

Convergence of Genetic Disease Association and Ocular Expression

by

Felicia Alessandra Hawthorne

University Program in Genetics and Genomics
Duke University

Date: _____

Approved:

Terri L. Young, Supervisor

Michael Hauser

Allison Ashley-Koch

Catherine Bowes Rickman

Douglas Marchuk

Dissertation submitted in partial fulfillment of
the requirements for the degree of Doctor of Philosophy
in the University Program in Genetics and Genomics
in the Graduate School of Duke University

2012

ABSTRACT

Convergence of Genetic Disease Association and Ocular Expression

by

Felicia Alessandra Hawthorne

University Program in Genetics and Genomics
Duke University

Date: _____

Approved:

Terri L. Young, Supervisor

Michael Hauser

Allison Ashley-Koch

Catherine Bowes Rickman

Douglas Marchuk

An abstract of a dissertation submitted in partial
fulfillment of the requirements for the degree of Doctor of Philosophy
in the University Program in Genetics and Genomics
in the Graduate School of Duke University

2012

Copyright by
Felicia Alessandra Hawthorne
2012

Abstract

The visual system in humans provides the ability to interpret our surroundings from many distances. This complex system serves as a powerful sense which can drastically impact the quality of life when threatened or eliminated. While the mechanisms involved in visual interpretation are largely understood, many of the mechanisms of ocular diseases remain elusive. The most common ocular disorders are refractive errors, where failure of normal growth processes results in eye components with shape and sizes that are not matched to provide uncorrected sharp visual acuity without correction. Myopia, or nearsightedness, is a refractive error with prevalence rates of epidemic proportions in some urban Asian settings, and rising in other developed countries. Pathological, or high myopia, has an increased risk for potentially blinding ocular morbidities which can be irreversible and further negatively impact quality of life. Myopia, like other common ocular disorders, results from a combination of environmental and genetic factors. Over 20 candidate genomic regions have been identified as involved in myopic development progression.

One such locus, *MYP3*, on chromosome 12q21-23 spans nearly 44 Mb with more than 200 protein-encoding genes mapped within. Sizable candidate disease genomic regions typically require refinement to identify genes or variants within them which may contribute to disease development. Without an understanding of the underlying

mechanistic framework of a disease, as is the case with myopia, biological inferences are difficult to make in prioritizing candidates, which can make finding true disease causing variants seem like finding a needle in a haystack. A better understanding of human ocular growth, as it relates to refractive error, may lead an improved ability to prioritize reasonable candidate genes related to myopic development and associated ocular diseases.

To identify genes involved in ocular growth and development, whole genome expression patterns were assessed in human ocular tissues of fetal versus adult eyes, and adult posterior versus peripheral tissues. Fetal ocular tissue gene expression has not been previously described. In addition to providing insights into expression patterns during ocular development, these tissues were also compared as a surrogate to study rapid eye growth states such as in myopia. Only ocular tissue types with clinical phenotypes associated with myopic development were considered. Human retina/retinal pigment epithelium (RPE), choroid, sclera, cornea* and optic nerve* tissues were isolated from fetal (N=9; *N= 6) and adult (N=6) normal donor eyes. The Illumina® whole genome expression microarray platform was used to assess differential expression of genes. Fetal tissues were compared to their adult counterparts while adult posterior tissues were compared to their peripheral counterparts, and the differences in each were assessed using Ingenuity Pathway Analysis (IPA) for enriched functional groups and canonical pathways. Statistical significance for all tissue comparisons was

determined using the Benjamini and Hochberg False Discovery Rate (FDR, $q=0.05$)).

Differentially expressed genes were compared to previously identified candidates for myopic development.

Additionally, qualitative and quantitative association studies in a large family (N=82) based high myopia cohort by genotyping 768 single nucleotide polymorphisms (SNPs) in the peak linkage area was performed to fine map the *MYP3* linkage peak. Qualitative testing for high myopia (≤ -5 diopter (D) affected, > -5 D unaffected) and quantitative testing on the average (avg) dioptric sphere (SPH) was performed. Five candidate SNPs were genotyped in a replicate high myopia cohort for independent validation. Additionally, the most significant SNPs were screened in a previously genotyped twin cohort as a second independent validation cohort.

Ocular growth expression data were used to help prioritize the resulting *MYP3* association candidate genes as supporting evidence and was not used on its own to identify or exclude candidates. Candidate genes (within 100 kilobases (kb) of highly associated SNPs) identified through either qualitative or quantitative association testing were screened in the most disease relevant tissues (retina/ retinal pigment epithelium (RPE), choroid and sclera) for differential expression during ocular growth and by physical regions of the tissues within the eye. Genes that were identified by microarray studies as being differentially expressed in one or more tissue were validated using quantitative real time PCR (RT-qPCR).

Significant gene expression changes with fold changes > 1.5 were found in adult versus fetal retina/RPE (N=1185), choroid (N=6446), sclera (N=1349), and cornea (N=3872), but not the optic nerve nor any of the central versus peripheral tissues. In all adult versus fetal tissues, differentially expressed genes belonging to cancer, development, and cell death/growth functional groups, as well as signaling canonical pathways were enriched. Seventeen genes previously associated with increased susceptibility for non-syndromic high myopia were in the most significant functional assignments for at least one adult versus fetal ocular tissue. In adult central versus peripheral tissues, there was considerably more variation by tissue in enriched functions and canonical pathways of differentially expressed genes. The only functional category shared by all three tissue types was development.

MYP3 association testing yielded several genetic markers as nominally significant in association with high myopia in qualitative testing including *rs3803036* ($p=9.1 \times 10^{-4}$), a missense mutation in protein tyrosine phosphatase receptor type R (*PTPRR*); and *rs4764971* ($p = 6.1 \times 10^{-4}$), an intronic SNP in UHRF1 binding protein 1-like (*UHRF1BP1L*). After correction for multiple testing, quantitative tests found statistically significant SNPs *rs4764971* ($p = 3.1 \times 10^{-6}$), also found by qualitative testing; *rs7134216* ($p = 5.4 \times 10^{-7}$), in the 3' UTR of DEP domain containing protein 4 (*DEPDC4*); and *rs17306116* ($p < 9 \times 10^{-4}$), intronic within *PTPRF* interacting liprin alpha 2 (*PPFIA2*). The intronic SNP in *UHRF1BP1L*, *rs4764971*, was validated for association with the quantitative trait of

sphere (SPH) using an independently collected non-syndromic, high myopia cohort. SNPs within *PTPRR* (for quantitative association) and *PPFIA2* (for qualitative and quantitative association) both approached significance in the independent high myopia cohort.

As with screening genes previously implicated in myopic development, qualitative and quantitative association candidates were screened in the independent whole genome expression array analyses, comparing normal rapidly growing fetal to normal grown adult ocular tissues. *PTPRR* and *PPFIA2*, candidates from qualitative and quantitative association respectively, were both validated by RT-qPCR with differential expression in at least one disease relevant ocular tissue. *PTPRR* and *PPFIA2* belong to the same gene family of protein tyrosine phosphatase (PTP) genes. This family of genes relays extracellular signals that regulate cell growth, division, maturation and function, and its differential expression is consistent with our myopia surrogate model.

Many genes implicated in either syndromic or non-syndromic myopia were present in the most significantly enriched adult versus fetal functional and/or canonical pathways together. The adult versus fetal choroid and cornea tissue types had the most overlap with known non-syndromic myopic-associated genes in the most significantly enriched functional groups. Further exploration of the connections amongst these known genes may elucidate possible mechanistic roles for disease progression and/or reveal related novel candidate genes. Differentially expressed genes in central versus

peripheral tissues yielded minimal overlap with genes implicated in myopia; however, in addition to broadening our understanding of the spatial variances in these tissues they may contain clues to the development and/or progression of other ocular diseases such as retinopathy of prematurity development.

The overlap with previously identified myopia-associated genes supports the model of eye growth for studying myopic development in human tissues. This expression data can be used both in prioritizing candidate genes other proposed genomic myopia loci, and also in detailed pathway analyses to identify potential biological mechanisms for candidates within these loci. Our most strongly associated candidate gene both in the discovery and replicate cohort was *UHRF1BP1L*, which was not differentially expressed in our data; however, interacting genes regulate the expression of at least one differentially expressed gene, indicating a possibly pathway connection. It is possible that differential expression may have been missed by the microarray data, or it may not be differentially expressed and affects myopic development through alternative or indirect means. While the expression data is a useful tool in prioritizing and inferring mechanistic roles for candidates, it should not be used to exclude candidates. Deeper study of the pathways of candidate genes for myopic development may reveal connections to genes involved in ocular growth. Despite these potential limitations, two of the three novel candidates, *PTPRR* and *PPFIA2*, were supported by genomic convergence with the expression data, in addition

to our discovery genetic association data. The other novel candidate, *UHRF1BP1L*, was validated in an independent Caucasian high-grade myopia cohort. Further validation and refinement of these three novel *MYP3* candidate genes is necessary to make further claims about their possible involvement in myopic progression.

Dedication

I would like to dedicate my doctoral dissertation to the people who have most inspired and motivated me throughout my life. My family has always been loving and supportive, and without them I could not have accomplished all of the things that I have. Particularly my sisters Sabrina, Stephanie and Francesca have each inspired me to persevere through difficult times. I also want to dedicate my dissertation to Josh, who has taught me to believe in myself and has permanently changed my perspective on life for the better.

Contents

Abstract	iv
List of Tables	xix
List of Figures	xxi
List of Abbreviations	xxii
Acknowledgements	xxvi
1. Introduction	1
1.1 Ocular Background	1
1.1.1 Vision	1
1.1.1.1 Ocular Anatomy	1
1.1.1.2 The Cell Biology of Vision	3
1.1.1.3 Refractive Power of the Eye	9
1.1.2 Ocular Growth and Regulation	11
1.2 Common Ophthalmic Diseases	14
1.3 Ocular Tissue Expression	15
1.3.1 Disease Related Ocular Tissue Expression	15
1.4 Myopia	17
1.4.1 Phenotype	17
1.4.1.1 Associated Tissue Changes	17
1.4.2 Prevalence and Health Concerns	21
1.4.2.1 Prevalence Rates of Myopia	21

1.4.2.2 Impact and Health Concerns of Myopia.....	22
1.4.3 Environmental Effects.....	23
1.5 Genetics of Myopia.....	24
1.5.1 Heritability of Refractive Error.....	24
1.5.2 Candidate Myopia Loci	25
1.5.2.1 Candidate Loci for Quantitative Myopia	27
1.5.2.2 Candidate Loci for Any Myopia	28
1.5.2.3 Candidate Loci for Mild to Moderate Myopia.....	28
1.5.2.4 Candidate Loci for Pathological High Myopia.....	29
1.5.3 Genes Implicated in Myopic Development	32
1.5.3.1 Non-Syndromic Myopia	32
1.5.3.2 Non-Syndromic High Myopia	33
1.5.3.3 Myopic Choroidal Neovascularization.....	36
1.5.3.4 Syndromes with a Myopic Component.....	41
1.6 High Myopia Locus MYP3.....	41
1.6.1 <i>MYP3</i> Genetic Studies.....	41
2. Ocular Tissue Expression.....	44
2.1 Ocular Sample Selection	46
2.1.1 Tissues of Interest	48
2.2 Methods	49
2.2.1 Ocular Dissection.....	49
2.2.1.1 Tissue Preservation.....	49

2.2.1.2 Tissue Isolation.....	52
2.2.2 RNA Extraction and Whole Genome Expression Processing	53
2.2.3 Whole Genome Expression Analyses.....	54
2.2.4 Pathway Analyses	54
2.2.4.1 Functional Annotation Analyses	55
2.2.4.2 Canonical Pathway Analysis.....	56
2.2.4.3 Disease Gene Overlap with Ocular Growth	56
2.3 Results	57
2.3.1 Differential Expression of Ocular Growth.....	60
2.3.1.1 Enriched Functional Annotation Analyses	60
2.3.1.2 Predicted Activation Functional Annotation Analyses.....	62
2.3.1.3 Canonical Pathway Analyses	67
2.3.1.4 Non-Syndromic High Myopia Susceptibility Genes	69
2.3.1.5 Syndromic Myopia Genes.....	80
2.3.2 Central versus Peripheral Differential Expression	81
2.3.2.1 Enriched Functional Annotation Analyses	82
2.3.2.2 Predicted Activation Functional Annotation Analyses.....	85
2.3.2.3 Canonical Pathway Analyses	87
2.4 Conclusions	88
2.4.1 Differential Expression of Ocular Growth.....	88
2.4.1.1 Retina/RPE	90
2.4.1.2 Choroid.....	92

2.4.1.3 Sclera.....	93
2.4.1.4 Optic Nerve.....	94
2.4.1.5 Cornea.....	95
2.4.1.6 Syndromic Myopia and Ocular Growth.....	96
2.4.1.7 Conclusions.....	98
2.4.2 Central versus Peripheral Differential Expression	98
3. Refining the <i>MYP3</i> Locus	101
3.1 Methods	101
3.1.1 Patient Cohort.....	101
3.1.2 Genotyping Methods	103
3.1.2.1 SNP Selection.....	103
3.1.2.2 Genotyping and Quality Control.....	103
3.1.3 Association Analyses	105
3.1.3.1 Qualitative Association Analyses	105
3.1.3.2 Quantitative Analyses	105
3.1.4 Independent Cohort Validation	106
3.1.4.1 International High Myopia Cohort	106
3.1.4.2 The Twin Eye Study	107
3.2 Results	108
3.2.1 Qualitative Association.....	108
3.2.2 Quantitative Association	108
3.2.3 International High Myopia Cohort.....	113

3.2.4 The Twin Eye Study	116
3.2.5 Concordance of SPH and SE Endophenotypes and Complete Multi-Ethnic Cohort in Discovery Data.....	116
3.3 Conclusions	121
3.3.1 Validation in Replicate Cohorts	122
3.3.2 Novel <i>MYP3</i> Candidate Genes.....	124
4. Genomic Convergence of Expression and Association	125
4.1 Methods	125
4.1.1 Ocular Tissues Relevant to Myopic Development	125
4.1.2 Overlap with <i>MYP3</i> Association.....	126
4.1.3 RT-qPCR Validation.....	126
4.2 Results	129
4.2.1 RT-qPCR Validation.....	130
4.3 Conclusions	132
4.3.1 Genomic Convergence of Association Candidates and Ocular Expression. ..	132
4.3.2 Limitations of Ocular Expression Prioritization	133
4.3.3 <i>MYP3</i> Candidate Genes.....	134
5. Conclusions.....	135
5.1 Implications of Genomic Convergence	135
5.1.1 Ocular Growth as a Model for Myopic Development	135
5.1.2 Candidates Genes for Myopic Development from Animal Models	136
5.1.3 Whole Genome Array Studied of Animal Models of Myopic Development...	137

5.1.4 Differentially Expressed Genes within Known Myopia Linkage Loci	141
5.2 Novel Insights into Possible Biological Mechanisms for Refractive Error	141
5.2.1 Protein Tyrosine Phosphatases (PTPs)	141
5.2.1.1 PTP Enrichment in <i>MYP3</i> Quantitative Analyses	142
5.2.2 <i>PTPRR</i> and <i>PPFIA2</i> as <i>MYP3</i> Candidates for Myopic Development	145
5.2.2.1 <i>PTPRR</i>	145
5.2.2.2 <i>PPFIA2</i>	147
5.2.3 <i>UHRF1BP1L</i> , <i>ACTR6</i> , <i>DEPDC4</i> and <i>NAV3</i> as <i>MYP3</i> Candidates for Myopic Development	148
5.2.3.1 <i>UHRF1BP1L</i>	148
5.2.3.2 <i>ACTR6</i> , <i>DEPDC4</i> and <i>NAV3</i>	150
5.3 Future Directions	151
5.3.1 Ocular Expression	151
5.3.1.1 Candidates in Genomic Myopia Loci	151
5.3.1.2 Animal Model Comparison by Tissue	152
5.3.2 Refinement of the <i>MYP3</i> locus	152
5.3.2.1 Validation by Additional Cohorts and/or Ethnicities	152
5.3.2.2 Tagging SNPs	153
5.3.2.3 Functional Validation	153
5.3.2.4 Differential Expression in Animal Models of Myopia	154
5.4 Conclusions	154
5.4.1 Ocular Growth as a Model for Myopia	154

5.4.2 Refinement of the <i>MYP3</i> Locus	155
Appendix A.....	156
Appendix B	159
Appendix C.....	167
References	179
Biography	198

List of Tables

Table 1: Genes Previously Implicated in or Proposed for the Progression of Myopic Development.	37
Table 2: Donor Information for Adult Ocular Whole Globes Used in Tissue Expression Analyses.	47
Table 3: Number and Fold Change Range of Filtered Probes and Unique Genes.....	58
Table 4: Ten Most Significant Adult versus Fetal Functional Assignments.	61
Table 5: Significant Predicted Activation of Functional Assignments for Ocular Growth Expression.	64
Table 6: Five Most Significant Adult versus Fetal Tissue Canonical Pathways.....	68
Table 7: Differentially Expressed Non-Syndromic High Myopia Susceptibility Genes. ...	77
Table 8: Genes Implicated in Myopic Development Which Belong to the Ten Most Significant Functional Assignments.	79
Table 9: Ten Most Significant Central versus Peripheral Functional Assignments.....	84
Table 10: Significant Predicted Activation Functional Assignments for Central versus Peripheral Expression.....	86
Table 11: Five Most Significant Central versus Peripheral Tissue Canonical Pathways. .	88
Table 12: Taqman® Genotyping Assay Identification Numbers.	107
Table 13: Most Significant SNPs from Qualitative and Quantitative Association Testing.	110
Table 14: Evolutionary Conservation of Candidate SNPs from Association.	111
Table 15: Validation of the Most Significantly Associated SNPs in an Independent High Myopia Cohort.	115
Table 16: Validation of the Most Significantly Associated SNPs in a Previously Genotyped Independent Cohort.....	118

Table 17: APL Concordance with SPH, SE and Mixed Ethnicities.....	119
Table 18: QTLD Concordance with SPH, SE and Mixed Ethnicities.	120
Table 19: Differentially Expressed Genes Related to Candidate Genes from <i>MYP3</i> Association.....	128
Table 20: Taqman® Gene Expression Assay Identification Numbers.....	129
Table 21: Our Human Expression Array Study Compared to Expression Array Studies of Animal Growth or Myopia.	139
Table 22: PTP Related Genes in Known Myopia Linkage Loci.	143

List of Figures

Figure 1: Eye Diagram.....	3
Figure 2: Distribution of Photoreceptors.	9
Figure 3: Ocular Refraction.....	11
Figure 4: Rate of Axial Elongation in Human Eyes During Normal Growth.	12
Figure 5: Localized Ocular Growth in Animal Models.	14
Figure 6: Relative Axial Elongation in Myopic Eyes.....	18
Figure 7: Tissues changes of the Posterior Wall in Refractive Error.....	19
Figure 8: Candidate Myopia Loci Identified by Whole Genome Analyses.	31
Figure 9: <i>MYP3</i> Locus Linkage Studies.	43
Figure 10: Posterior and Peripheral Ocular Tissue Isolation.	48
Figure 11: Fetal Ocular Histology.....	51
Figure 12: Association in the Presence of Linkage (APL) and Quantitative Trait Linkage Disequilibrium (QTL) Association Results by $-\log(p)$	112
Figure 13: Fetal Versus Adult Fold Changes of Real Time Quantitative PCR (RT-qPCR) Validated Genes.	131
Figure 14: Quantitative Association by $-\log(p)$ for All SNPs in PTP Related Genes.	144
Figure 15: Possible Mechanistic Roles for Novel Candidates <i>PTPRR</i> , <i>PPFIA2</i> and <i>UHRF1BP1L</i>	150

List of Abbreviations

AA	African Americans
A	association
AL	axial length
APL	Association in the Presence of Linkage
avg	average
BED	Bornholm Eye Disease
CEPH	Centre d'Etude du Polymorphisme Humain
CNV	copy number variant
D	diopter
DEP	Dishevelled, Egl-10 and Pleckstrin
DNA	deoxyribonucleic acid
EST	expressed sequence tag
FC	fold change
FDM	form deprivation myopia
FDR	false discovery rate
GABA	gamma-aminobutyric acid
GDA	Genetic Data Analysis
GF	genotype frequency

GOLD	Graphical Overview of Linkage Disequilibrium
G-protein	guanine nucleotide-binding proteins
GWAS	genome-wide association study
HA	haplotype association
HWE	Hardy-Weinberg equilibrium
IPA	Ingenuity® Pathway Analysis
L	linkage
LAR	leukocyte common antigen-related
LD	linkage disequilibrium
LOD	logarithm of odds
LR	logistic regression
M	loss of function mutation
MA	meta-analysis
MAF	minor allele frequency
MIM	Mendelian inheritance in man
<i>miR</i>	microRNA
<i>MYP</i> (#)	myopia locus (one, two, etc.)
N	number
NEI	National Eye Institute
OPA	oligo pool assay

p	short arm of chromosome
p-value	probability value
PTI	preservation time interval
PTP	protein tyrosine phosphatase
q	long arm of chromosome
QA	quantitative association
QC	quality control
QTL	quantitative trait locus
QTLD	Quantitative Trait Linkage Disequilibrium
Qual.	qualitative
Quant.	quantitative
RFLP	restriction fragment length polymorphism
RNA	ribonucleic acid
RPE	retinal pigment epithelium
RT-qPCR	reverse transcriptase quantitative polymerase chain reaction
SAGE	serial analysis gene expression
SE	spherical equivalence
SNP	single nucleotide polymorphism
SOLAR	Sequential Oligogenic Linkage Analysis Routines
SPH	sphere

UK	United Kingdom
US	United States
USV	unique sequence variant
UTR	untranslated region
VF	variant frequency

Acknowledgements

There are many people that I would like to acknowledge who have helped me to accomplish this body of work. First, I would like to thank my advisor, Terri Young, who took a chance on me and supported my interests in and out of the lab. My lab members over the years have also helped with support, encouragement and scientific advice. Ravi Metlapally in particular helped me to navigate the field and served as a great role model in the lab. I also want to acknowledge the support and advice of my committee, all of whom I have turned to in times of need. I would also like to thank all of the other lab members of the Center for Human Genetics who helped me in times of need, especially Karen Abramson and Karen Soldano. I could not have completed my dissertation without the assistance and guidance of many of the analysts. Tina Markunas was instrumental in my learning data analyses and I will be forever grateful. Lastly, I would like to acknowledge all of my friends who have made graduate school an enjoyable experience and contributed to my overall successes in my time here.

1. Introduction

1.1 *Ocular Background*

1.1.1 Vision

Human perceptions of the world around them are largely influenced by their vision. Our highly specialized eyes allow us to interpret visual signals through a complex network of cells by absorbing photons of light and converting them into electrical signals. These signals are transmitted to our brains where we decode them into an image. This powerful sense that humans possess is not without faults. Impairment or loss of sight may not be life threatening, but the quality of life may be reduced in those suffering from partial or complete loss of vision.

1.1.1.1 Ocular Anatomy

The eye globe is a round structure used to interpret light signals from the world around it and transmit them to the brain for processing. Figure 1 shows a diagram of the ocular anatomy with the structures discussed below. The outer wall of the eye is called the sclera, which is comprised of white fibrous tissue that extends as a shell ending at the cornea at the anterior segment and the optic nerve posteriorly. The optic nerve is responsible for transmitting visual signals from the internal retina to the brain. The cornea is a translucent 'window' at the front of the eye, through which light waves are refracted through the lens and ultimately to the inner retina in the posterior chamber

of the eye. Together the cornea and the lens constitute the major refractive components of the eye. As photons of light energy enter the eye and are focused on the posterior wall of the globe, they pass through the retina and are absorbed either by the photoreceptors (visual signaling), located at the posterior side of the retina, or the retinal pigment epithelium (RPE; protective excess energy absorption), immediately posterior to the retina. The photon absorption by the photoreceptors, rods and cones, sets off a signaling cascade, known as phototransduction, back via the retina through a complex neural circuit. In humans, rod photoreceptors are the most abundant, and are more sensitive than the cones and are therefore responsible for vision in low light – they are so sensitive, in fact, that they are capable of responding to a single photon of light. Cone photoreceptors are most concentrated in the center of the retina, within the macula, and provide our visual acuity and color vision. There are three types of color-sensitive cones corresponding roughly to red, green, and blue sensitive detectors. Visual signals interpreted by rods and cones are eventually sent via retinal ganglion cells, whose axons form the interior of the optic nerve, to the brain. The RPE is a single layer of epithelial cells that form the blood-eye barrier between the retina and the choroid. It serves multiple functions including maintaining photoreceptor outer segment length, visual pigment recycling, nutrient uptake, metabolite transportation and absorption of excess light energy. The choroid is a thin, vascularized layer sandwiched between the

retina/RPE and the sclera. It is primarily responsible for oxygen/ free radical exchange with the retina, and for providing nutrients to its surrounding tissues. (Rodieck 1998; Strauss 2005; Hildebrand and Fielder 2011)

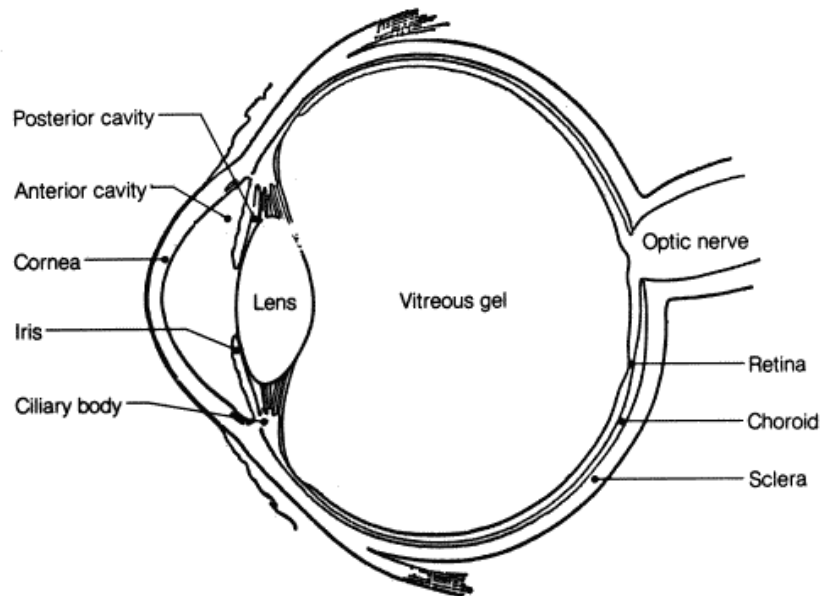


Figure 1: Eye Diagram.

This model shows the basic components of the eye in a cross section including the posterior retina, choroid and scleral tissues. (Freely licensed image)

1.1.1.2 The Cell Biology of Vision

The retina, made up of three cell layers, is the primary ocular tissue responsible for visual interpretation. Light is transmitted through the ganglion, second order and photoreceptor cell layers until it reaches the photoreceptor outer segments where it is

absorbed by opsin molecules embedded in the disc organelle membrane. Light absorption in the photoreceptors initiates a signaling network, through the three cell layers, responsible for transmitting the visual signals to the brain for further processing. Located at the posterior pole of the human eye globe, the macula (lutea) is a yellow oval shaped region of the retina approximately 5 mm in diameter. At the center of the macula, the fovea (centralis) is a depression approximately 1.5 mm in diameter. The foveola is at the center of the fovea spanning approximately 0.35 mm in diameter. This central region of the retina allows for the highest acuity vision. (Hildebrand and Fielder 2011)

Light signal transduction starts in the rod and cone photoreceptors, which have variable distribution throughout the retina (Figure 2). The most numerous photoreceptors, rods, interpret low levels of light and are absent from the center-most region of the retina, the foveola. Rods are concentrated within the fovea, forming a rod-rich ring, located within the macula about 4.5 mm from the foveola, and then gradually decreasing in density as you continue peripherally. Cone photoreceptors, which interpret color vision and high levels of light, are most concentrated in the fovea, with decreased density in the peripheral retina. (Rodieck 1998; Purves 2001)

Photoactivation of retinal by photons, termed phototransduction, sets off a biochemical cascade in the photoreceptors resulting in hyperpolarization of their cell

membrane. The outer segment of photoreceptors contains the transmembrane protein opsin, a photopigment that captures photons of light and initiates the signaling cascade. When a photon is absorbed, the opsin-bound chromophore 11-cis retinal is photoisomerized to all-trans retinal. The RPE aids in the visual cycle of retinal by reisolomerizing retinal and transporting it back to the photoreceptors, which are unable to reisolomerize retinal on their own as necessary to maintain photon excitability. As a result of this signaling cascade initiated by photoisomerization of 11-cis retinal to all-trans, the synaptic channels pumping calcium into the photoreceptor cells close. This decrease in internal calcium reduces the rate of glutamate, a neural signaling molecule, release. The synaptic ribbons of spherules and pedicles (single and multi-synaptic sites at the base of rods and cones, respectively) each connect to multiple second order neurons (bipolar and horizontal cells). However, rods with just two synaptic ribbons per spherule connect to four second order neurons, while cones with about 30 synaptic ribbons per pedicles connect to over 100 second order neurons. (Rodieck 1998; Strauss 2005; Hildebrand and Fielder 2011)

Horizontal cells provide lateral inhibition to enhance spatial differences in photoreceptor activation at the level of the photoreceptor and the bipolar cell connecting to them via a negative feedback loop. These cells extend laterally connecting to many photoreceptors (typically more in the peripheral retina) helping to increase sensitivity to

contrast and spatial differences in light intensities. The three types of horizontal cells differ in their dendrite and axon size/shape as well as the type of photoreceptor they connect to. HI and HIII cells both have dendritic fields which contact cones at ribbon synapses in pedicles and long axons terminating in clusters of contacts. HI cells' axons terminate at rod spherules and HIII axon terminals are believed to terminate at both cone pedicles and rod spherules. The dendrites of HII cells also connect to cone pedicles, however, their axons are shorter, curved and connect to cone pedicles via smaller terminals. (Rodieck 1998; Kolb 2011)

In the human retina there are 11 different types of bipolar cells, 10 of which connect to cones and only one of which connects to rods. The differences in cone bipolar cell types include the number of cones they connect to and the types of contacts that are made. Rod bipolar cells depolarize in response to light signals received from dendrites connecting to 15-20 rod spherules in the central retina and up to 50 in the peripheral retina per cell. Rod bipolar cells connect to ganglion cells via amacrine cells, allowing for convergence of signals relayed from many rods to each ganglion cell. (Rodieck 1998; Kolb 2011)

Unlike rod bipolar cells, cone bipolar cells can signal through direct synaptic connections with ganglion cells without the need for intermediate amacrine cell circuitry. Cone bipolar cells can either depolarize (on-bipolar cells) or hyperpolarize

(off-bipolar cells) in response to light, depending on the kind of glutamate receptors on each bipolar cell type. The diffuse cone bipolar cells comprise of seven of the 10 cone bipolar cell types and receive information from many cones at once (between five and 20 depending on the type, typically with more in the peripheral retina). The other three types of cone bipolar cells, midget bipolar cells and blue-cone specific, connect with only one cone each. (Rodieck 1998; Kolb 2011)

Within the fovea, the cones pathways achieve high acuity vision via divergent signaling to bipolar and ganglion cells. While midget bipolar cells receive input from only one cone within the fovea, each cone connects to two midget bipolar cells (one on-bipolar cell and one off-bipolar cell) in addition to diffuse bipolar cells, resulting in divergent signaling. On and off midget bipolar cells each connect with a distinct on or off midget ganglion cell. This divergent cone midget pathway (one cone to two ganglion cells) in the fovea explains the concentration of ganglion cells in the region. (Rodieck 1998; Kolb 2011)

With about 40 sub-types, only a few of which have been well characterized, amacrine cells are the most diverse and least understood cell type in the retina. These sub-types are characterized by the size and regions of their dendritic fields. Amacrine cells receive signals from bipolar cells and other amacrine cells and all respond to light by depolarizing. They can send signals to bipolar cells, other amacrine cells, and also to

ganglion cells. Amacrine signals constitute the majority of signals to the ganglion cells. (Rodieck 1998; Kolb 2011)

Lastly, retinal ganglion cells, like those found in the brain, are a diverse group of neurons. The rate of action potentials, generated to send signals to the brain, is influenced by the activity of the connection to amacrine and bipolar cells. Generally, bipolar cell activity increases the firing rate, while amacrine activity decreases it. The retinal ganglion cells are the only retinal cells to send signals out of the eye rather than to other cells within it. Retinal ganglion cell types are specialized for particular visual components, such as contrast or movement. The long axons of these specialized retinal ganglion cells travel through the optic nerve to six different regions in the primate brain, each also adapted for different visual functions. (Rodieck 1998; Kolb 2011)

In summary, the retina is a highly specialized tissue made up of numerous cell types. These cells communicate in a backward loop through the retina and back out via the optic nerve. Despite this complicated signaling network within the retina interpreting visual signals, no known mechanism exists which send signals to or from the nearby ocular tissues such as the choroid and sclera.

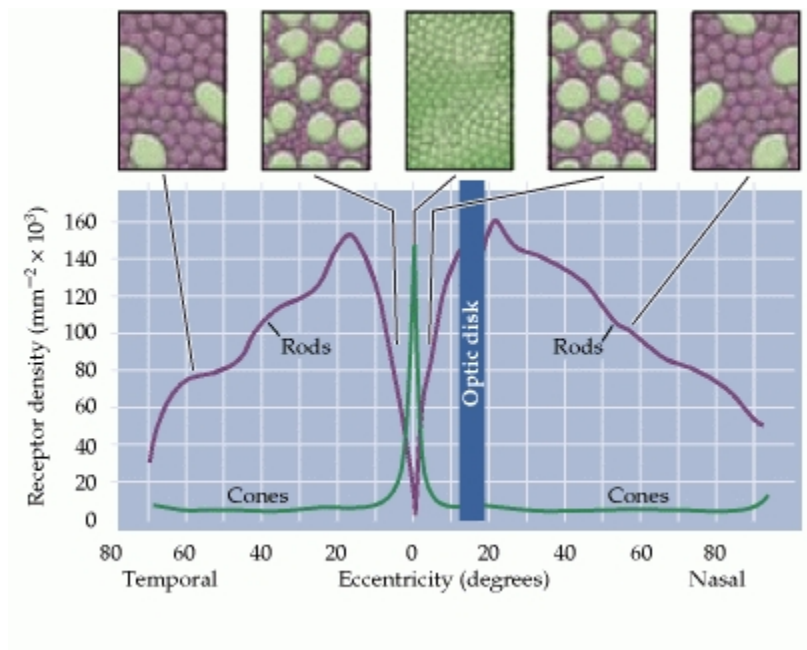


Figure 2: Distribution of Photoreceptors.

The distribution of rods and cones in the retina are variable. The rods are relatively dense across the entire retina, with the exception of the foveola where their density sharply declines. Conversely, the cones are most dense in the center of the fovea and have relatively low density as the eccentricity (degrees) increases from the center of the fovea increases. (Image © (Purves 2001))

1.1.1.3 Refractive Power of the Eye

In emmetropia, or absence of refractive error, the globe axial length (AL) is coordinated with the combined optical powers of the cornea and the lens such that the object image on the retinal plane is not distorted (Figure 3). As light passes through the cornea and lens it is bent to a focal point at the image plane. The cornea is responsible

for the majority of the refractive power of the eye. The thickness and curvature of the cornea and lens affect the degree of refraction of light.

Refractive errors, resulting in reduced visual acuity, are the most common ocular disorders affecting hundreds of millions worldwide (Pascolini and Mariotti 2012).

Sphere (SPH), measured in diopters (D), determines the amount of optical correction in the axis meridian needed. Spherical equivalence (SE; $SPH + \text{cylinder}/2$) is also measured in D and is used to determine the optical correction needed to compensate for AL in addition to curvature of the cornea and/or the lens. Both SPH and SE are commonly used in measuring refractive error and prescribing corrective lenses to resolve visual impairment. Refractive errors resulting in the image plane anterior to the retina are termed myopia, while errors resulting in the image plane posterior to the retina are termed hyperopia (Figure 3).

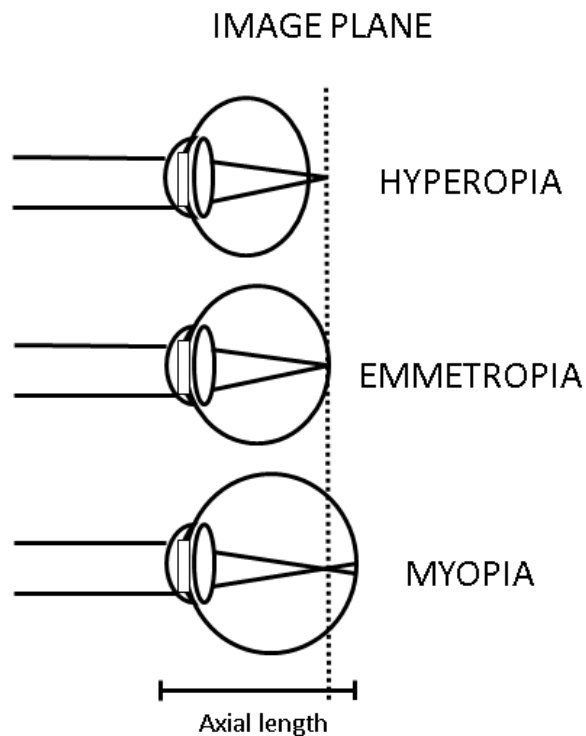


Figure 3: Ocular Refraction.

Hyperopic (top), Emmetropic or normal (middle), and myopic (bottom) vision. Changes in refraction relative to axial length (AL) of the globe results in refractive error or blurred vision. (Lab image adapted from (Sundin, Dharmaraj et al. 2008))

1.1.2 Ocular Growth and Regulation

Human ocular growth exponentially declines over time, slowing considerably by the age of two or three years (Fledelius and Christensen 1996) (Figure 4). Newborn humans are typically born slightly hyperopic, with postnatal axial elongation shifting

toward emmetropia. Animal studies provide insights into how ocular growth is regulated, but the mechanisms involved largely remain a mystery.

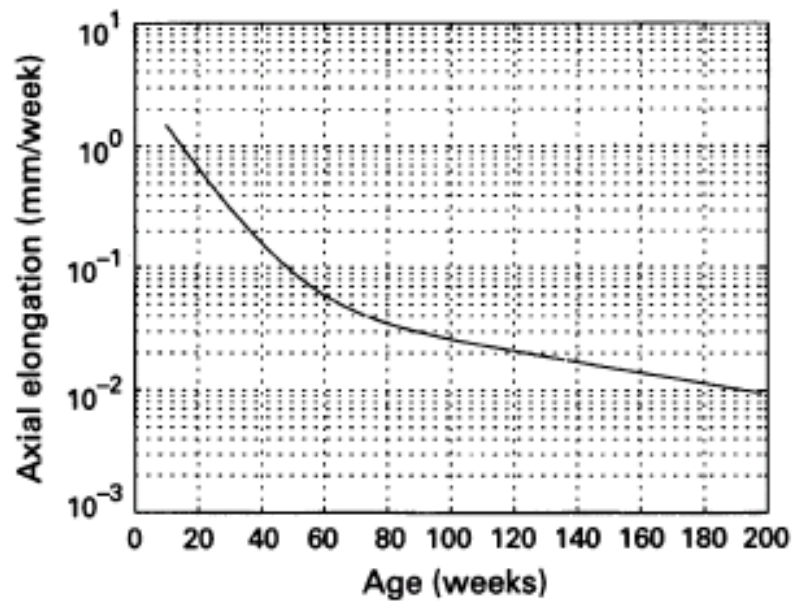


Figure 4: Rate of Axial Elongation in Human Eyes During Normal Growth.

Ocular growth exponentially decreases over time. Age is given in weeks starting at conception. (Fledelius and Christensen 1996)

Eye growth is self-regulated by visual cues interpreted by the retina and signaled through the choroid and sclera by unknown mechanisms. During growth and development of a normal eye, myopic defocus (focal point of light is in front of the retina) can be corrected by pushing the retina forward through expansion of the choroid

layer and also slowing the progression of axial elongation (Wildsoet and Wallman 1995; Wallman and Winawer 2004). For hyperopic defocus (focal point of light is behind the retina), vision modulation occurs by pulling the retina back, with choroidal thinning, and increased AL by growth or sclera modifications (Wildsoet and Wallman 1995; Wallman and Winawer 2004).

Scientists have exploited these self-corrective pathways to create animal models of myopia using form-deprivation or lens-defocus (Wildsoet and Wallman 1995; Wallman and Winawer 2004; Faulkner, Kim et al. 2007; Tkatchenko, Shen et al. 2009). These animal models support local control of eye shape and size (Figure 5). If the optic nerve connecting the eye to the brain is cut, form-deprivation or lens-defocus can still affect eye shape with some alterations. Furthermore, deprivation or defocus affects only the portion of the posterior wall tissues deprivation is applied to (Wallman and Winawer 2004). While animal models show features of human myopia, the exact mechanisms by which they occur remain under study (Tkatchenko, Shen et al. 2009).

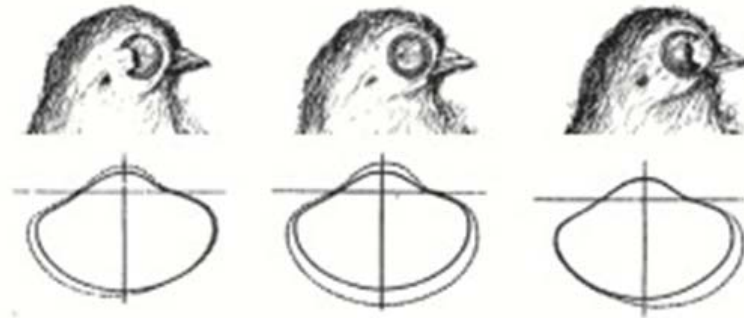


Figure 5: Localized Ocular Growth in Animal Models.

Visual deprivation of nasal (left) or temporal (right) half of the retina versus the entire (center) retina shows that ocular growth is regulated locally. (Wallman, Gottlieb et al. 1987)

1.2 Common Ophthalmic Diseases

The complex workings of vision are susceptible to many disruptions leading to a variety of diseases. The most common ophthalmic diseases include refractive errors, cataract, age-related macular degeneration, and glaucoma. Most cases of refractive error, can be resolved with corrective lenses representing a multi-billion dollar industry (Vision 2007). However, prevalence rates are rapidly increasing, reaching epidemic proportions in Asia (Saw 2003). A better understanding of the genetic and environmental mechanisms involved in myopic development is necessary before strides can be made in fighting this disease. Similarly, cataract, typically presenting later in life, is treatable through ophthalmic surgery to remove clouded lenses and replace them

with synthetic materials. Other common ocular diseases including age-related macular degeneration, where the retina is damaged, and glaucoma, where the optic nerve is damaged, have no cures. Treatments instead focus on slowing the progression toward blindness. A better understanding of how these diseases develop relative to the normal functions of their relevant ocular tissues may help to improve treatment strategies.

1.3 Ocular Tissue Expression

Publically available databases currently have an underrepresentation of genes specific to the eye (Zarepari, Hero et al. 2004). The introduction of microarray technology into mainstream science following the completion of the Human Genome Project has made expression analysis of ocular diseases feasible, yet the arrays have not contained all the genes expressed in the eye (Zarepari, Hero et al. 2004).

1.3.1 Disease Related Ocular Tissue Expression

Ocular tissue expression studies in common diseases can sometime be difficult due to the barrier of collecting tissue. Tissue can be collected from patients of some ocular diseases such as glaucoma and cataract during surgical procedures. However, normal tissue for comparisons can be obtained post-humerously from donor samples. The extra variables introduced by comparing living to deceased tissues likely represents noise when attempting to identify differences in expression in diseased tissue. Other ocular disorders such as refractive error typically do not undergo surgery of the relevant

tissues during development, and diseased human tissue is not obtainable.

Consequently, many scientists have turned to animal models as a surrogate to study ocular diseases – particularly those where no human diseased tissue is available.

Expression analyses have been performed on normal human adult samples but only from single tissue types (Young, Guo et al. 2003; Young, Scavello et al. 2004). The NEIBank's EyeSAGE database (Bowes Rickman, Ebright et al. 2006) has annotated ocular disease loci and candidate loci as well as serial analysis of gene expression (SAGE) data (Wistow, Peterson et al. 2008). Expression studies of myopic refraction, an early developmental disease, thus far include single tissue expression on model systems, such as mice using EST sequencing and cDNA libraries (Mu, Zhao et al. 2001; Zhou, Rappaport et al. 2006), chicks undergoing imposed myopic defocus (Schippert, Schaeffel et al. 2008) or comparisons of *in vivo* and *in vitro* development (Liu, Li et al. 2008). These animal models induce myopic ocular growth for comparison at any stage to control eyes. However, whole genome comparisons have yet to be done on human ocular tissues in relation to ocular growth. Whole genome expression comparisons between developing and developed human eyes in multiple ocular tissues may elucidate many of the genes involved in ocular growth and related diseases.

1.4 Myopia

1.4.1 Phenotype

Myopia is a condition of refractive error in the eye characterized by the focal point of parallel light rays in front of the fovea, resulting in blurred vision (Kempen, Mitchell et al. 2004). After birth, the human eye grows in length an average of 7 mm (Gordon and Donzis 1985). During this period of growth a myopic shift, characterized by an increased AL (Atchison, Jones et al. 2004), can occur from six years of age onward (Gordon and Donzis 1985). While criteria vary between studies, criterion for high myopia begins with a corrective lens of -5 D or more with onset prior to 12 years of age (Shih, Ho et al. 2006) and are sometimes higher in D requirements.

1.4.1.1 Associated Tissue Changes

Highly myopic eyes have distinct clinical phenotypes including changes to their size, shape and tissue structure (Xu, Li et al. 2007). Highly myopic eyes tend to be larger than their emmetropic counterparts, with primary axial elongation (Atchison, Jones et al. 2004) (Figure 6). High myopia is also characterized by thinner sclera, the outermost tunic of the eye (Rada, Shelton et al. 2006). Changes in the sclera can alter the shape of the eye potentially resulting in refractive error (Rada, Shelton et al. 2006). The tissues of the posterior pole, most significantly the sclera, are thinner as though stretched in highly myopic eyes (McBrien and Gentle 2003) (Figure 7).

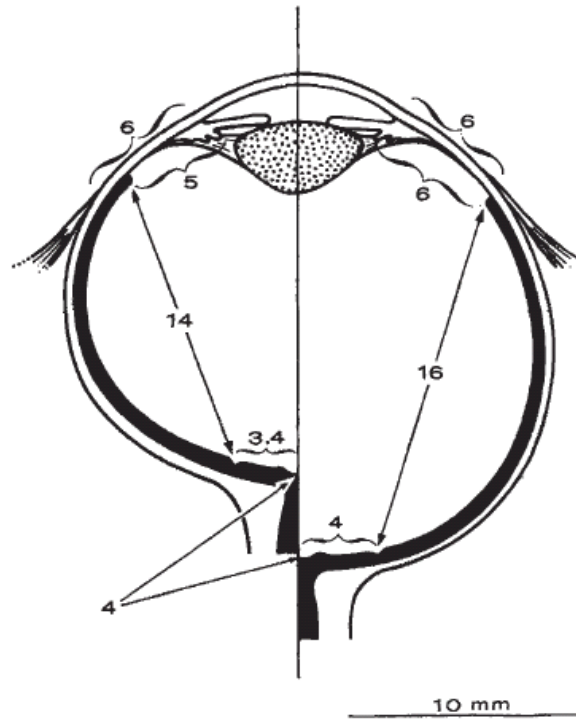


Figure 6: Relative Axial Elongation in Myopic Eyes.

Left) The size and shape of a normal emmetropic eye. Right) The size and shape, particularly the axial elongaion, is represented. Numbers represent distance in mm. (Torsten et al. 1977)

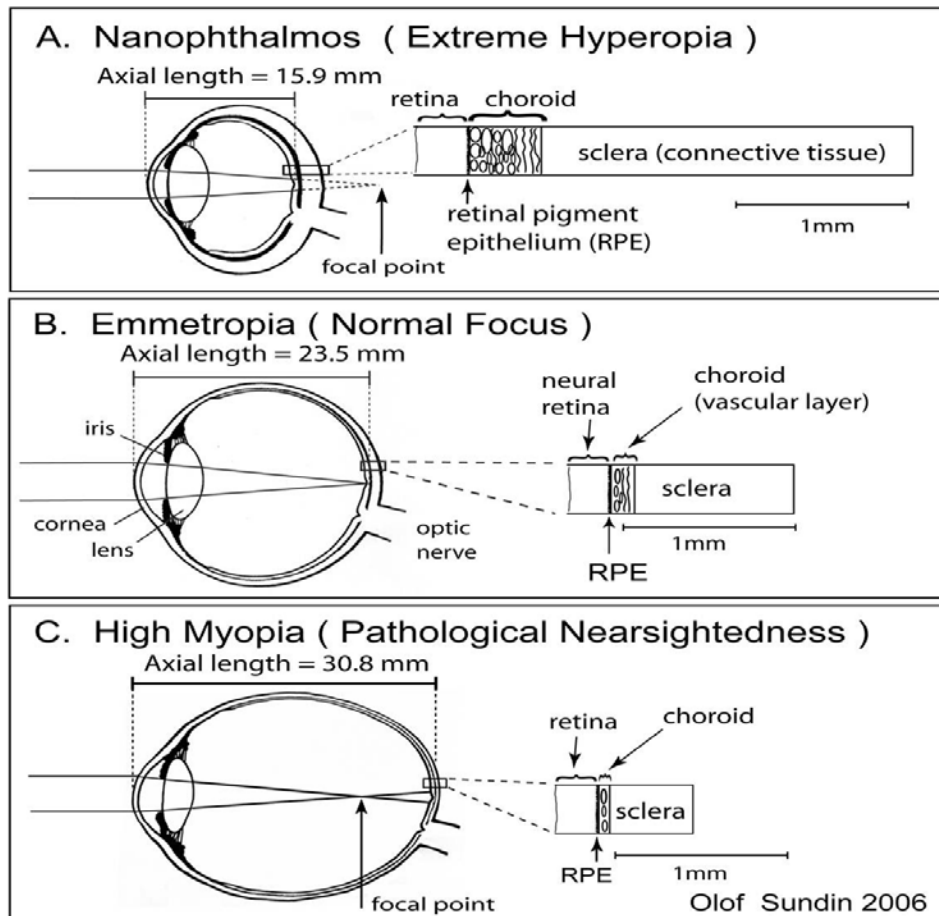


Figure 7: Tissues changes of the Posterior Wall in Refractive Error.

A) An extremely hyperopic, or far sighted, eye showing thickening of the posterior retina, choroid and scleral wall. B) An emmetropic, or normal, eye. C) A highly myopic, or near sighted, eye showing increased globe size, axial elongation and thinning of the posterior retina, choroid and scleral wall. (Sundin, Dharmaraj et al. 2008)

Particularly in highly myopic eyes, the sclera is believed to be a major factor in chorio-retinal damage responsible for the majority of resulting blindness (McBrien and

Gentle 2003). This thinning of the sclera, particularly at the posterior pole, is also characterized by extracellular matrix changes within the tissue itself. The collagen fibrils have shown distinct morphology changes, shifting toward smaller diameters of fibrils including those with altered shapes (Curtin, Iwamoto et al. 1979; McBrien and Gentle 2003). Active remodeling and passive stretch during myopic development of myopia have both been suggested to account for these changes in the posterior scleral extracellular matrix (McBrien and Gentle 2003). Studies in young tree shrews have supported remodeling by showing a net tissue loss consistent with the degree of thinning (McBrien, Lawlor et al. 2000).

While collagen degradation in the thin sclera is seen in myopic patients (McBrien and Gentle 2003), the choroid has been speculated to release growth factors upon retinal signal stimulation (Nickla and Wallman 2010). The roles of the other tissues suggest that the signal may originate in either of these tissues, and the visually striking scleral changes may be a downstream effect (McBrien and Gentle 2003).

In addition to axial growth and elongation seen in these posterior tissues, other ocular tissues have physical characteristics associated with or exploited in treatment of high myopia. Highly myopic eyes are frequently accompanied by higher corneal astigmatisms and have been shown to have distinct morphological changes of their optic nerve head (Jonas, Gusek et al. 1988; Xu, Li et al. 2007; Samarawickrama, Mitchell et al.

2011; Hwang and Kim 2012; Ohno-Matsui, Akiba et al. 2012). In current treatments of high myopia, the cornea has been manipulated by surgical flattening, thereby reducing refractive power.

1.4.2 Prevalence and Health Concerns

1.4.2.1 Prevalence Rates of Myopia

Myopia is the most common ocular disorder in the world, which raises significant public health and economic concerns (Pararajasegaram 1999). The most recent estimates show 41.6% of the United States (US) population has some form of myopia (Javitt and Chiang 1994; Kempen, Mitchell et al. 2004; Vitale, Sperduto et al. 2009). The US prevalence of myopia has increased in the last 25 years from 25%, when Western Europe had a similar prevalence of about 26%, while Australia had a slightly lower estimated prevalence of about 16% (Kempen, Mitchell et al. 2004). The highest known prevalence rates, reaching epidemic proportions, are those in urban Asian countries, such as China where 82% of adults are myopic (Saw 2003; Quek, Chua et al. 2004). Similarly, 68% of adult Indians and 65% of adult Malaysians living in Singapore are myopic (Saw 2003). Certain ethnic groups have been shown to have higher rates of myopia including Chinese, Japanese and Jews, while Hispanics, Africans and African Americans have lower rates (Saw, Katz et al. 1996; Katz, Tielsch et al. 1997). Although not statistically significant, females have been shown to have a slightly higher rate of

myopia (Kempen, Mitchell et al. 2004). High myopia in the US and Western Europe is estimated to be about 2%, while in Australia is estimated to be just under 3% (Burton 1989; Kempen, Mitchell et al. 2004; Vitale, Sperduto et al. 2009).

1.4.2.2 Impact and Health Concerns of Myopia

When accounting for products, services and time away from work, it is estimated that in 1990 the US spent nearly 14 billion dollars on the correction of refractive errors, nearly five billion of which is attributable to myopia (Javitt and Chiang 1994; Kempen, Mitchell et al. 2004; Vitale, Cotch et al. 2006; Vision 2007). Myopia has been shown to be a financial burden (Javitt and Chiang 1994), and also negatively affects self-perception, job and activity ocular health (Rose, Harper et al. 2000; Pesudovs, Garamendi et al. 2006). It has that higher degrees of myopia were more significantly associated with disadvantaged vision related quality of life (Rose, Harper et al. 2000). The reported effects on the quality of life in patients with high myopia are comparable to visually disabling diseases (Rose, Harper et al. 2000).

Myopia or more specifically high myopia is associated with higher risks of retinal detachment, glaucoma, cataracts, myopic degeneration and ocular morbidity (Burton 1989; Kempen, Mitchell et al. 2004). Despite relatively low risks for loss of vision loss associated with myopic patients, the high numbers of myopic individuals

suggests an absolute number of individuals that is higher than other at risk groups (Kempen, Mitchell et al. 2004).

1.4.3 Environmental Effects

Environmental effects on myopia are evident by the recent rapid changes in the prevalence of both myopia and high myopia in places such as East Asia (Saw 2003; Morgan and Rose 2005). Increased levels of education have been shown to be associated with myopia (Katz, Tielsch et al. 1997; Saw 2003; Morgan and Rose 2005). It is thought that higher education affects myopia by increasing the amount of time spent doing near work activity such as reading in competitive academic institutions (Katz, Tielsch et al. 1997; Saw 2003). It is unclear whether people with myopia pursue certain careers due to their myopic disadvantage or if their myopia develops due to their affinity for those careers with increased near work activities (Saw, Katz et al. 1996). Children who spend more time engaging in outdoor activities have shown a reduced prevalence of myopia (Rose, Morgan et al. 2008). Additionally, prevalence of myopia varies by residential environments; urban populations have higher proportions of myopic individuals than rural environments (Saw, Katz et al. 1996; Katz, Tielsch et al. 1997).

1.5 Genetics of Myopia

1.5.1 Heritability of Refractive Error

Twin and family studies have estimated the heritability of refractive error including myopia. Intra-pairwise correlations are higher for monozygotic twins than dizygotic twins; however, both have shown high heritability of myopia (Tsai, Lin et al. 2009). Heritability of refractive error has been estimated using twin studies to be between 0.31 and 0.91, while the heritability of AL is estimated to be 0.95 (Lyhne, Sjolie et al. 2001; Klein, Suktitipat et al. 2009; Lopes, Andrew et al. 2009; Tsai, Lin et al. 2009). SE, another common measurement in determining refractive error, has been estimated to have heritability between 0.58 and 0.83 (Klein, Suktitipat et al. 2009; Parssinen, Jauhonen et al. 2010). Other biometric parameters in the eye which may play a role in the heritability of refractive error are similarly highly heritable. Recent studies note heritability's of 0.95 for corneal curvature, and 0.78 for anterior chamber depth (Klein, Suktitipat et al. 2009). Relative lens thickness has also been estimated to have additive genetic effects contributing to a heritability of nearly 0.90 (Shen, Ding et al. 2012). Environmental effects and gene-environment interactions also play a role in myopic development; however the genetic component is significant (Lyhne, Sjolie et al. 2001; Lopes, Andrew et al. 2009; Tsai, Lin et al. 2009). Selective breeding studies in a chick

model of myopia support genes- environment interaction in myopia development (Chen, Hocking et al. 2011).

1.5.2 Candidate Myopia Loci

Advanced genomic technology has allowed scientists to use common variants, such as microsatellites and SNPs, to identify regions which may contain causal or susceptibility loci. Families with high myopia, or any other genetic phenotype, can be used to detect either linkage or association to genomic regions. Genetic linkage is defined by a particular region of the genome which has a statistically significant increase in segregation with the disease phenotype (Hodge 1993). Utilizing large numbers of families with the same disease can increase the power to identify these regions (Vieland, Wang et al. 2001). In the case of linkage with multiple families, linkage is established by genomic region rather than by the genotype of the variant. Association studies, however, require that the same variant in the same genomic location segregate significantly more frequently with the disease (Hodge 1993). Association studies are commonly conducted with large cohorts of families or with unrelated cases and controls (with care to ensure the populations share similar ethnicity and other factors which could affect background genotype frequencies) (Cordell and Clayton 2005).

Linkage and association studies have identified over 30 regions of the human genome, including nearly all chromosomes, which may contain either susceptibility or

causal variants for myopia (Figure 8; Appendix A). Appendix A contains a list of all candidate loci for myopia, their reference studies and degree of myopia. The majority of these studies were of non-syndromic familial high myopia. Some studies have considered refractive error as quantitative traits and performed quantitative trait locus (QTL) mapping, while other studies have included individuals with any level of myopia, or only common, mild to moderately, myopic individuals as a phenotype.

Since the first genome-wide association study (GWAS) reported a novel susceptibility locus for pathological (high) myopia at 11q24.1 (Nakanishi et al., 2009), six additional GWAS have been reported for myopia, refractive error, or AL (Fan et al., 2012; Hysi et al., 2010; Li et al., 2011a; Li et al., 2011b; Shi et al., 2011b; Solouki et al., 2010) (Appendix A). Each of these studies has implicated a distinct region of the genome in refractive error, though many have since been replicated. A recent large scale international GWAS meta-analysis of myopia replicated association with 15q14 for Caucasians (Solouki et al., 2010; Verhoeven et al., 2012). A Japanese cohort also replicated association with 15q14 and was suggestive for 15q25 (Hayashi et al., 2011). Two studies have replicated association to 5p15.1 in Chinese populations (Lu et al., 2011; Yu et al., 2012); one of which also replicated association with 11q24.1 (Yu et al., 2012). Association with myopia in Chinese has also been replicated by an independent study (Gao et al., 2012). Most recently, 23andme (Mountain View, CA) announced a GWAS

with the largest ever cohort from a European population (Data Unpublished). This study, of over 40,000 participants, identified 19 significant associations including replication of two previously identified regions: 15q14 and 15q25. The replication of many of these regions suggests that large scale GWAS studies have great power to detect true associations with myopia and should be further utilized.

1.5.2.1 Candidate Loci for Quantitative Myopia

The majority of identified loci (Red Stars in Figure 8) do not overlap with qualitative myopia or high myopia loci. The two exceptions are on the short arm of chromosome 1, the myopia locus 14 (*MYP14*; MIM 610320), and the short arm of chromosome 7, the myopia locus 17 (*MYP17*; MIM 608367) (Figure 8). Three years after the first establishment of the *MYP14* locus for myopia using QTL mapping of a high myopia cohort of Ashkenazi Jewish families (Wojciechowski, Moy et al. 2006), multipoint, qualitative, high myopia linkage analyses of a Caucasian and Asian cohort nominally replicated the locus (Li, Guggenheim et al. 2009). Six years after the establishment of the myopia locus four (*MYP4*; MIM 608367) on the short arm of chromosome 7 for non-syndromic myopia (Naiglin, Gazagne et al. 2002), a larger study including French families and the same original two Algerian families identified a novel, adjacent high myopia locus 17 (*MYP17*; MIM 608367) (Paget, Julia et al. 2008). That

same year, quantitative linkage was established for the same region in a cohort of African American (AA) individuals (Ciner, Wojciechowski et al. 2008).

1.5.2.2 Candidate Loci for Any Myopia

In 2004, genome-wide linkage analyses of twins from the United Kingdom (UK) Twin Registry identified four genomic regions for any level of myopia ($< 0D$) (Figure 8) (Hammond, Andrew et al. 2004). The strongest linkage peak Hammond et al. identified was on the short arm of chromosome 11, the myopia locus seven (*MYP7*; MIM 609256). The other three loci identified were on the long arm of chromosome three (*MYP8*; MIM 609257), the long arm of chromosome four (*MYP9*; MIM 609258), and the short arm of chromosome eight (*MYP10*; MIM 609259).

1.5.2.3 Candidate Loci for Mild to Moderate Myopia

To date, nearly ten genomic regions have been identified for mild to moderate ($< 0D$ to $-6D$). Several of these studies have overlapped with studies of other myopic criteria. The myopia locus ten (*MYP10*; MIM 609259) identified for any myopia ($< 0D$) (Hammond, Andrew et al. 2004) on the short arm of chromosome eight, was suggestively replicated under a recessive model in a population of mild to moderately myopic Old Order Amish individuals (Stambolian, Ciner et al. 2005). Linkage using three Australian families with moderate levels of myopia replicated the high myopia locus 12, (*MYP12*; MIM 609995) (Paluru, Nallasamy et al. 2005; Chen, Stankovich et al.

2007). However, later refinement of the region using the same families and an independent case-control cohort identified an adjacent, but not overlapping genomic location (Schache, Chen et al. 2009).

1.5.2.4 Candidate Loci for Pathological High Myopia

The majority of the candidate genomic loci for myopia have been identified using high myopia (< -5 D) cohorts. While over 20 regions have been identified, fewer than half of them have been replicated by independent cohorts- many with only suggestive significance. Some of the candidate loci were identified with nominal significance, while others were identified using genetically inbred populations, such as a Hutterite population from South Dakota used to identify the myopia locus 15 (*MYP15*; MIM 612717) (Nallasamy, Paluru et al. 2007). Both of these factors may contribute to the lack of candidate loci replication. Myopia locus three (*MYP3*; MIM 603221) and myopia locus one (*MYP1*; MIM 310460) are two of the most highly replicated high myopia loci (Schwartz, Haim et al. 1990; Young, Ronan et al. 1998; Farbrother, Kirov et al. 2004; Young, Deeb et al. 2004; Nurnberg, Jacobi et al. 2008; Li, Guggenheim et al. 2009). The *MYP1* locus was the first identified genomic locus for familial high myopia of a large Danish family with Bornholm Eye Disease (BED) (Schwartz, Haim et al. 1990). In addition to replication with a Caucasian and Asian non-syndromic high myopia cohort (Li, Guggenheim et al. 2009) and a replicate BED family (Young, Deeb et al. 2004),

several adjacent but non-overlapping loci have also been identified. Two of these adjacent loci have been identified with Chinese high myopia families (Zhang, Guo et al. 2006; Zhang, Li et al. 2007), while the other was identified using an Old Order Amish population with moderate myopia (Stambolian, Ciner et al. 2005). One of the more recent whole-genome linkage analyses, with five international sites contributing families, replicated at least six myopia loci (Li, Guggenheim et al. 2009) – *MYP1* (Schwartz, Haim et al. 1990), *MYP3* (Young, Ronan et al. 1998), *MYP6* (MIM 608908) (Stambolian, Ciner et al. 2005), *MYP11* (MIM 609994) (Zhang, Guo et al. 2005), *MYP12* (Paluru, Nallasamy et al. 2005), and *MYP14* (Wojciechowski, Moy et al. 2006).

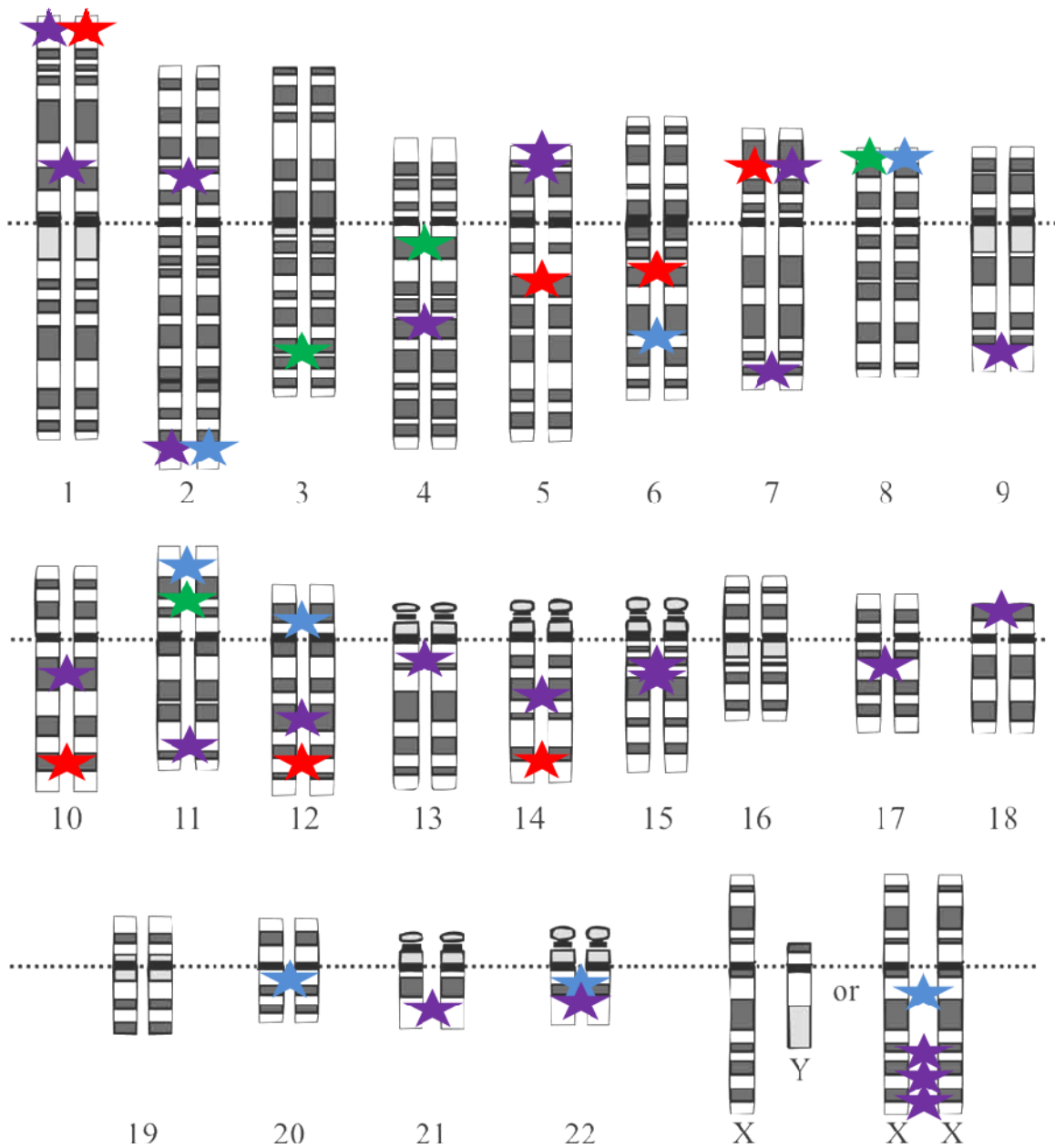


Figure 8: Candidate Myopia Loci Identified by Whole Genome Analyses.

Stars indicate loci identified for myopia across the whole genome. Red, Quantitative; Green, Any Myopia; Blue, Mild to Moderate Myopia (0 D to -6 D); Purple, High Myopia (<-5 D). (Freely licensed image modified by Felicia Hawthorne, 2012)

1.5.3 Genes Implicated in Myopic Development

To date, over 40 genes have been identified as possibly contributing to myopia and its associated clinical phenotypes. The majority of these genes have been identified for high myopia, which carries the biggest risk for other ocular morbidities. However, few of these identified genes have been found within previously identified non-syndromic myopia linkage peaks. Even fewer of these genes have been found with variants believed to be causal for myopic development.

1.5.3.1 Non-Syndromic Myopia

For non-syndromic myopia, seven genes have been identified as associated or linked (Table 1). The majority of these genes have been identified using qualitative measures of affection, but two genes, matrix metalloproteinase 1 and 2 (*MMP1* [MIM 120353]; *MMP2* [MIM 120360]) have both been identified using the average SPH and SE as quantitative traits. The genes previously identified as associated with myopia are variable in their functions and may reflect a diverse set of mechanisms for myopic development.

The earliest identified gene, *PAX6* (paired box 6; MIM 607108), was in a region showing linkage to all myopia (< 0 D) (Hammond, Andrew et al. 2004). The involvement of *PAX6* in myopic development has also been supported by three independent animal model studies. In infant rhesus monkeys, hyperopic defocus

caused significantly higher expression of *PAX6* in the retina (Zhong, Ge et al. 2004). In normal chick retina, *PAX6* expression decreases after hatching and then steadily increases into adulthood; however, form deprivation myopia (FDM) prevented the level of expression from attaining normal control adult levels (Bhat, Rayner et al. 2004). A later study of *PAX6* in the chick retina also found lower expression in the time period seven to ten days after of FDM, but diffuser removal allowed recovery (Ashby, Megaw et al. 2009). Additionally, *miR328* (microRNA 328; MIM 613701) has been shown to suppress expression of *PAX6* and a *miR328* binding site within *PAX6* has been proposed as a susceptibility loci for high myopia (Chen, Hsi et al. 2012). The other genes identified for non-syndromic myopia have not yet been validated using animal models or other functional assays. However, in addition to *PAX6*, two of these genes have also shown association with high myopia – *COL2A1* (collagen, type II, alpha 1; MIM 120140) and *HGF* (hepatocyte growth factor; MIM 142409) (Table 1).

1.5.3.2 Non-Syndromic High Myopia

For non-syndromic, high myopia (<5 D), 34 genes have been implicated (Table 1). However, many of these genes have not been replicated or supported by follow-up functional or expression studies. Few of these genes lie within known myopia linkage peaks, and some have not been shown to account for myopic development in individuals showing linkage to the regions. The main exception to this rule thus far is

the triple replicated high myopia (< -6 D) gene (Li, Goh et al. 2011; Lu, Jiang et al. 2011; Yu, Zhou et al. 2012) catenin (cadherin-associated protein), delta 2 (*CTNND2*; MIM 604275), which is located within the *MYP16* locus on the short arm of chromosome 5 (5p15.33-p15.2).

Three genes have also shown association to general myopia (*COL2A1*, *HGF*, and *PAX6*). Like *PAX6*, a number of these genes have been supported by tissue expression data – primarily in animal models of myopia. Deletion of the adenosine A2a receptor (*ADORA2A*; MIM 102776), which has significant differences in genotype frequencies with high myopia (< -8 D) (Chen, Xue et al. 2011), has been shown to cause the development of relative myopia in mice (Zhou, Huang et al. 2010). Collagen, type I, alpha 1 (*COL1A1*; MIM 120150) has reduced expression in the sclera of FDM mice (Zhou, Ji et al. 2012), and has been associated with high myopia (< -9.25 D) in a Japanese population (Inamori, Ota et al. 2007). Double knockout *FMOD* (fibromodulin; MIM 600245) and *LUM* (lumican; MIM 600616) mice have presented with distinct features of myopia including increased AL, frequent retinal detachments, and thinner sclera (Chakravarti, Paul et al. 2003). Unique sequence variants within *FMOD* and *LUM* have been discovered in highly myopic (< -6 D) UK subjects (Majava, Bishop et al. 2007) and in regulatory domains of *LUM* in highly myopic (< -10 D) Taiwanese (Lin, Kung et al. 2010). *LUM* has also been associated with associated with high myopia (< -6 D) in Han

Chinese (Lin, Wan et al. 2010). Haplotypes within another gene, *IGF1* (insulin-like growth factor 1; MIM 147440) have shown association to high myopia (< -8 D) and also has been shown to be involved in myopic development in an animal model (Mak, Yap et al. 2012; Ritchey, Zelinka et al. 2012). Postnatal chicks injected with *IGF1* and *FGF2* (fibroblast growth factor 2; MIM 134920) developed myopia after two weeks (Ritchey, Zelinka et al. 2012). Lastly, *TGFB1* (transforming growth factor, beta 1; MIM 190180) and *TGFB2* (transforming growth factor, beta 2; MIM 190220) both have been shown to be major contributors to extracellular matrix remodeling in tree shrew sclera, but not the retina or choroid, with down-regulated expression in an occlusion model resulting in a 15% decrease in collagen synthesis (Jobling, Nguyen et al. 2004; Jobling, Gentle et al. 2009; Jobling, Wan et al. 2009; Gao, Frost et al. 2011). In a mouse model, increased expression of *TGFB1* was suggested to account for increased scleral thickness by preventing degradation of collagen (Liu, Xiang et al. 2007). In the outer RPE layer of FDM chicks, *TGFB2* had decreased expression (Xie and Chen 2008). Three independent genotyping studies have implicated *TGFB1* in high myopia (< -5 D) (Lin, Wan et al. 2006; Zha, Leung et al. 2009; Khor, Fan et al. 2010). Genotype frequencies have been associated in high myopia (< -6 D) for *TGFB2* (Lin, Wan et al. 2009).

Few of the genes implicated in myopic development have been proposed to be causal for high myopia. Leprecan-like 1 (*LEPREL1*; MIM 610341), however, in Bedouin

Israeli consanguineous individuals with autosomal-recessive high myopia (< -5 D) has shown a mutation on exon 10 which has been shown to inactivate the protein in an insect cell line (Mordechai, Gradstein et al. 2011). Most recently, new whole exome sequencing technology has identified novel mutations in zinc finger protein 644 (*ZNF644*; MIM 614159) segregating in a Han Chinese family with autosomal dominant high myopia (< -6.27 D) (Shi, Li et al. 2011). Screening of the same gene in a Caucasian high myopia (< -5 D) dataset revealed additional novel mutations (Tran-Viet, St Germain et al. 2012).

1.5.3.3 Myopic Choroidal Neovascularization

Myopic choroidal neovascularization is a complication of high myopia (Silva 2012). Complement factor I (*CFI*; MIM 217030) has been shown to be associated with highly myopic (<-6 D) choroidal neovascularization. Gene polymorphisms in vascular endothelial growth factor A (*VEGFA*; MIM 192240) on the other hand has been shown to be associated with the size, rather than occurrence, of choroidal neovascularization in highly myopic eyes, suggesting a possible role in their growth rather than initiation.

Table 1: Genes Previously Implicated in or Proposed for the Progression of Myopic Development.

Genes implicated in the development of myopia, high myopia and myopic choroidal neovascularization. MIM, Mendelian Inheritance in Man; p, short arm of chromosome; q, long arm of chromosome; D, diopter; A, association; L, linkage; GWAS, genome-wide association study; LR, logistic regression; MA, meta-analysis; USV, unique sequence variant; CNV, copy number variant association; GF, genotype frequency; VF, variant frequency; HA, haplotype association; M, loss of function mutation; RFLP, restriction fragment length polymorphism association; QA, quantitative association.

Gene Symbol	Gene Name	MIM	Cytogenic Location	Reference Study	Myopia Severity	Study Type
Myopia						
<i>COL2A1</i>	collagen, type II, alpha 1	120140	12q13.11	(Metlapally, Li et al. 2009)	< -0.75	A
<i>HGF</i>	hepatocyte growth factor	142409	7q21.11	(Yanovitch, Li et al. 2009)	< -0.5	A
<i>MMP1</i>	matrix metalloproteinase 1	120353	11q22.2	(Veerappan, Pertile et al. 2010)	-5.99 to -2 D	A
<i>MMP2</i>	matrix metalloproteinase 2	120360	16q12.2	(Wojciechowski, Bailey-Wilson et al. 2010)	Mean -1.61 D	QA
<i>PAX6</i>	paired box 6	607108	11p13	(Hammond, Andrew et al. 2004)	-12.12 D to +7.25 D	L
<i>RASGRF1</i>	RAS protein-specific guanine nucleotide-releasing factor 1	606600	15q25	(Hysi, Young et al. 2010)	< -1 D	GWAS
<i>SERPINI2</i>	serpin peptidase inhibitor, clade I, member 2	605587	3q26.1	(Hysi, Simpson et al. 2012)	< -1 D	A

<i>VDR</i>	vitamin D receptor	601769	12q13.11	(Mutti, Cooper et al. 2011)	< -0.75	A
High Myopia						
<i>ADORA2A</i>	adenosine A2a receptor	102776	22q11.23	(Chen, Xue et al. 2011)	< -8 D	GF
<i>BMP2K</i>	BMP2 inducible kinase		4q21.21	(Liu, Lin et al. 2009)	< -6 D	A
<i>C1QTNF9B</i>	C1q and tumor necrosis factor related protein 9B	614148	13q12.12	(Shi, Qu et al. 2011)	< -6 D	GWAS
<i>C1QTNF9B-AS1</i>	C1QTNF9B antisense RNA 1 (non-protein coding)		13q12.12	(Shi, Qu et al. 2011)	< -6 D	GWAS
<i>CHRM1</i>	cholinergic receptor, muscarinic 1	118510	11q12.3	(Lin, Wan et al. 2009)	< -6.5 D	A
<i>CHRM2</i>	cholinergic receptor, muscarinic 2	118493	7q33	(Lin, Wan et al. 2012)	< -10	CNV
<i>CHRM3</i>	cholinergic receptor, muscarinic 3	118494	1q43	(Lin, Wan et al. 2012)	< -6 D; < -10 D; -6 to -10 D	CNV
<i>CHRM4</i>	cholinergic receptor, muscarinic 4	118495	11p11.2	(Lin, Wan et al. 2012)	< -6 D	CNV
<i>COL1A1</i>	collagen, type I, alpha 1	120150	17q21.33	(Inamori, Ota et al. 2007)	< -9.25 D	A
<i>COL2A1</i>	collagen, type II, alpha 1	120140	12q13.11	(Metlapally, Li et al. 2009)	< -5 D	A
<i>CRYBA4</i>	crystallin, beta A4	123631	22q12.1	(Ho, Yap et al. 2012)	< -8 D	A
<i>CTNND2</i>	catenin (cadherin-associated protein), delta 2	604275	5p15.2	(Lu, Jiang et al. 2011)	< -6 D	A
				(Li, Goh et al. 2011)	< -6 D	MA
				(Yu, Zhou et al. 2012)	< -6 D	GWAS
<i>FMOD</i>	fibromodulin	600245	1q32.1	(Majava, Bishop et al. 2007)	< -6 D	USV
<i>GRM6</i>	glutamate receptor, metabotropic 6	604096	5q35.3	(Xu, Li et al. 2009)	< -6 D	USV
<i>HGF</i>	hepatocyte growth factor	142409	7q21.11	(Han, Yap et al. 2006)	< -10 D	QA
				(Yanovitch, Li et al. 2009)	< -5 D	A

<i>HLA-DQB1</i>	major histocompatibility complex, class II, DQ beta 1	604305	6p21.32	(Li, Ji et al. 2000) (Li, Ji et al. 2001)	unknown unknown	RFLP RFLP
<i>IGF1</i>	insulin-like growth factor 1	147440	12q23.2	(Mak, Yap et al. 2012)	< -8 D	HA
<i>LAMA1</i>	laminin, alpha 1	150320	18p11.31- p11.23	(Zhao, Zhang et al. 2011)	< -6 D	A
<i>LEPREL1</i>	leprecan-like 1	610341	3q28	(Mordechai, Gradstein et al. 2011)	< -5 D	M
<i>LUM</i>	lumican	600616	12q21.33	(Majava, Bishop et al. 2007) (Lin, Kung et al. 2010) (Lin, Wan et al. 2010)	< -6 D < -10 D < -6.5 D	USV A A
<i>LYPLAL1</i>	lysophospholipase-like 1		1q41	(Fan, Barathi et al. 2012)	variable	MA
<i>MIPEP</i>	mitochondrial intermediate peptidase	602241	13q12.12	(Shi, Qu et al. 2011)	< -6 D	GWAS
<i>MYOC</i>	myocilin	601652	1q24.3	(Tang, Yip et al. 2007) (Vatavuk, Skunca Herman et al. 2009)	< -6 D < -6 D	L & A A
<i>NYX</i>	nyctalopin	300278	Xp11.4	(Zhang, Xiao et al. 2007)	< -6 D	USV
<i>OPTC</i>	opticin	605127	1q32.1	(Majava, Bishop et al. 2007)	< -6 D	VF
<i>PAX6</i>	paired box 6	607108	11p13	(Hewitt, Kearns et al. 2007) (Tsai, Chiang et al. 2008) (Han, Leung et al. 2009) (Ng, Lam et al. 2009) (Liang, Hsi et al. 2011)	< -9 D < -10 D < -6 D < -6 D < -11 D	A A A A A

<i>PRELP</i>	proline/arginine-rich end leucine-rich repeat protein	601914	1q32.1	(Jiang, Yap et al. 2011) (Majava, Bishop et al. 2007)	< -8 D < -6 D	A USV
<i>SLC30A10</i>	solute carrier family 30, member 10	611146	1q41	(Fan, Barathi et al. 2012)	variable	MA
<i>TGFB1</i>	transforming growth factor, beta 1	190180	19q13.2	(Lin, Wan et al. 2006) (Zha, Leung et al. 2009) (Khor, Fan et al. 2010)	< -6 D < -8 D < -5 D	GF A A
<i>TGFB2</i>	transforming growth factor, beta 2	190220	1q41	(Lin, Wan et al. 2009)	< -6.5 D	GF
<i>TGIF</i>	transforming growth factor-beta-induced factor	602630	18p11.31	(Lam, Lee et al. 2003)	< -6 D	LR
<i>UMODL1</i>	uromodulin-like 1	613859	21q22.3	(Nishizaki, Ota et al. 2009)	< -9.25 D	A
<i>ZC3H11B</i>	zinc finger CCCH-type containing 11B pseudogene		1q41	(Fan, Barathi et al. 2012)	variable	MA
<i>ZNF644</i>	zinc finger protein 644	614159	1p22.2	(Shi, Li et al. 2011) (Tran-Viet, St Germain et al. 2012)	-6.27 to -20.00 < -6 D	USV USV
Myopic Choroidal Neovascularization						
CFI	complement factor I	217030	4q25	(Leveziel, Yu et al. 2012)	< -6 D	A
VEGFA	vascular endothelial growth factor A	192240	6p21.1	(Akagi-Kurashige, Kumagai et al. 2012)	unknown	A

1.5.3.4 Syndromes with a Myopic Component

Over 150 syndromes caused by single gene mutations contain familial high myopia as a component (Morgan 2003; Hornbeak and Young 2009). Genes involved in sclera extracellular matrix are the most common in syndromic forms of high myopia (Morgan, Ohno-Matsui et al. 2012). Some of the genes implicated in non-syndromic myopia have also been implicated in syndromic myopia such as *COL2A1* for Stickler syndrome (Francomano, Liberfarb et al. 1987).

1.6 High Myopia Locus *MYP3*

1.6.1 *MYP3* Genetic Studies

Over ten years ago, Professor Terri Young, MD first established the myopia three, *MYP3*, locus for familial high-grade non-syndromic myopia (Figure 9). A linkage study using a single large multigenerational family of German/Italian descent mapped to chromosome 12q21-23, *MYP3*, using microsatellite markers with a maximum LOD score of 3.85 (Young, Ronan et al. 1998). The *MYP3* locus was replicated by Farbrother et al. in the UK using 51 myopia families again using microsatellite markers with a maximum logarithm of odds (LOD) score of 2.54, however, the p-values only just reached significance (Farbrother, Kirov et al. 2004). Next, Nurenberg et al. again replicated the *MYP3* locus using a single family of German descent with dominant Mendelian high myopia using 10K whole genome SNP chips with a maximum LOD

score of 3.9 in *MYP3* (Nurnberg, Jacobi et al. 2008). Most recently, our lab performed a whole genome SNP linkage scan using 254 high myopia families with a peak LOD score of 3.48 for *MYP3* (Li, Guggenheim et al. 2009). These same data were used in identifying suggestive quantitative trait linkage in the *MYP3* locus (Abbott, Li et al. 2012). The regions on chromosome 12 identified by the four independent linkage studies are shown in Figure 9. The two linkage studies performed in our lab (Young, Ronan et al. 1998; Li, Goh et al. 2011) have significant overlap, however, we were unable to reduce the region using conserved haplotypes. The other two linkage studies do not overlap with each other, however, they overlap on opposing ends with our linkage region. The overlap on opposing ends may be indicative of the region containing multiple variants or genes influencing myopia or related ocular traits, which could explain the large size of the initial linkage peak.

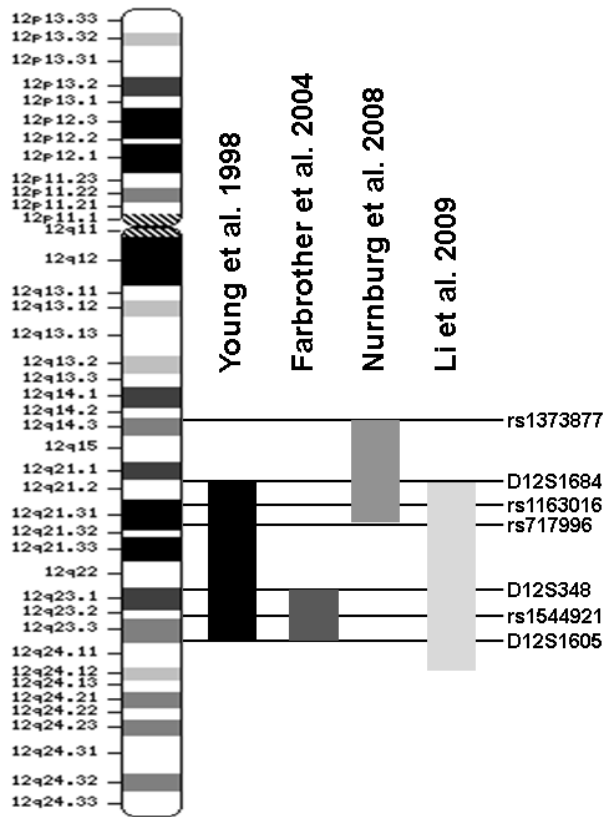


Figure 9: *MYP3* Locus Linkage Studies.

This diagram shows the four independent linkage studies which replicated the region on chromosome 12 and their regions of overlap. (Young, Ronan et al. 1998; Farbrother, Kirov et al. 2004; Nurnberg, Jacobi et al. 2008; Li, Guggenheim et al. 2009) (Image adapted by Felicia Hawthorne from Nurnberg, Jacobi et al. 2008)

2. Ocular Tissue Expression

The National Eye Institute Eye Bank contains a database of expression information, EyeSAGE, for adult human trabecular meshwork, as well as posterior and peripheral retina and RPE (Bowes Rickman, Ebright et al. 2006; Liu, Munro et al. 2011). However, no database exists for these same human tissues for fetal samples, nor for other ocular tissues. Ocular tissues (retina, RPE, choroid, sclera, optic nerve, and cornea) were collected from human adult and fetal normal donors to evaluate expression patterns in the context of growth and development.

The posterior pole of the human eye contains the retinal macular region adjacent to the optic nerve, which has an increased density of photoreceptors and confers highest visual acuity. The physical changes such as retinal thinning, breaks in Bruch's membrane, choroidal neovascularization, choroidal show, and thinned sclera, seen in highly myopic individuals are primarily localized to the posterior pole. In addition to the major changes seen in these posterior tissues, less prominent changes in the shape and size of the cornea and optic nerve can be seen in myopic individuals.

While these tissues have been studied in animal models, they have not been studied in humans as diseased tissue is difficult to collect. Since diseased tissue was not accessible, a model for the rapid growth of myopia would be necessary to study human tissue. Herein we propose the use of rapidly growing fetal tissue as a surrogate model

to study the exaggerated growth seen in myopia. While normal fetal growth may not represent only those mechanisms of growth seen in myopia, these normal growth mechanisms may include mechanisms involved during the exaggerated growth in myopic development. As a physiological surrogate of rapid ocular growth during myopic development, gene expression of human fetal ocular tissue types of central retina/ retinal pigment epithelium, choroid, sclera, optic nerve and cornea were compared to their adult counterparts from normal donor eyes. Functional and pathway roles in these tissues for genes previously identified as associated with myopia were assessed in normal human growth to gain an understanding of how their disruptions may lead to myopic development. To our knowledge this is the first whole genome expression analysis comparing human adult versus fetal ocular tissues. This data can provide an understanding of normal changes these tissues undergo during growth in humans. It also may contain clues to understand how diseases may result from disruptions to these normal processes in the context of myopia associated genes.

The same tissues of the posterior pole (retina, RPE, choroid, and sclera) extend anteriorly covering much of the eye. To further understand the spatial differences in the roles these tissues play in ocular disease development whole genome expression analysis was performed. To assess for differential expression specific to this posterior

pole, adult central retina, choroid and sclera were collected and compared to their non-macular, peripheral counterparts.

Functional and pathway roles in these tissues for genes previously identified as associated with myopia were assessed in normal human growth to gain an understanding of how their disruptions may lead to myopic development. To our knowledge this is the first whole genome expression analysis comparing human adult versus fetal ocular tissues. This data can provide an understanding of normal changes these tissues undergo during and after growth in humans. It also may contain clues to understand how diseases may result from disruptions to these normal processes either in understanding normal roles for myopia associated genes or identifying possible novel candidates.

2.1 Ocular Sample Selection

To compare gene expression between rapidly growing to fully grown ocular tissue types, normal samples from two age groups were used: fetal eyes and adult eyes. The fetal donor eyes were obtained from Advanced Biosciences Resources (Alameda, CA, USA), while the adult eyes were obtained from the North Carolina Eye Bank (Winston-Salem, North Carolina, USA). Fetal gestational age was determined by most recent menstruation in addition to fetal foot measurements. The group of fetal eyes consisted of late prenatal fetal eyes of approximately 24-weeks' gestation. Twenty-four-

week old eyes were the oldest group of prenatal eyes readily available. All layers and cell types are differentiated in the posterior, macular retina by 11 weeks' gestation (Linberg and Fisher 1990; Hendrickson 1992). Nine fetal donor eyes (4 male and 5 female samples), and six fully grown adult donor eyes (3 of each gender) were used for microarray analyses. Space and cost limitations required that optic nerve and cornea sample sizes were reduced to six adult and six fetal samples each. All adult donors were Caucasian and donors with known ocular disorders were excluded (Table 2). Ethnic and health information was not available for fetal donors.

Table 2: Donor Information for Adult Ocular Whole Globes Used in Tissue Expression Analyses.

Preservation time interval (PTI) is listed in hours. Age is listed in years.

Individual	Race	Sex	Age	PTI	Cause of Death
2809	Caucasian	Female	76	4:00	Acute Myeloid Leukemia
2835	Caucasian	Female	55	4:55	Dementia
2217	Caucasian	Female	77	6:24	Chronic Obstructive Pulmonary Disease
2828	Caucasian	Male	80	5:20	Pneumonia
2834	Caucasian	Male	56	5:22	Abdominal Aortic Aneurysm Rupture
2836	Caucasian	Male	67	5:10	Heart Disease

2.1.1 Tissues of Interest

Retina/RPE, choroid, and sclera were isolated from the posterior macular region (adjacent to the optic nerve) of adult and fetal whole globes (Figure 10). Comparison of these posterior tissues over different developmental stages was used to identify genes involved in rapid growth states such as in myopic development. Additionally, the optic nerve and central cornea were isolated from adult and fetal globes to identify genes involved in growth in tissues which display myopic-associated clinical phenotypes. A second region of retina, choroid, and sclera were collected in the same adult globes peripheral and opposite the optic nerve. These tissues were used to identify expression differences between the tissues of the axial pole, which is elongated in myopic individuals, and the same tissues extending peripherally.

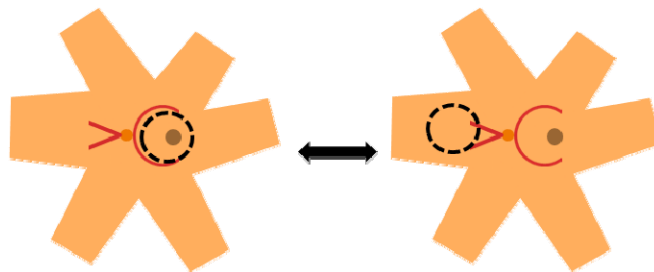


Figure 10: Posterior and Peripheral Ocular Tissue Isolation.

Flat mount diagram of posterior cup of ocular globe. Left) Posterior wall tissues of interest centered on the retinal fovea (brown dot). Right) Peripheral wall tissues of interest opposite the optic nerve (orange centered dot) and offset toward the equator of the globe. (© Felicia Hawthorne, 2012)

2.2 Methods

2.2.1 Ocular Dissection

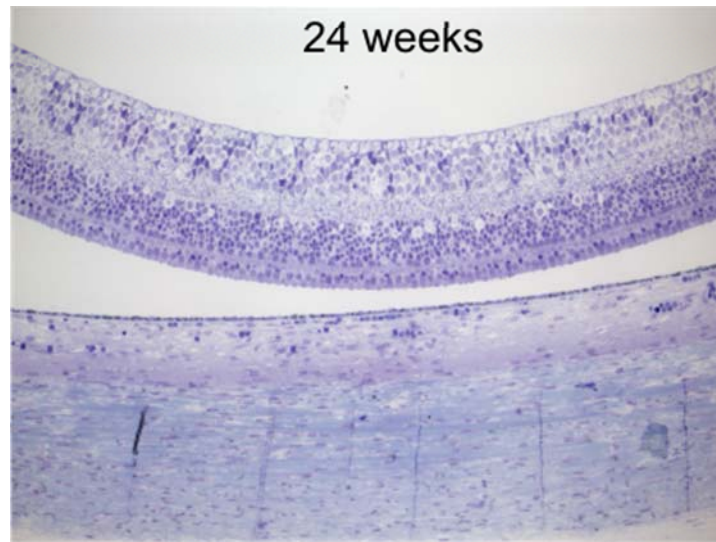
2.2.1.1 Tissue Preservation

All adult whole globes collected for expression analyses were immersed in RNAlater® (Qiagen, Hilden, Germany) within 6.5 hours of collection (Table 2), and shipped overnight on ice. Fetal whole globes collected for expression analyses were collected and preserved in RNAlater® within minutes of collection and shipped overnight on ice. Prior to immersion in RNAlater®, a 2 mm incision was cut equatorially into all whole globes to allow permeation of the solution to the inner tissues. All whole globes were dissected on the same day as arrival.

An additional fetal whole globe was collected for histological examination of the posterior ocular tissues. The whole globe was collected and fixed in 4% paraformaldehyde for 24 hours at 4°C. Eyes were then shipped overnight on ice to the lab for immunohistological staining. Immunohistological staining was performed by Jindong Ding, Ph.D. Figure 11 shows the histology of fetal ocular tissue (24-weeks' gestation) obtained from the same source and with the same selection criteria as those used in this study for expression analyses. Preservation artifacts are present in the immunohistological staining of the 24-week fetal posterior ocular tissues shown in Figure 11. As seen at both magnifications, the retina is separated from the RPE, choroid and sclera. The osmolarity of 4% buffered formaldehyde has been demonstrated to be

high enough to cause volume contraction of whole eyes, resulting in complete or partial separation of the retina (Margo and Lee 1995).

A.



B.

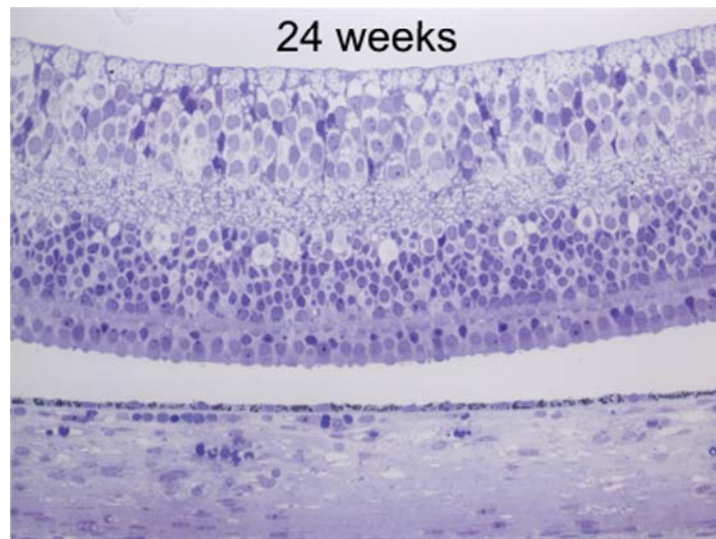


Figure 11: Fetal Ocular Histology.

A). Macular section of 24-week fetal eye showing from top to bottom the differentiated retina, RPE, choroid and sclera. **B).** Increased magnification of retina in 24-week fetal eye showing developing layers and cell types. (© Jindong Ding, Ph.D., 2012)

2.2.1.2 Tissue Isolation

The retina, RPE, choroid and scleral tissues were isolated at the posterior pole using a circular, double embedded technique using round 7 mm and 5 mm biopsy punches. To reduce contamination of retina to the other tissues samples, the second biopsy punch of 5 mm was used in the center of the 7 mm punch after retinal removal. The adult RPE was collected in RNAlater® by gentle brushing from the choroid, pipetting the solution, and centrifuging at 4°C to remove the RNAlater®. Fetal eye samples proved difficult to separate the RPE from the retina. Consequently, the retina and RPE were collected in total. The retina, RPE, choroid and scleral tissues were isolated from two distinct regions in each sample for each age group. First, the central region (macular region of the eye adjacent to the optic nerve) of the posterior wall, then approximately 3 mm peripheral to the edge of the central region was also collected.

Additionally, optic nerve and corneal samples were isolated from each eye in each age group. Central corneal samples were isolated using a clean 5 mm biopsy punch. The whole optic nerve was collected using clean dissection scissors. The fibrous sclera, optic nerve and cornea samples were cut into smaller portions (about 1 mm²) using a scalpel to aid in subsequent homogenization. After dissection all tissues were immediately frozen in liquid nitrogen for storage at -80°C until RNA extraction.

2.2.2 RNA Extraction and Whole Genome Expression Processing

RNA was extracted from each tissue sample using the mirVana™ total RNA extraction (Ambion, Austin, Texas, USA) kit following the manufacturer's protocol. The tissue samples were homogenized at 4°C in Ambion lysis buffer using a Bead Ruptor Tissue Homogenizer (Omni, Kennesaw, Georgia, USA) with 2.38 mm metal bead tubes using the following machine settings: 4 cycles X 30 seconds at speed 4.0 with 30 seconds break between cycles. Quality control for each sample included measuring RNA concentration and 260/280 nm ratios using a Nanodrop® (Invitrogen, Carlsbad, California, USA).

The ocular tissue RNA samples were labeled and amplified using the Illumina® Total Prep kit (Ambion, Austin, Texas, USA). RNA samples were hybridized to Illumina® HumanHT-12 v4 Expression BeadChips (San Diego, California, USA), which target over 25,000 annotated genes (over 48,000 probes). All protocols were performed following the manufacturer's recommendations. Twelve samples were per chip were processed and chips were run in two batches, each containing samples of at least two tissue types. The first batch (N = 75) included all retina/RPE, choroid and sclera samples. The second batch included all cornea and optic nerve samples (N=24).

2.2.3 Whole Genome Expression Analyses

The microarray data preprocessing procedures were conducted separately for each batch. After the data were generated for each batch, background noise was subtracted from the intensity values using the Illumina® GenomeStudio program. The data were exported from GenomeStudio and \log_2 transformed. Sample outliers were determined by principle component analyses using the Hotelling's T2 test (Hotelling 1931) (at 95% confidence interval) and removed from further analyses. The data intensity was normalized by Quantile normalization followed by Multichip Averaging (Irizarry, Hobbs et al. 2003) to reduce chip effects. The exact Wilcoxon rank sum test (Wilcoxon 1945) was used to identify differentially expressed genes because of the relatively small sample size. Fetal ocular tissues were compared to their adult counterparts, and assessed for relative fold changes per probe. Adult retina and RPE samples were averaged for comparison to fetal retina/RPE. The Benjamini and Hochberg False Discovery Rate (Benjamini 1995) (FDR) procedure was applied, and FDR was set at $q=0.05$ to determine statistical significance for all comparisons.

2.2.4 Pathway Analyses

In total, five adult versus fetal and three central versus peripheral expression comparisons were made, representing each tissue type. Lists of differentially expressed probes were generated for each comparison for functional and pathway assessment

using Ingenuity® Pathway Analysis ([IPA], Ingenuity® Systems, www.ingenuity.com). The retina/RPE, choroid, sclera and cornea probes were FDR controlled at $q=0.05$. The adult versus fetal optic nerve and all central versus peripheral samples did not produce any probes meeting the FDR significant cut-offs. Consequently, the adult versus fetal optic nerve probes were filtered by a raw p-value for each probe of < 0.05 . For central versus peripheral tissues a raw p-value cut-off of $<.10$ was used. To focus on biologically important changes in each tissue, those probes with fold changes < 1.5 were also removed. For each comparison, Table 3 contains the number of probes and representative unique genes. Each comparison was assessed using IPA for enriched functional groups of genes as well as for significant canonical pathways.

2.2.4.1 Functional Annotation Analyses

To identify overrepresentation of genes within known functional pathways involved in rapid or depressed growth we performed IPA functional annotation analyses. Probes including their associated gene, p-value, and fold change were analyzed separately for each comparison. The significance of each functional group is given as a p-value (Table 4). Additionally, IPA calculated a z-score, or standard score, for each functional classification. A z-score of < -2.00 indicates that that function has a significantly decreased predicted activation. Conversely, a z-score of > 2.0 indicates a predicted increased activation of that functional group. Functional assignments with a

significantly predicted activation are shown in Table 5. For presentation purposes, functional assignments containing redundant genes and functions were consolidated.

2.2.4.2 Canonical Pathway Analysis

To identify specific pathways involved in rapid growth or lack of growth in relevant ocular tissues we performed canonical pathway analyses using IPA (Table 6). Probes including their associated gene, p-value, and fold change were analyzed simultaneously for each comparison to identify overrepresentation of genes within known canonical pathways. The significance of each pathway was given a p-value. Additionally, IPA calculates a ratio of genes differentially expressed within each canonical pathway.

2.2.4.3 Disease Gene Overlap with Ocular Growth

A number of genes implicated in either non-syndromic or syndromic high myopia in various degrees were differentially expressed between rapidly growing/developing and mature ocular tissues. Seventeen differentially expressed genes associated with non-syndromic high myopia were present in the most significant functional classifications for at least one ocular tissue type (Tables 7 and 8). Ten differentially expressed genes found to either be associated with or causal for syndromes with a myopic component were present in the ten most significant functional

classifications for at least one ocular tissue (data not shown). Many of these myopic-associated genes were found in the same functional groupings as discussed below.

2.3 Results

The number and fold change of genes differentially expressed varied by tissue type. For the adult versus fetal tissues, the retina/RPE had the lowest average fold change and the fewest number of genes, while the cornea had the largest fold changes and the highest number of differentially expressed genes (Table 3). Many of the highest differentially expressed genes per tissue type have either previously been implicated or may be relevant in ocular diseases particular to these tissues. The extracellular matrix collagens were among the most differentially expressed genes in all adult versus fetal tissue types tested (Appendix B). For the central versus peripheral tissues, no genes reached statistical significance and the fold changes averaged around two for all tissues tested. Sufficient peripheral RPE was not obtained to compare central and peripheral expression.

As microarray chips were redundant, many genes had multiple probes tagging the same genes. Given the stringent quality control and fold change criteria used in our testing, all probes for a given gene did not always meet that threshold. Consequently, some genes have differing numbers of probes in different tissue types. Probes with near/below background readings in one or both ages tended to have very high fold

changes. These low readings may have resulted either from failed probes or absent expression. Probes with near or below background intensity readings are noted below.

Table 3: Number and Fold Change Range of Filtered Probes and Unique Genes.

Retina/RPE, Choroid, Sclera and Cornea were filtered by False Discovery Rate (FDR) < 0.05. *Optic Nerve was filtered by raw p-value < 0.05. **Central versus peripheral tissues were filtered by raw p-value < 0.10. All tissues were filtered by a fold change (FC) > 1.5. Average FC is by absolute value.

	Tissue	FC Range	Average FC	Probes	Unique Genes
Adult versus Fetal	Retina/RPE	-8.50 ↔ 21.09	1.86	1236	1185
	Choroid	-617.57 ↔ 550.49	5.56	7124	6446
	Sclera	-125.11 ↔ 6.40	2.28	1423	1349
	Optic Nerve*	-205.22 ↔ 1695.34	5.90	2399	2179
	Cornea	-1252.45 ↔ 205.77	7.34	4354	3872
Central versus Peripheral	Retina**	-10.22 ↔ 14.65	1.88	1066	1015
	Choroid**	-5.28 ↔ 12.68	2.04	1290	1269
	Sclera**	-6.33 ↔ 14.98	2.29	658	654

Although the presence of all cell types and layers in fetal retina have already been established in 11-weeks' gestation fetal tissue (Linberg and Fisher 1990); the raw expression signals of phototransduction cascade genes were screened in our array data for confirmation. The expression of major genes of the phototransduction cascade (including but not limited to opsin, transducing, and cycle nucleotide gated channels)

was confirmed in the fetal and adult ocular retina/RPE. Additionally, differential expression of these genes was screened as a positive control of our averaging methods of adult retina and RPE relative to fetal retina/RPE. As expected, most of these genes were more highly expressed in the adult retina/RPE relative to the fetal tissue. The fold changes of these genes were comparable to the average fold changes seen in the adult versus fetal retina/RPE, which were low overall. In some cases where the raw gene expression signals were either very high or very low for both fetal and adult retina/RPE, fold changes were absent or very low. The quantile normalization methods, which most strongly affect these extremes, in combination with the averaging methods likely contributed to these genes not showing differential expression. This limitation should be kept in mind when analyzing other genes within the retina/RPE. Another limitation identified by screening the phototransduction cascade genes was the possible differences in contribution of foveal retina to the posterior retina/RPE in the fetal versus adult tissues. The use of a biopsy punch of the same size in fetal and adult tissue collection may have influenced differential expression of some genes due to differences in the cellular density and makeup in the central retina. Some differences detected may be the result of variation between cell types in the retina rather than growth and development. In the fetal retina/RPE, short-wave sensitive opsin was expressed 1.3 fold higher in the fetal relative to adult tissue. Given that short-wave sensitive opsin is

lacking from central foveal retina (Rodieck 1998), it is possible that the fetal tissue collected may have included a higher proportion of non-foveal retina/RPE than the adult tissue either due to the size of the punch in the smaller fetal eyes or variation in punch location during adult tissue sample collection.

2.3.1 Differential Expression of Ocular Growth

2.3.1.1 Enriched Functional Annotation Analyses

In all comparisons of ocular tissues the most significant functional assignments included cancer, development, and cell growth/death categories. Other common categories included cell cycle, movement, function morphology, and expression. These most significant functional assignments showed that genes involved in basic cellular regulations were differentially activated in rapidly growing and developing tissues relative to their adult counterparts. The lower significance for the optic nerve in the array data was reflected in its lower significance for functional classifications. Despite large variances in the number and significance of genes between tissue type comparisons, the most significant functional assignments across all adult versus fetal comparisons, including the optic nerve, were comparable (Table 4).

Table 4: Ten Most Significant Adult versus Fetal Functional Assignments.

Significance (p-value) of functional groups is determined by Fischer's exact test. Total number of genes in the groups which are included in the dataset is given as # Genes.

Tissue	Functions Annotation	P-Value	# Genes
Retina/RPE	differentiation	7.15X10 ⁻¹⁶	156
	tumorigenesis	2.48X10 ⁻¹²	260
	proliferation of cells	8.05X10 ⁻¹²	182
	cell movement	8.36X10 ⁻¹¹	133
	tissue development	9.28X10 ⁻¹¹	182
	function of blood cells	4.33X10 ⁻¹⁰	57
	immune response	1.14X10 ⁻⁹	116
	cell death of blood cells	3.18X10 ⁻⁹	60
	development of lymphocytes	4.35X10 ⁻⁹	60
	quantity of cells	1.06X10 ⁻⁸	118
Choroid	tumorigenesis	3.19X10 ⁻²⁸	1317
	cell death	1.37X10 ⁻²³	1058
	cell cycle progression	3.81X10 ⁻²⁰	376
	proliferation of cells	1.07X10 ⁻¹⁶	835
	growth of cells	1.22X10 ⁻¹⁴	588
	expression of RNA	2.95X10 ⁻¹⁴	658
	transcription	1.63X10 ⁻¹³	610
	differentiation	2.10X10 ⁻¹³	617
	transcription of RNA	2.37X10 ⁻¹³	599
	organization of cytoplasm	6.20X10 ⁻¹³	329
Sclera	tumorigenesis	6.17X10 ⁻¹⁸	365
	cell division of chromosomes	3.73X10 ⁻¹²	43
	cell cycle progression	1.14X10 ⁻¹⁰	110
	tissue development	1.35X10 ⁻¹⁰	237
	proliferation of cells	2.13X10 ⁻¹⁰	231
	differentiation	4.42X10 ⁻¹⁰	179
	cell death	2.39X10 ⁻⁹	272
	cell movement	6.59X10 ⁻⁹	164
	interphase	1.30X10 ⁻⁸	73
	morphology of organ	8.54X10 ⁻⁸	132

Optic Nerve	tumorigenesis	5.22X10 ⁻¹⁰	548
	tissue development	1.31X10 ⁻⁸	371
	expression of RNA	8.54X10 ⁻⁸	288
	proliferation of cells	9.32X10 ⁻⁸	357
	microtubule dynamics	8.38X10 ⁻⁷	100
	cell cycle progression	9.49X10 ⁻⁷	152
	transcription	9.68X10 ⁻⁷	263
	morphology of basement membrane	1.24X10 ⁻⁶	9
	immortalization	4.28X10 ⁻⁶	17
	morphology of blood vessel	1.18X10 ⁻⁵	44
Cornea	tumorigenesis	9.15X10 ⁻²⁸	1060
	tissue development	6.71X10 ⁻¹⁹	702
	cell death	7.63X10 ⁻¹⁹	831
	proliferation of cells	1.51X10 ⁻¹⁸	684
	growth of cells	1.05X10 ⁻¹⁷	492
	encephalopathy	3.18X10 ⁻¹⁷	363
	cell movement	1.96X10 ⁻¹⁶	483
	invasion of cells	2.00X10 ⁻¹⁶	199
	movement disorder	2.52X10 ⁻¹⁴	289
	organization of cytoplasm	3.77X10 ⁻¹⁴	275

2.3.1.2 Predicted Activation Functional Annotation Analyses

Adult versus fetal compared tissues shared major functional categories in common, but with some differences from those most significantly present. When taking direction of fold changes and their predicted effects on a functional assignment, all tissues had predicted activation changes for cancer and cell movement categories. Many tissue types also had development and cell growth/death categories in common. Even within the same tissue type these shared categories were not consistently predicted to have the same directional activation; however, those shared categories had differing

functional assignments and contained distinct genes. Functionally assigned groups containing redundant genes which were removed from the data for publication did not contradict one another in the direction of predicted activation.

Functions with a predicted activation state between fetal and adult tissues are listed in Table 5. A large number of functions from all tissues were significantly predicted to be activated in adult or fetal tissues, but those in the optic nerve were all predicted to be increased in the fetal tissues. In the adult retina/RPE, choroid and sclera, functions predicted to have increased activation included cell proliferation, while those predicted to have decreased activation included lymphocyte movement and/or proliferation. In the adult optic nerve, predicted increased functions included cell growth, formation, and organization. Lastly in the adult cornea, predicted functional increases included development, differentiation, and cell cycle progression, while decreased included cell invasion and survival.

Table 5: Significant Predicted Activation of Functional Assignments for Ocular Growth Expression.

Negative z-scores predict higher functional activation in adult tissues, while positive z-scores predict lower activation in adult tissues. Significance of each functional group (with number [#] of genes) is given as a p-value.

Tissue	Functions Annotation	p-Value	Regulation z-score	# Genes
Retina/ RPE	hyperplasia of secretory structure	6.03X10 ⁻⁴	-2.399	10
	proliferation of cells	8.05X10 ⁻¹²	-2.307	182
	inflammation of colon transformation	2.98X10 ⁻⁴	-2.197	5
		1.43X10 ⁻³	-2.018	36
	recruitment of cells	9.89X10 ⁻⁷	2.812	31
	cell movement of lymphocytes	4.02X10 ⁻⁶	2.137	33
	fatty acid metabolism	1.13X10 ⁻³	2.107	37
	apoptosis of hematopoietic progenitor cells	5.16X10 ⁻⁴	2.041	17
	migration of mononuclear leukocytes	1.31X10 ⁻⁵	2.039	30
	digestive organ tumor	5.68X10 ⁻⁶	2.005	100
Choroid	replication of Influenza A virus	2.13X10 ⁻³	-2.737	91
	genital tumor	7.87X10 ⁻⁸	-2.683	89
	size of embryo	3.14X10 ⁻⁵	-2.675	109
	cell movement of tumor cell lines	8.64X10 ⁻⁶	-2.567	193
	proliferation of tumor cell lines	1.09X10 ⁻⁹	-2.523	285
	transformation	5.88X10 ⁻⁷	-2.318	172
	cell death of embryonic cell lines	5.35X10 ⁻⁷	-2.274	80
	interphase/ S phase/ entry into	3.16X10 ⁻⁵	-2.109	198

	S phase				
	head and neck cancer	1.55X10 ⁻⁴	-2.079	173	
	cellular homeostasis	1.67X10 ⁻⁴	3.64	371	
	developmental process of lymphocytes	1.18X10 ⁻⁴	2.915	197	
	excretion of Na ⁺	2.28X10 ⁻⁴	2.554	20	
	development of blood cells	2.19X10 ⁻⁵	2.531	198	
	maturation of cells	1.05X10 ⁻³	2.525	111	
	heart disease	2.25X10 ⁻³	2.439	225	
	cell movement of blood cells	4.59X10 ⁻⁵	2.224	244	
	immune response	1.03X10 ⁻³	2.146	438	
	chemotaxis	1.08X10 ⁻³	2.096	144	
	differentiation of blood cells	8.06X10 ⁻⁸	2.066	236	
	organismal death	2.25X10 ⁻¹⁰	2.051	494	
	organogenesis	1.81X10 ⁻⁷	-3.137	165	
	tumorigenesis of malignant tumor	1.56X10 ⁻⁵	-2.796	34	
	proliferation of tumor cell lines	4.73X10 ⁻⁶	-2.511	82	
	transformation	1.78X10 ⁻³	-2.279	46	
	S phase	1.32X10 ⁻⁶	-2.169	34	
	solid tumor	3.47X10 ⁻¹⁶	-2.135	281	
Sclera	invasion of cells	1.05X10 ⁻⁵	-2.122	62	
	benign tumor	2.23X10 ⁻⁵	-2.057	68	
	immune response	2.14X10 ⁻³	2.994	119	
	release of histamine	2.12X10 ⁻³	2.848	7	
	cell death of bone cancer cell lines	3.54X10 ⁻³	2.563	15	
	proliferation of B-1 lymphocytes	2.16X10 ⁻⁴	2.451	4	
	cell death of carcinoma cell lines	6.36X10 ⁻⁴	2.377	19	

	accumulation of cells	1.30X10 ⁻³	2.369	29
	generation of hematopoietic progenitor cells	2.91X10 ⁻³	2.305	5
	cell movement of mononuclear leukocytes	1.01X10 ⁻³	2.23	40
	clearance of lipid	3.15X10 ⁻³	2.203	6
	cell movement of phagocytes	3.92X10 ⁻⁴	2.182	46
	cell death of kidney cancer cell lines	8.34X10 ⁻⁴	2.123	7
	cell death of cancer cells	1.39X10 ⁻³	2.083	24
Optic Nerve	tumorigenesis of tissue	4.25X10 ⁻³	2.212	14
	formation of cytoplasmic aggregates	1.16X10 ⁻²	2.112	6
	organization of cytoplasm	9.69X10 ⁻⁵	2.079	134
	cell movement of brain cancer cell lines	3.25X10 ⁻⁴	2.011	17
	development of connective tissue / bone	6.51X10 ⁻¹⁰	-3.275	240
Cornea	size of body	1.50X10 ⁻⁷	-3.203	138
	tissue development	6.71X10 ⁻¹⁹	-2.917	702
	differentiation of red blood cells	4.87X10 ⁻⁴	-2.552	33
	phagocytosis of testicular/epithelial cells	1.33X10 ⁻⁴	-2.497	5
	tumorigenesis of organ	1.19X10 ⁻⁵	-2.205	74
	cell cycle progression	7.02X10 ⁻⁸	-2.177	260
	cytostasis	4.63X10 ⁻⁴	-2.145	70
	development of bone marrow	6.93X10 ⁻⁴	-2.13	35
	osteoclastogenesis	7.22X10 ⁻⁶	-2.107	26
	mass of body	2.73X10 ⁻⁶	-2.1	155
cell movement of brain cancer cell lines	3.48X10 ⁻⁴	-2.09	25	

formation of filaments	1.29X10 ⁻⁶	-2.033	95
development of skeleton / ossification	2.91X10 ⁻⁵	-2.023	93
invasion of embryonic cell lines	6.54X10 ⁻⁴	2.383	7
cell survival	5.60X10 ⁻⁶	2.348	272
tumorigenesis of breast cancer cell lines	5.68X10 ⁻⁴	2.279	16
breakage of blood vessel	9.77X10 ⁻⁵	2.168	7

2.3.1.3 Canonical Pathway Analyses

In all tissues signaling pathways were among the most significant, and there was overlap in pathways between tissue types (Table 6). The retina/RPE and sclera both included atherosclerosis signaling among the most significant pathways. The most significant in the choroid and cornea both included axonal guidance signaling. The most significant pathways in the sclera and optic nerve tissues both included those involving cell cycle regulations. The other most significant five pathways in retina/RPE involved expression, regulation and immune responses of the cell. In the choroid, the most significant pathways included growth, expression and immune responses. In the sclera, most of the most significant pathways involved cell cycle regulation. In the optic nerve, the most significant pathways were cell fate, growth, regulation and expression. For the cornea, the most significant pathways were cell fate and growth.

Table 6: Five Most Significant Adult versus Fetal Tissue Canonical Pathways.

Significance (-log[p-value]) of pathways is determined by Fischer's exact test of probability of genes in the dataset fit into the pathway by chance alone and by proportion (ratio) of genes in pathway that are included in the dataset (# Genes).

Tissue	Ingenuity Canonical Pathways	-log(p)	Ratio	# Genes
Retina/ RPE	Atherosclerosis Signaling	3.99	1.09X10 ⁻¹	14
	LXR/RXR Activation	3.25	9.56X10 ⁻²	13
	p38 MAPK Signaling	3.25	1.13X10 ⁻¹	12
	MIF Regulation of Innate Immunity	3.15	1.40X10 ⁻¹	7
	Hepatic Fibrosis / Hepatic Stellate Cell Activation	3.14	9.52X10 ⁻²	14
Choroid	Axonal Guidance Signaling	7.03	2.98X10 ⁻¹	128
	Molecular Mechanisms of Cancer	5.55	2.88X10 ⁻¹	109
	CXCR4 Signaling	5.33	3.39X10 ⁻¹	57
	Ephrin Receptor Signaling	5.09	3.12X10 ⁻¹	62
	EIF2 Signaling	4.85	3.22X10 ⁻¹	66
Sclera	ATM Signaling	5.31	2.20X10 ⁻¹	13
	Role of CHK Proteins in Cell Cycle Checkpoint Control	3.68	2.29X10 ⁻¹	8
	Atherosclerosis Signaling	3.53	1.24X10 ⁻¹	16
	Mitotic Roles of Polo-Like Kinase	2.37	1.38X10 ⁻¹	9
	Cell Cycle: G2/M DNA Damage Checkpoint Regulation	2.17	1.43X10 ⁻¹	7
Optic Nerve	Wnt/β-catenin Signaling	5.61	2.03X10 ⁻¹	35
	Hereditary Breast Cancer Signaling	4.99	2.05X10 ⁻¹	26
	Human Embryonic Stem Cell Pluripotency	4.58	1.80X10 ⁻¹	27
	Cell Cycle: G1/S Checkpoint Regulation	3.64	2.31X10 ⁻¹	15
	RAR Activation	3.47	1.60X10 ⁻¹	30
Cornea	Breast Cancer Regulation by Stathmin1	6.67	2.93X10 ⁻¹	61
	Mitochondrial Dysfunction	6.35	2.64X10 ⁻¹	46
	Wnt/β-catenin Signaling	6.16	3.14X10 ⁻¹	54
	Axonal Guidance Signaling	5.89	2.37X10 ⁻¹	102
	Molecular Mechanisms of Cancer	5.79	2.41X10 ⁻¹	91

2.3.1.4 Non-Syndromic High Myopia Susceptibility Genes

A total of 17 genes associated with high myopia were differentially expressed and present in the most significant functional groups for at least one tissue type (Tables 7 and 8). Nine of these associated genes were found differentially expressed in multiple tissue types: collagen type I alpha-1 (*COL1A1* (Inamori, Ota et al. 2007); MIM 120150), collagen type II alpha-1 (*COL2A1* (Metlapally, Li et al. 2009); MIM 120140), fibromodulin (*FMOD* (Majava, Bishop et al. 2007; Lin, Wan et al. 2009); MIM 600245), insulin-like growth factor I (*IGF1* (Mak, Yap et al. 2012); MIM 147440), laminin alpha-1 (*LAMA1* (Zhao, Zhang et al. 2011); MIM 150320), lumican (*LUM* (Wang, Chiang et al. 2006; Majava, Bishop et al. 2007; Chen, Wang et al. 2009; Zhang, Zhu et al. 2009; Lin, Kung et al. 2010; Lin, Wan et al. 2010); MIM 600616), myocilin (*MYOC* (Tang, Yip et al. 2007); MIM 601652), transforming growth factor beta two (*TGFB2* (Lin, Wan et al. 2009); MIM 190220), and vitamin D receptor (*VDR* (Annamaneni, Bindu et al. 2011); MIM 601769). Four genes associated with myopia were present in the most significant functional classifications for only one tissue type each: bone morphogenetic protein two inducible kinase (*BMP2K* (Liu, Lin et al. 2009)), cholinergic receptor muscarinic two (*CHRM2* (Lin, Wan et al. 2012); MIM 118493), cholinergic receptor muscarinic three (*CHRM3* (Lin, Wan et al. 2012); MIM 118494), hepatocyte growth factor (*HGF* (Han, Yap et al. 2006; Veerappan, Pertile et al. 2010); MIM 142409), complement factor I (CFI

(Leveziel, Yu et al. 2012); MIM 217030), leprecan-like one (*LEPREL1* (Mordechai, Gradstein et al. 2011); MIM 610341), prolargin (*PRELP* (Majava, Bishop et al. 2007); MIM 601914), and paired box gene six (*PAX6* (Jordan, Hanson et al. 1992; Tsai, Chiang et al. 2008; Jiang, Yap et al. 2011; Liang, Hsi et al. 2011); MIM 607108).

The *COL1A1* gene was present in the most significant functional assignments with lower expression in adult versus fetal choroid, optic nerve and cornea. In the choroid, *COL1A1* was expressed at -17.95 lower fold in the adult relative to fetal tissue. In the optic nerve and cornea, the fold changes were larger at -205.22 and -209.79 respective lower expression in the adults, despite adult detection intensities well above background. In the choroid, *COL1A1* was present in the tumorigenesis, cell cycle progression, proliferation and growth of cells, and expression of RNA functional assignments. For the optic nerve, *COL1A1* was associated with tumorigenesis, tissue development, expression of RNA, proliferation of cells, and cell cycle progression. Lastly in the cornea, *COL1A1* was present in tumorigenesis, tissue development, proliferation and growth of cells, and cell movement functional assignments.

The other collagen gene, *COL2A1*, present in multiple of the most significant functional assignments was also expressed lower in adult relative to fetal tissue. In the retina/RPE, *COL2A1* was detected as down-regulated at -2.74 and -1.67 lower expression fold changes in adults. In the sclera, only one probe for *COL2A1* passed all quality

control criteria with a -2.55 lower expression fold change. In the retina/RPE groups of genes functioning in differentiation, tumorigenesis, proliferation of cells, cell movement, tissue development and immune response included *COL2A1*. For the sclera, *COL2A1* functional assignments were tumorigenesis, tissue development, proliferation and differentiation of cells, cell death, cell movement, and organ morphology.

The *FMOD* gene was present in the ten most significant functional assignments in the adult versus fetal retina/RPE, optic nerve and cornea. *FMOD* was up-regulated in adult retina/RPE and down-regulated in adult optic nerve and cornea (with 1.65, -4.32 and -18.62 lower expression fold changes respectively). In the retina/RPE, the most significant functional assignments for *FMOD* were cancerous growth, tissue development and immune responses. In the optic nerve *FMOD* expression was associated with cancerous growth, tissue development, and morphology of blood vessel groups. Lastly, in the cornea *FMOD* was associated with cancerous growth, tissue development and cell death.

IGF1 was present in all ten of the most significant categories in both the choroid and sclera. In the choroid, *IGF1* was up-regulated in adults in two probes at fold changes of 7.72 and 5.98. In the sclera, only one probe met the fold change criteria at -1.62 times lower in the adult. *IGF1* was present in all ten of the most significant functional assignments for both the choroid and the sclera. *IGF1* and *FMOD* were the

only two non-syndromic myopic-associated genes to have differential expression not follow the same direction for all tissue types.

LAMA1 was differentially expressed in all tissues of the posterior wall: the retina/RPE, choroid and sclera. In the retina/RPE, *LAMA1* had lower expression fold change in the adult tissue (-1.85 and -1.56). A third probe passed quality control criteria only in the choroid (with lower detection and fold change p-values), which contradicted the other two probes at 2.85 higher expression fold change in adults relative to the other probes at -30.80 and -5.67 lower expression fold change. In the sclera, the same probes as the retina/RPE showed -4.47 and -2.56 lower expression fold change in the adult relative to fetal tissue. In the retina/RPE, *LAMA1* was present in differentiation, tumorigenesis, cell proliferation, cell movement, and tissue development functional groups. For the choroid, *LAMA1* functional groups were tumorigenesis, cell death, proliferation of cells, and differentiation. For the sclera, *LAMA1* was present in tumorigenesis, tissue development, cell proliferation, differentiation, cell death, and movement functional assignments.

LUM was present in the most significant functional classifications for both the choroid and the optic nerve. In the adult versus fetal choroid comparisons, *LUM* was present in four of the most significant ten functional assignments. In the adult versus fetal optic nerve comparisons *LUM* was present in three of the ten most significant

functional assignments. In our testing, *LUM* showed a -7.82 and -12.53 lower expression fold change in adult relative to fetal choroid and optic nerve respectively. In the choroid, the most significant functional assignments for *LUM* were cellular growth, proliferation, and death. For the optic nerve the most significant functional assignments that *LUM* was present in were cellular growth and proliferation, as well as tissue development.

The *MYOC* gene was present in three of the most significant functional categories, each in different tissue types. In the choroid, with an 8.6 higher expression fold increase in adults, expression of RNA included *MYOC*. In both the sclera and cornea, *MYOC* was present in functional groups of cell movement. In the sclera *MYOC* was up-regulated in adults in two probes at 2.22 and 6.40 fold. *MYOC* demonstrated its highest differential expression in the cornea with up-regulation in adult expressions with a fold change of 74.20, largely inflated by a near background reading in fetal samples.

TGFB2 was differentially expressed and present in the most significant functional groups for the choroid and optic nerve. In the choroid, *TGFB2* was present in seven of the most significant functional assignments including tumorigenesis, cell death, cell growth, cell cycle progression, expression, and differentiation. It was expressed 2.94 fold higher in the adult versus fetal tissue. In the optic nerve, expression was -2.59 fold

lower in adult tissue. *TGFB2* shared to the most significant functions of tumorigenesis, tissue development, expression, cell cycle progression, immortalization, and morphology of blood vessels.

The last gene previously identified with myopia susceptibility present in the most significant functional assignments in multiple tissue types, *VDR*, was up-regulated in both the adult choroid and cornea. In the choroid, *VDR* had 3.11 higher expression fold change in the adult versus fetal tissue. In the cornea, an 11.86 higher expression fold change was seen in the adults. *VDR* was present in eight of the ten most significant functional groups involving cell turn over, development, and differentiation. In the cornea, *VDR* was present in comparable functional categories in seven of the ten most significant functional assignments.

BMP2K was present in the 10th most significant functional group for only one tissue - the adult to fetal choroid. The function of the genes within the group was involvement in the organization of the cytoplasm. It had -4.15 lower fold expression in the adult versus fetal choroid. *CHRM2* and *CHRM3* were each present in the most significant functional assignments for the choroid and sclera respectively. *CHRM2* had 1.95 fold higher expression in adult sclera while *CHRM3* had -3.76 fold lower expression in the adult choroid. *CHRM2* was present in the sclera's most significant functional groups for tumorigenesis and organ morphology. *CHRM3* belonged to significant

functional groups for tumorigenesis, cell proliferation, and cell growth. *HGF* was present in nine of the ten most significant functional assignments for only one tissue type - the adult versus fetal scleral comparisons. Two probes within the *HGF* gene down-regulated in adult, with fold changes of -2.2 and -1.61, met the criteria for the pathway analyses list for the sclera. The functional assignments for *HGF* in the sclera involved cancerous growth, cell cycle progression, tissue development, proliferation, differentiation, cell death, cell movement, interphase, and organ morphology. Another gene with association with myopia that was present in our most significant functional groups for the tissues tested was *CFI*. However, *CFI* was present in only one of the most significant functional annotation group, tumorigenesis, in only one tissue, the optic nerve. In the optic nerve, *CFI* had a -2.28 lower expression fold change in the adult. In addition to this functional group containing the largest number of genes in the optic nerve, *CFI* was only present in this tissue, which failed to meet statistical significance. *LEPREL1* was present in one of the most significant functional groups for cell cycle progression in the choroid. It had 2.41 fold higher expression in the adult. In addition to *MYOC*, two other genes associated with high myopia were present in the most significant functional categories for the adult versus fetal cornea – *PRELP* and *PAX6*. *PRELP* was present in two of the ten most significant adult versus fetal cornea comparisons. Two probes, with fold changes of -6.3 and -5.55, were down-regulated in

adult for the *PRELP* gene for the cornea. The two functional assignments for *PRELP* were cancerous growth and tissue development. The last myopic-associated gene present in only one tissue type, *PAX6*, was present in six of the ten most significant classifications. *PAX6* was found to be up-regulated in the adult cornea for two probes at fold changes of 2.71 and 3.84. The range of functions for *PAX6* was diverse, including growth, development, movement, and organization. *PAX6* and *PRELP* were the only two genes found only in the cornea.

Table 7: Differentially Expressed Non-Syndromic High Myopia Susceptibility Genes.

Fold change (FC) and significance (p-value) are listed for each differentially expressed (FC > 1.5) probe (given on separate lines) of genes previously implicated in myopic development. Underlined FC and p-values were not present in the ten most significant functional assignments.

	Retina/RPE		Choroid		Sclera		Optic Nerve		Cornea	
	FC	p-value	FC	p-value	FC	p-value	FC	p-value	FC	p-value
<i>BMP2K</i>			-4.15	< .01						
<i>CFI</i>							-2.28	< .05		
<i>CHRM2</i>					1.95	< .01				
<i>CHRM3</i>			-3.76	<.001						
<i>COL1A1</i>			-17.95	<.001			205.22	< .01	-209.79	< .01
<i>COL2A1</i>	-1.67	< .0001			-2.55	< .0001				
	-2.74	< .001								
<i>FMOD</i>	1.65	< .001					-4.32	< .05	-18.62	< .01
<i>GRM6</i>			<u>4.05</u>	<u>< .01</u>						
<i>HGF</i>					-2.2	< .001				
					-1.61	< .01				
<i>IGF1</i>			-2.73	< .01	-1.62	< .001				
			-45.62	< .001						
<i>LAMA1</i>	-1.85	< .01	-5.67	< .001	-4.47	< .001				
	-1.56	< .01	-30.8	< .001	-2.56	< .0001				
			2.85	< .01						
<i>LEPREL1</i>			2.41	< .01						
<i>LUM</i>			-7.82	< .001			-12.53	< .01		
<i>LYPLAL1</i>			<u>-2.59</u>	<u>< .01</u>					<u>3.9</u>	<u>< .01</u>

			<u>-5.72</u>	<u>< .01</u>			<u>4.59</u>	<u>< .01</u>
<i>MMP1</i>	<u>1.61</u>	<u>< .01</u>	<u>2.42</u>	<u>< .01</u>				
<i>MMP2</i>							<u>-9.52</u>	<u>< .01</u>
<i>MYOC</i>			8.6	< .01	6.4	< .0001		
					2.22	< .0001	74.2	< .01
<i>PAX6</i>							2.71	< .01
							3.84	< .01
<i>PRELP</i>							-6.3	< .01
							-5.55	< .01
<i>TGFB2</i>			2.94	< .01				
						-2.59	< .01	
<i>VDR</i>			3.11	< .001			11.86	< .01
<i>ZC3H11B</i>							<u>-2.90</u>	<u>< .05</u>

Table 8: Genes Implicated in Myopic Development Which Belong to the Ten Most Significant Functional Assignments.

Presence of myopic- associated genes in the ten most significant functional groups is indicated by an 'X'.

Tissue	Functions Annotation	Myopic-Associated Genes																
		<i>BMP2K</i>	<i>CFI</i>	<i>CHRM2</i>	<i>CHRM3</i>	<i>COL1A1</i>	<i>COL2A1</i>	<i>FMOD</i>	<i>HGF</i>	<i>IGF1</i>	<i>LAMA1</i>	<i>LEPREL1</i>	<i>LUM</i>	<i>MYOC</i>	<i>PAX6</i>	<i>PRELP</i>	<i>TGFBR2</i>	<i>VDR</i>
Retina/RPE	differentiation					X				X								
	tumorigenesis					X	X			X								
	proliferation of cells					X				X								
	cell movement					X				X								
	tissue development					X	X			X								
	function of blood cells																	
	immune response						X	X										
	cell death of blood cells																	
	development of lymphocytes																	
	quantity of cells																	
Choroid	tumorigenesis				X	X				X	X	X				X	X	
	cell death									X	X	X				X	X	
	cell cycle progression				X	X				X	X					X		
	proliferation of cells				X	X				X	X	X				X	X	
	growth of cells				X	X				X		X				X	X	
	expression of RNA					X				X			X			X	X	
	transcription									X							X	
	differentiation									X	X					X	X	
	transcription of RNA									X							X	
	organization of cytoplasm	X								X								
Sclera	tumorigenesis			X		X		X	X	X								
	cell division of chromosomes								X									
	cell cycle progression							X	X									

	tissue development		X	X	X	X		
	proliferation of cells		X	X	X	X		
	differentiation		X	X	X	X		
	cell death		X	X	X	X		
	cell movement		X	X	X	X	X	
	interphase			X	X			
	morphology of organ	X	X	X	X			
Optic Nerve	tumorigenesis	X	X	X		X	X	
	tissue development		X	X		X	X	
	expression of RNA		X				X	
	proliferation of cells		X			X	X	
	microtubule dynamics							
	cell cycle progression		X				X	
	transcription							
	morphology of basement membrane							
	immortalization						X	
	morphology of blood vessel						X	
	Cornea	tumorigenesis		X	X			X
		tissue development		X	X		X	X
		cell death			X		X	X
proliferation of cells			X			X	X	
growth of cells			X				X	
encephalopathy						X		
cell movement			X			X	X	
invasion of cells							X	
movement disorder								
organization of cytoplasm						X		

2.3.1.5 Syndromic Myopia Genes

A number of genes associated with or causal for ocular syndromes including myopia as a component were also found to be differentially expressed in adult versus

fetal ocular tissues (data not shown). Several collagen genes (N=4), known to be associated with or causal for such syndromes, were among the most differentiated genes in tissues believed to be important in the progression of myopia - the retina/RPE, choroid, sclera and cornea. Each of these collagen genes and a few other (N=5) syndromic myopia genes were present in our most significant functional classifications in at least one tissue analyzed. The most prominently found syndromic myopia genes were collagen genes found in the fibrous sclera, optic nerve and cornea. Interestingly, *COL9A1* (MIM 120210), was not present in any of the most significant functional classifications in the choroid despite being one of the most down-regulated genes in the tissue (Appendix B)

2.3.2 Central versus Peripheral Differential Expression

All of the central-to-peripheral comparisons did not meet FDR cut-offs, thus a raw p-value of < 0.10 was used to identify the most likely differentially expressed genes for pathway analysis. To focus on biologically important changes in each comparison, those probes with fold changes < 1.5 were also removed. The number of genes meeting this threshold was considerably lower than previously performed adult-to-fetal comparisons, which met FDR significance cut-offs. In addition to the lack of significantly, differentially expressed genes, the average fold changes were generally lower in the central versus peripheral tissues. In the retina, the fold changes were

comparable to the adult versus fetal retina/RPE; however, the choroid and sclera were both lower than their adult to fetal counterparts (Table 3). The enriched functional groups in the central versus peripheral tissues varied substantially more between tissue types (Table 9).

2.3.2.1 Enriched Functional Annotation Analyses

The most significant central versus peripheral functional classifications, which are fewer than adult versus fetal comparisons as expected by lower input significance due to smaller sample sizes, for each tissue comparison are listed in Table 9. Adult central versus peripheral comparisons yielded significant functional categories and assignments more variable from one another than adult versus fetal comparisons. The only category shared across all three tissues was development, but the functional assignments within the category were varied. Central versus peripheral retina had significant functional assignments mostly involving neurological disease and organization. Central versus peripheral choroid's most significant functional assignments were more variable and included tumorigenesis, arterial pressure and miscellaneous biochemical processes. Lastly, central versus peripheral sclera comparisons also yielded variable functional assignments such as actin bundle formation, vasodilation and cytoskeletal organization.

Functional assignments of central versus peripheral tissues based on predicted activation states also varied by tissue type (Table 10). In the retina, the peripheral retina is predicted to be lower than the central retina in functions of polymerizations, quantity of retinal cells, proliferation and movement of cells and atherosclerosis. The peripheral retina is predicted to have increased functions of lipid metabolisms and contractility of cardiomyocytes. Peripheral choroid is predicted have increased activation of cellular organizations, quantity of hormones, lipid metabolisms, cell death and artery remodeling relative to the central choroid. Central sclera is predicted to have higher cell death and proliferation; while the peripheral sclera is predicted to have higher tubulation of cells.

Table 9: Ten Most Significant Central versus Peripheral Functional Assignments.

Significance (p-value) of functional groups is determined by Fischer's exact test. Total number of genes in the groups which are included in the dataset is given as # Genes. *Indicates redundant genes in the functional groups with independent functional annotations.

Tissue	Functions Annotation	P-Value	# Genes
Retina	movement disorder	4.12X10 ⁻¹⁴	106
	tumorigenesis	9.63X10 ⁻¹³	298
	neuromuscular disease	6.90X10 ⁻¹²	99
	encephalopathy	9.65X10 ⁻¹²	118
	organization of cytoplasm	4.69X10 ⁻¹¹	94
	neuritogenesis	1.13X10 ⁻¹⁰	51
	growth of neurites	1.97X10 ⁻¹⁰	50
	tissue development	3.75X10 ⁻¹⁰	204
	cell movement	5.48X10 ⁻¹⁰	147
	schizophrenia	3.36X10 ⁻⁹	57
Choroid	tumorigenesis	1.90X10 ⁻⁶	312
	mean arterial pressure of artery	9.30X10 ⁻⁵	6
	accumulation of diacylglycerol	9.57X10 ⁻⁵	4
	expression of RNA	1.34X10 ⁻⁴	161
	transcription	1.60X10 ⁻⁴	150
	hydrolysis of nucleotide	3.68X10 ⁻⁴	15
	hydrolysis of fatty acid	6.65X10 ⁻⁴	6
	import of metal	7.10X10 ⁻⁴	4
	export of protein	8.61X10 ⁻⁴	6
	fusion of eyelid	1.10X10 ⁻³	6
Sclera	maintenance of intercellular junctions	5.95X10 ⁻⁴	3
	formation of actin bundles	6.10X10 ⁻⁴	5
	vasodilation of aorta *	7.70X10 ⁻⁴	4
	astrocytosis *	9.94X10 ⁻⁴	6
	organization of cytoskeleton	9.99X10 ⁻⁴	36
	processing of RNA	1.10X10 ⁻³	16

abnormal morphology of nasal cavity	1.23X10 ⁻³	3
DNA damage checkpoint	1.23X10 ⁻³	5
cell death	1.34X10 ⁻³	113
cell spreading	1.35X10 ⁻³	14

2.3.2.2 Predicted Activation Functional Annotation Analyses

Functions with predicted activation in in all central versus peripheral tissues are shown in Table 10. The central versus peripheral retina had the most significant predicted activation states for functional groups. Functions that were predicted to be activated in the central rather than peripheral tissues included quantity of retinal cells/photoreceptors and arterial occlusive disease/atherosclerosis. A functional increase in the quantity of photoreceptors can be explained by the increase in photoreceptors in the central or macular region isolated (Rodieck 1998). Increases in functions relating to vascular disease may reflect interactions with the increased vasculature in the choroid surrounding the macular retina (Nickla and Wallman 2010). Other functions predicted to have increased activation in the central retina included polymerization of filaments and microtubules, cell movement and growth. Functions predicted to have lower activation in the central tissues included metabolism and contractility of cardiomyocytes (muscle cells). All the functions with predicted activation in the central versus peripheral choroid were predicted to have lower activation in the central tissue. The functions included cytoplasm organization, hormone quantity, filament and cellular

protrusion formation phospholipid release, podocyte apoptosis, and arterial remodeling.

In the central versus peripheral sclera, cell death and formation of cells were predicted as increased in the central tissue, while tabulation of cells was predicted as decreased.

Table 10: Significant Predicted Activation Functional Assignments for Central versus Peripheral Expression.

Negative z-scores predict higher functional activation in central tissues, while positive z-scores predict lower activation in central tissues. Significance of each functional group (with number [#] of genes) is given as a p-value.

Tissue	Functions Annotation	p-Value	Regulation z-score	# Genes
Retina	polymerization of filaments	2.09X10 ⁻³	-3.095	11
	proliferation of liver cells	7.61X10 ⁻³	-2.837	14
	quantity of retinal cells/ photoreceptors	4.15X10 ⁻⁴	-2.559	9
	polymerization of microtubules	7.82X10 ⁻⁴	-2.515	7
	fusion of embryonic tissue	4.22X10 ⁻³	-2.488	4
	proliferation of mammary epithelial cells	4.22X10 ⁻³	-2.446	4
	cell movement of prostate cancer cell lines	9.37X10 ⁻⁴	-2.431	10
	arterial occlusive disease/ atherosclerosis	5.40X10 ⁻⁴	-2.394	33
	invasion of cells	7.13X10 ⁻⁸	-2.32	61
	cell movement of tumor cells	4.85X10 ⁻³	-2.31	12
	cleavage of cells	7.67X10 ⁻³	-2.108	12
	metabolism of acylglycerol	7.20X10 ⁻³	2.099	12
	synthesis of triacylglycerol	5.54X10 ⁻³	2.079	7
	contractility of cardiomyocytes	6.51X10 ⁻³	2.034	5
metabolism of triacylglycerol	3.69X10 ⁻³	2.031	10	
Choroid	organization of cytoplasm	1.34X10 ⁻²	2.516	72
	quantity of hormone	2.19X10 ⁻²	2.303	31

	formation of filaments	4.56X10 ⁻²	2.282	26
	release of phospholipid	1.19X10 ⁻²	2.227	4
	formation of cellular protrusions	9.53X10 ⁻³	2.188	32
	apoptosis of podocytes	2.46X10 ⁻³	2.032	4
	remodeling of artery	2.46X10 ⁻³	2.009	4
	cell death of tumor cell lines	1.15X10 ⁻²	-2.174	46
Sclera	formation of cells	5.59X10 ⁻³	-2.029	16
	tubulation of cells	8.65X10 ⁻³	2.753	5

2.3.2.3 Canonical Pathway Analyses

The most significant central versus peripheral pathways for all tissues all included signaling pathways like the adult versus fetal tissues (Table 11). However, none of the tissues shared signaling pathways in their five most significant pathways. The most significant pathway in the central versus peripheral retina was axonal guidance signaling. Other significant pathways in the retina involve growth, expression and immune regulation. In the choroid, pathways involve B-cell biology and the immune response. In the sclera that pathways involve cell growth, regulation and lipid synthesis.

Table 11: Five Most Significant Central versus Peripheral Tissue Canonical Pathways.

Significance (p-value) of pathways is determined by Fischer's exact test of probability of genes in the dataset fit into the pathway by chance alone and by proportion (ratio) of genes in pathway that are included in the dataset (# Genes).

Tissue	Ingenuity Canonical Pathways	-log(p)	Ratio	# Genes
Retina	Axonal Guidance Signaling	8.23	1.02X10 ⁻¹	44
	Ephrin Receptor Signaling	4.24	1.01X10 ⁻¹	20
	14-3-3-mediated Signaling	3.75	1.23X10 ⁻¹	15
	CXCR4 Signaling	3.49	1.01X10 ⁻¹	17
	Breast Cancer Regulation by Stathmin1	3.15	9.13X10 ⁻²	19
Choroid	April Mediated Signaling	2.54	1.63X10 ⁻¹	7
	B Cell Activating Factor Signaling	2.41	1.56X10 ⁻¹	7
	CXCR4 Signaling	2.29	9.52X10 ⁻²	16
	Role of IL-17A in Arthritis	2.22	1.27X10 ⁻¹	8
	IL-17A Signaling in Fibroblasts	2.09	1.50X10 ⁻¹	6
Sclera	PAK Signaling	3.03	7.48X10 ⁻²	8
	Glycine, Serine and Threonine Metabolism	2.92	4.76X10 ⁻²	7
	Thrombin Signaling	2.87	5.83X10 ⁻²	12
	ATM Signaling	2.75	1.02X10 ⁻¹	6
	Glycosphingolipid Biosynthesis - Globoseries	2.71	9.76X10 ⁻²	4

2.4 Conclusions

2.4.1 Differential Expression of Ocular Growth

Phenotypic changes in the tissues examined in this study have been seen in myopic eyes, consequently, genetic changes in any or all of these tissues may contribute to myopic development (Rada, Shelton et al. 2006). We hypothesized that genes which

when altered contribute to the development of myopia, may be part of normal growth and development mechanisms in ocular tissues. We assessed differentially expressed genes between rapidly growing fetal tissues relative to their mature adult counterparts. We examined the functions of those differentially expressed genes to extrapolate information regarding the mechanisms of ocular disease relating to excess axial growth and other associated physical characteristics.

Of nearly 40 genes previously identified as being associated with increased susceptibility for non-syndromic high myopia in in one or more multi-family cohort, we identified 17 in the ten most significant functional assignments in at least one adult versus fetal tissue comparison (*BMP2K, CHRM2, CHRM3, CFI, COL1A1, COL2A1, FMOD, HGF, IGF1, LAMA1, LEPREL1, LUM, MYOC, PAX6, PRELP, TGFB2* and *VDR*). An additional five myopic-associated genes were also differentially expressed; however, they were not part of the most significant functional assignments (Table 8). Of these genes in the most significant functional groups, nine were down-regulated in adults for all tissue types, five were up-regulated in adults for all tissue types, and three had contradicting directions of expression fold changes by tissue type. Further functional and pathway analyses of genes previously implicated in myopic growth which are differentially expressed and belonging to the most significant functional assignments in

the adult versus fetal tissue comparisons may help to further elucidate their tissue specific roles in myopic development as well as other potentially new candidates.

Additionally, knowing in which tissue(s) these genes are changing their activity during and after growth may help to understand their diversity and possible contributions to disease progression. This data showed that a number of structural genes are differentially expressed in tissues upstream of the sclera, the retina/RPE and choroid. A better understanding of what changes may be occurring within these tissues may help to understand how the signal is carried from tissue to tissue without any known direct communication channels.

2.4.1.1 Retina/RPE

In our data, only three non-syndromic myopic-associated genes, *COL2A1*, *FMOD* and *LAMA1* were found in the most significant functional classifications in the retina/RPE. However, two other genes, *HGF* and *LUM*, were slightly below fold change cut-offs in this tissue with the lowest average fold changes. Our methods of averaging the adult retina and RPE may have contributed to the reduced fold changes seen. *HGF*, *LUM* and other non-syndromic high myopia associated genes may be playing larger roles in the retina/RPE than indicated by our data, and should be investigated further.

In the retina/RPE both *COL2A1* and *FMOD* belonged to the only most highly significant group in any of the tissues with immune response functions in common,

while their other functional annotations were similar in all tissues. These two genes also both have been implicated in connective disorders beyond non-syndromic myopia (Brown, Vandenberg et al. 1995; Jepsen, Wu et al. 2002). Further, these two genes are both differentially expressed in the retina/RPE and sclera, but not the choroid despite the choroid containing the largest number of differentially expressed myopic associated genes. This detected pattern suggests that further exploration of the potential connection in their roles in myopic development may be warranted.

Multiple factors must be considered when drawing conclusions from the results of the retina/RPE tissue comparisons. First, the tissue was collected differently in fetal and adult samples due to physical constraints with the tissue. The methods of averaging the adult tissue almost certainly are imprecise and are difficult to qualitatively assess. Second, the differences in cellular makeup within the human macula may contribute to differences seen that are unrelated to growth. Lastly, the overall low fold changes seen in the tissue make it difficult to assess the biological importance of differences identified. Taken together, these limitations suggest that biologically important differences may not be detected in this analysis, while additional noise may be present in the current dataset. However, despite these limitations there are similarities in this tissue with the other tissues identified which suggest it can still be used for its intended purpose of studying candidate genes and pathways for myopic development so long as adequate

consideration is given to the limitations and sufficient validations are performed before drawing conclusions.

While this data alone cannot substantiate any claims of mechanistic roles, it may be used to generate hypotheses for further testing. Possible research pursuits based on this information include but are not limited to tissue specific manipulations to understand how the same genes could yield different physical characteristics, particularly in the retina/RPE, which unlike the sclera is not predominantly a tissue of structural support, and exploration of a possible role in defects of the immune system resulting in ocular disease. *LAMA1* on the other hand was present in the retina/RPE, choroid and sclera. Further research is needed to determine if the expression is related to a signaling cascade resulting in extracellular matrix remodeling in the sclera, or if the same gene may be playing different developmental roles in other tissues.

2.4.1.2 Choroid

In the choroid, *CHRM3*, *COL1A1*, *IGF1*, *LAMA1*, *LEPREL1*, *LUM*, *MYOC*, *TGFB2*, and *VDR* belonged to some of the most significantly enriched functions. The largest number of differentially expressed genes was in the choroid, supporting its diverse roles in many aspects and mechanisms of ocular growth and development. Given the choroids intermediate location and functional interactions between the retina/RPE and sclera one might reasonably expect to find these myopia associated genes given the

diverse functionality of the tissue and numerous possible roles in ocular growth and development. It is possible that other genes regulating the extracellular matrix and surrounding tissues may have yet to be discovered for their roles in myopic development. Screening our growth differentiated genes for genes in pathways upstream of these six myopic-associated genes may yield promising novel candidates. The presence of *IGF1* and *TGFB2* fits with the model of the choroid acting as an intermediate tissue transmitting signals to nearby tissues such as the sclera. However, like in the retina/RPE the presence of genes thought to play physical, structural roles such as collagens and proteoglycans, should be further studied to elucidate their possible developmental roles in the choroid. These genes could play a structural role within the choroid itself or signaling to the nearby sclera.

2.4.1.3 Sclera

In the sclera *CHRM2*, *COL2A1*, *HGF*, *IGF1*, *LAMA1* and *MYOC* were all present in the most significant functional assignments. This fibrous tissue is most visibly remodeled or thinned in highly myopic eyes permitting elongation of the eye; however, these resultant changes are likely a consequence of upstream signals from the retina. The presence of two growth factor genes and three structural genes associated with high myopia may reflect their roles in extracellular matrix changes seen in highly myopic eyes which may or may not be sufficient to initiate or maintain disease progression on

their own. Further exploration of these and related genes functions in normal growth may help to explain their contributions to myopic development. Also, upstream analyses of genes regulating their change may help explain how they are regulated in myopic development. The low fold changes seen in the sclera may reflect a delicate mechanism of tissue remodeling, disruption of which could yield substantial physical changes such as the significantly thinned tissue in highly myopic eyes.

2.4.1.4 Optic Nerve

In the optic nerve, differentially expressed genes *COL1A1*, *CFI*, *FMOD*, *LUM*, and *TGFB2* were present in the most significant functional assignments. However, *CFI*, which is implicated in choroidal neovascularization associated with high myopia rather than myopia itself (Leveziel, Yu et al. 2012), was only differentially expressed in the optic nerve and present in just one functional group. Given that the analyses failed to meet statistical significance, it was present in only the largest functional group and the fold change for *CFI* was relatively small in the tissue, it cannot be considered conclusive evidence. *FMOD* and *LUM* are believed to play important roles in collagen assembly (such as *COL1A1*), which occurs during development in the optic nerve. Changes to the collagens in the optic nerve independently may not likely play a significant role in myopic development as changes in the optic nerve are not prominent physical characteristics of highly myopic eyes. The functional categories for each of these genes

also include genes implicated in syndromic myopia, suggesting these changes may affect more phenotypes than those seen in non-syndromic high myopia. Given the significance limitations, minimal inferences can be drawn from the data of the optic nerve. However, this information may be compared to other fibrous tissues, such as the cornea and sclera for patterns in ocular growth.

2.4.1.5 Cornea

Lastly, in the cornea, *COL1A1*, *FMOD*, *MYOC*, *PAX6*, *PRELP* and *VDR* were all present in the most significant functional categories. While the cornea had only a little over half the number of differentially expressed genes as the choroid, the average fold change was highest for the cornea despite it being one of two tissues with a reduced sample size. The most significant functional groups in the cornea shared the highest number of non-syndromic myopic-associated genes with the choroid, and had the highest number of combined non-syndromic and syndromic myopic-associated genes of all tissue types. *COL1A1*, *FMOD*, *MYOC* and *VDR* all had their highest fold changes in the cornea, while *PAX6* and *PRELP* were only differentially expressed in the cornea. The relatively high fold-changes in the cornea may suggest significant changes, possibly on/off, take place in the developing versus mature cornea but these may or may not relate to myopic progression. These genes may be associated with high myopia due to their roles in other tissues, whether differentially expressed or not. Mutations and

normal variances in these genes may yield more significant physical changes due to this underlying framework. Other genes contributing to myopic associated clinical features may yet to be uncovered in this tissue. Further review of the functions and pathways of these differentiated genes may elucidate novel candidates.

2.4.1.6 Syndromic Myopia and Ocular Growth

In addition to cataloging genes known to be associated with non-syndromic high myopia, we also considered those genes identified in syndromes which include myopia as well as ocular conditions predisposed by myopia. While the focus of this paper was to use ocular growth to understand myopic development, the data collected has many potential uses in understanding normal growth as well as the development of other ocular disorders. Screening genes associated or causal for syndromes which include a myopic component may also help us to understand how myopic development relates to other diseases while at the same time demonstrating the yet to be reached potential of the data.

Within all tissue types tested the most significant functional groups containing non-syndromic high myopia genes also contained a number of genes either associated with or causal for syndromes including myopic components (data not shown). Those functional categories in tissues of the most overlap with known non-syndromic high myopia genes frequently included collagen genes implicated in syndromic forms of

myopia. The expression patterns of genes associated with myopic development support the idea that myopic growth can result from disruptions to the extracellular matrix's collagen (Yang, Li et al. 2009). However, causal mutations in collagen genes have not been found for non-syndromic myopia, suggesting these mutations likely effect more than AL or corneal refractive power.

In addition to those implicated in myopic growth, a number of other collagen genes were also overlapping, some of which have been implicated in other ocular disorders predisposed by high myopia such as glaucoma. Interestingly, a number of genes which have been associated with non-syndromic and syndromic myopia and numerous other ocular disorders were among the most differentially expressed genes in every tissue examined (Appendix B). Collagens, which have been implicated in a number of ocular disorders (Hansen 1963), made up the majority of these genes in every tissue type. As an example of further potential of the data, it may be worth noting that in addition to collagens, a number of genes associated with other ocular disorders were also among the most differentially expressed genes, such as *NTM* (MIM 607938), which was recently implicated in increased susceptibility to primary open angle glaucoma (Ulmer, Li et al. 2012).

2.4.1.7 Conclusions

We present here the first whole genome expression analysis comparing human adult versus fetal ocular retina/RPE, choroid, sclera, cornea and optic nerve. Since the samples were not completely randomized across chips, some true expression differences may have been removed in chip normalization steps. Additionally, combining the retina and RPE as well as possible differences in the contributing tissues cellular makeup may also have reduced our power to detect differences, which may account for the relatively low number of differentially expressed genes and their corresponding fold changes. While the optic nerve comparisons failed to reach statistical significance, they still shared much in common with other adult versus fetal comparisons, possibly lending some credibility to their validity. We have also shown promising supportive data for human ocular growth as a model for ocular growth disorders. However, our model includes genes that are involved in ocular growth and development, which is a good starting point to identify and interpret genes potentially contributing to myopic development.

2.4.2 Central versus Peripheral Differential Expression

The central versus peripheral tissues failed to reach statistical significance casting doubt on their validity. However, the most significant functional categories of differentially expressed genes in those tissues reflected many known differences in those

tissues spatially, such as changes in cell and vasculature concentration and extracellular matrix organization. Despite myopic axial elongation being localized to the posterior pole, few genes previously implicated in myopic development were differentially expressed between the posterior and peripheral tissues or present in enriched functional groups between the tissues. This may be explained by tissues exerting local control on ocular growth in response to visual stimuli which primarily affect the posterior region rather than underlying genetic differences. However, the spatial differences between the tissues can provide clues to ocular development and possibly other diseases.

For over 100 years, scientists have debated the origins of glaucoma as either mechanical or vascular (Sugiyama, Townsend et al. 1993; Flammer, Orgul et al. 2002; Barbara M. Wirostko 2009). The vasculature theory suggests that glaucoma is caused by atrophy of the ocular tissues due both to increased intraocular pressure as well as vasculature changes in providing nutrients (Sugiyama, Townsend et al. 1993; Flammer, Orgul et al. 2002; Barbara M. Wirostko 2009). In the central versus peripheral retina a functional group of arterial occlusive disease genes were predicted to be significantly decreased, and contains known central corneal thickness/glaucoma gene *CAV1* (Table 10). This increase in vascular functional groups may be due to the increased concentration of vasculature in the central relative to the peripheral region. However, the increased expression in peripheral tissues of vasodilators such as *ADRB2* (MIM

109690) (Hesse, Schroeder et al. 2010) and *NOS3* (MIM 163729) (Adams 2006) cannot be accounted for by the same means. The increased presence of these types of molecules in the peripheral tissues may explain the pattern of cell death if vasculature blockage indeed can cause glaucoma. Blockages in the posterior vasculature may reduce pressure and consequently blood flow to the peripheral tissues resulting in malnutrition and cell death of the outermost ganglion cells progressing inward as blood flow worsens over time (Waliszek-Iwanicka, Waliszek et al. 2010). Vasodilators may also account for the lack of a segmented form of cell death caused by a blockage in the peripheral tissue. Additionally, the peripheral choroid is predicted to have increased arterial remodeling which can help to maintain blood flow in the event of a lesion. Further analysis of functional characteristics and pathway interactions in spatial differences in these ocular tissues may further elucidate their possible roles in glaucoma development. However, follow up validation will be essential given the lack of significance in the array data.

3. Refining the *MYP3* Locus

In addition to evidence for linkage with the qualitative trait of high myopia (Young, Ronan et al. 1998; Farbrother, Kirov et al. 2004; Nurnberg, Jacobi et al. 2008; Li, Guggenheim et al. 2009), quantitative trait linkage analyses also revealed nominally significant LOD scores in the *MYP3* locus for SPH (Abbott, Li et al. 2012). The region implicated by the independent qualitative linkage studies, *MYP3*, spans nearly 44 Mb (Figure 9) making candidate sequencing studies impractical in narrowing down the region. Finer mapping, such as SNP association, may help to prioritize candidates within the region. *MYP3* may contain variants that associate with high myopia as well as those with quantitative traits used to measure the degree of refractive error. However, the size of this linkage peak limits the number of SNPs that can be cost and resource effective; thus further prioritization of candidate genes after association is necessary. To refine the chromosome 12 high myopia linkage peak, *MYP3*, we conducted a peakwide SNP qualitative and quantitative association mapping study in our high-grade myopia family cohort.

3.1 Methods

3.1.1 Patient Cohort

The cohort consisted of Caucasian families of three or more individuals previously collected by T. L. Young and used in whole genome linkage analyses

replicating the *MYP3* locus (Li, Guggenheim et al. 2009). Phenotypic information was collected by ocular examination for each family member included in the study. Affected individuals were characterized with high-grade non-syndromic myopia using the same criteria as in previous linkage analyses (dioptric SPH measurement of less than or equal to -5.00 in the better of two eyes and an onset by the age of 12 years) (Li, Guggenheim et al. 2009). Families with highly myopic phenotypes were preferentially selected and they were included in the analyses on the exclusive basis of the presence at least one high grade myopia family member. The average SPH for the individuals in the cohort was -4.78 D (affected: -10.44 D; others: -1.36 D). Previous evidence of positive linkage to *MYP3* was not considered when choosing families.

The cohort consisted of 530 individuals from 67 families of various sizes. The average family size was 7.91 individuals with a range of three to 35 individuals per family. The cohort was evenly comprised of males and females (N=265 each). Patients with ophthalmologic conditions, which might predispose them to high myopia or syndromic disorders, such as Stickler, Ehler-Danlos, or Marfan syndromes, were excluded from this study. The cohort was comprised entirely of Caucasians to reduce ethnic stratification issues. All participants provided written informed consent that was approved by Duke University's Institutional Review Board and adhered to the tenets of the Declaration of Helsinki guidelines.

3.1.2 Genotyping Methods

3.1.2.1 SNP Selection

A list of all potential SNPs was generated by Illumina® (San Diego, CA) upon submission of the requested 44 Mb region. The region was covered using non-uniform SNP density. Seven hundred and sixty eight SNPs were distributed across the region at a base density of one SNP every 60 kb with regions of a higher density SNP placement of one every 40 kb. The regions of higher density SNP placement were: 1) The region of overlap between Young et al. and Nürnberg et al.; 2) The region of overlap between Young et al. and Farbrother et al.; 3) The highest peak region of Li et al (Figure 9) (Young, Ronan et al. 1998; Farbrother, Kirov et al. 2004; Nurnberg, Jacobi et al. 2008; Li, Guggenheim et al. 2009). SNPs were selected using the following criteria: 1) location (as described above); 2) Minor Allele Frequency (MAF) > .05; 3) Illumina® designability score > 0.7 (with preference to higher scores); 4) coding non-synonymous > coding synonymous > UTR > intronic.

3.1.2.2 Genotyping and Quality Control

Genomic DNA was extracted from each individual from either blood or saliva as previously described (Oliveira, Li et al. 2005). Family members were genotyped using custom designed 768-plex Oligo Pool Assay (OPA) Goldengate Universal 32 BeadChip Kits from Illumina®. Samples were directly hybridized to the chips and detected by

Illumina®'s iScan system. The Goldengate assays were run with 672 samples on seven 96-well plates which included 28 quality controls. These samples included an additional 114 individuals from 15 families of Hispanic, Latino, Asian or African American descent, which were excluded from analyses due to ethnic stratification issues, but were later analyzed to assess consistency. Each genotyping plate included two Centre d'Etude du Polymorphisme Humain (CEPH) DNA samples as well as two internal replicates with masked identity during analysis. The internal replicates were selected from samples in the cohort, which had sufficient quantities of DNA for duplicate genotyping. The CEPHs and internal replicate genotypes were checked for concordance.

The data were cleaned using Illumina's® GenomeStudio. Samples with a call rate below 95% and parent to child Mendelian errors above 1% were removed (N= 59 and 12 respectively) from further analyses. SNPs with a call rate below 95% (N = 15) and Mendelian errors over 95% (N = 3) were also removed from further analyses. Mendelian inconsistencies and relationships within families were screened using Pedcheck (O'Connell and Weeks 1998). Deviations from Hardy-Weinberg equilibrium (HWE) were checked using Genetic Data Analysis (GDA) (Paul and Dmitri 2006). Markers were removed from analyses if the control population deviated from HWE ($p < 0.05$) (N = 32). Pairwise linkage disequilibrium (LD) within the population was checked using

Graphical Overview of Linkage Disequilibrium (GOLD) and LD Select (Abecasis and Cookson 2000; Carlson, Eberle et al. 2004).

3.1.3 Association Analyses

3.1.3.1 Qualitative Association Analyses

The Association in the Presence of Linkage test (APL) (Martin, Bass et al. 2003) was used in qualitative association tests because it infers absent parental genotypes using estimates of identity by descent allowing for single and multi-locus haplotype analysis. Individuals were classified as affected for high myopia if both of their eyes were ≤ -5 spherical D; individuals with ≥ -0.05 spherical D in both eyes were classified as unaffected; all other individuals- including those with missing phenotype data- were classified with an unknown affection status. Consistency of the data was checked with the same affection classifications using the additional non-Caucasian individuals as well as with another common biometric parameter used in determining myopic refraction, SE.

3.1.3.2 Quantitative Analyses

The Quantitative Trait Linkage Disequilibrium Test (QTLD) (Havill, Dyer et al. 2005) in Sequential Oligogenic Linkage Analysis Routines (SOLAR) (Almasy and Blangero 1998) was conducted by treating refractive errors as quantitative traits. Quantitative tests were run using the average (avg) SPH phenotype of the two eyes.

Additionally, quantitative analyses were conservatively performed for SPH and SE by taking the better, or less myopic, of the two eyes. The same affection classifications using the additional non-Caucasian individuals as well as SE were again tested for consistency. The QTLD tests were run using the default model including identity by descent calculations of our study population. The QTLD test calculations of identity by descent were obtained using SOLAR (Almasy and Blangero 1998).

3.1.4 Independent Cohort Validation

3.1.4.1 International High Myopia Cohort

Five (DNA quantities prohibited additional candidate screening; please refer to Results Section [3.2.3] for selection criteria) of the most significantly associated SNPs from qualitative and quantitative testing were genotyped in an independent collection of Caucasian high-grade myopia pedigrees recruited from four international collection sites. These pedigrees have been described previously (Li, Guggenheim et al. 2009). The validation SNPs were selected for their significance in each test as well as any overlap with other tests. Genotyping was performed using Taqman® allelic discrimination assays (Table 12) with quality control measures as previously described (Yanovitch, Li et al. 2009). Qualitative and quantitative tests, described above, for both SPH and SE were used for each SNP.

Table 12: Taqman® Genotyping Assay Identification Numbers.

SNP	Assay ID
<i>rs4764971</i>	C__30866249_10
<i>rs7134216</i>	C__30023434_10
<i>rs17306116</i>	C__33218892_10
<i>rs3803036</i>	C__25749934_20
<i>rs824311</i>	C__8342112_10

3.1.4.2 The Twin Eye Study

Qualitative and quantitative tests for SPH were previously carried out in a cohort comprised of a sample of twins (UK Twin Study) that were not recruited on the basis of their refractive error (Hysi, Young et al. 2010). These test results were used as a second independent validation cohort. As described (Hysi, Young et al. 2010), this cohort of twins had been SNP genotyped at high density across the entire genome. All of the SNPs selected for the discovery association tests, including some of our most significantly associated candidates, were not genotyped in this cohort. All the most significantly associated SNPs from both the qualitative and quantitative discovery analyses were screened in the twin test results. SNPs in high linkage disequilibrium with the most significantly associated SNPs not genotyped in the cohort were also screened, but none were genotyped in the cohort.

3.2 Results

3.2.1 Qualitative Association

Testing for association with high myopia status was carried out using APL with affection classified as individuals with a dioptric SPH ≤ -5 D and unaffected individuals as having ≥ -0.50 D. After stringent quality control (please refer to the Methods Section [3.1.2.2]), 702 SNPs remained. While no SNPs passed Bonferroni correction significance levels, the most associated SNPs were evaluated as possible candidates (Figure 12). Table 13 contains the five SNPs with the lowest p-values for APL ($p < 6 \times 10^{-3}$) and their corresponding quantitative p-values. The three SNPs with the highest probability of association are located over 50 kb from the nearest genes: *rs741525* ($p=7.80 \times 10^{-4}$), *rs790436* ($p=5.09 \times 10^{-4}$), and *rs1358228* ($p=1.29 \times 10^{-3}$). The two SNPs with the next highest association probabilities are located within coding genes: *rs7134216* ($p=2.74 \times 10^{-3}$) is intronic to the *UHRF1BP1L* gene (*UHRF1* [MIM 607990] binding protein 1-like isoform b), and *rs3803036* ($p=5.65 \times 10^{-3}$), is a non-synonymous coding variant in the *PTPRR* gene (protein tyrosine phosphatase receptor type R; MIM 602853).

3.2.2 Quantitative Association

Quantitative tests were performed to test each SNP for association with the average SPH endophenotype. The quantitative tests showed markers with overlapping significance with the qualitative results. Figure 12 shows both the qualitative and

quantitative association results for the 702 SNPs that passed quality control measures. The five most significantly associated SNPs that met the Bonferroni threshold with 702 SNPs of $p < 7.12 \times 10^{-5}$ ($\alpha=0.05$). The first and fourth most significant SNPs, *rs4764971* ($p=2.25 \times 10^{-7}$) and *rs7134216* ($p=4.49 \times 10^{-5}$), are over 100 kb apart, though not in LD (Table 13). The first SNP, *rs4764971*, is located in the 3' UTR of the longest isoform of the gene *DEPDC4* (DEP domain containing 4) and is also intronic in *ACTR6* (actin-related protein 6), while *rs7134216* is the same intronic SNP located in the gene *UHRF1BP1L* as in APL results. The second best SNP intronic in *PPFIA2* (*PTPRF* interacting; MIM 603143), *rs17306116* ($p=2.65 \times 10^{-5}$), was also statistically significant. While *rs1520562* and *rs1558726* also withstood Bonferroni correction, they are in regions that are at least 600 kb and 150 kb, respectively, from the nearest genes. The region containing *rs1520562* is conserved in higher primates, rhesus, marmoset and guinea pig but not in rats, mice, other mammals, or lower vertebrates (Table 14).

Table 13: Most Significant SNPs from Qualitative and Quantitative Association Testing.

P-values that withstood Bonferroni correction by number of SNPs (**bold**) and by number of tests including those not presented in this paper (**bold**). Base pairs are based on human genome build 36.2, chromosome 12. Minor allele frequency (MAF) is for Caucasians.

Base Pair Location	SNP	Gene Location	MAF	Qualitative SPH p-value	Qualitative SE p-value	Quantitative SPH p-value	Quantitative SE p-value
69425930	<i>rs3803036</i>	Coding nonsyn. in <i>PTPRR</i>	.258	5.65X10 ⁻³	5.68X10 ⁻³	9.39X10 ⁻³	3.92X10 ⁻⁴
71970854	<i>rs1520562</i>	> 600 kb from nearest gene	.271	0.875	0.606	3.51X10⁻⁵	6.07X10 ⁻⁴
76672201	<i>rs1358228</i>	76 kb upstream of <i>NAV3</i> (MIM 611629)	.415	1.29X10 ⁻³	1.60X10 ⁻³	2.22X10 ⁻²	0.152
80351222	<i>rs17306116</i>	Intronic <i>PPFIA2</i>	.119	0.195	0.428	2.65X10⁻⁵	1.76X10 ⁻³
86528808	<i>rs790436</i>	> 150 kb from nearest gene	.425	7.80X10 ⁻⁴	9.98X10 ⁻⁴	2.12X10 ⁻³	3.63X10 ⁻³
96200365	<i>rs1558726</i>	> 150 kb from nearest gene	.108	4.86X10 ⁻²	1.42X10 ⁻²	6.36X10⁻⁵	6.57X10 ⁻⁴
97316149	<i>rs741525</i>	55 kb from <i>SLC9A7P1</i>	.325	5.09X10 ⁻⁴	2.12X10 ⁻³	0.698	0.279
99043879	<i>rs7134216</i>	Intronic <i>UHRF1BP1L</i>	.233	2.74X10 ⁻³	4.71X10 ⁻³	4.49X10⁻⁵	4.64X10⁻⁶
99155927	<i>rs4764971</i>	3 ¹ UTR of <i>DEPDC4</i> , intronic <i>ACTR6</i>	.133	4.62X10 ⁻²	0.176	2.25X10⁻⁷	2.01X10⁻⁵

Table 14: Evolutionary Conservation of Candidate SNPs from Association.

'X' indicates SNP is conserved in the given species.

SNP	Chimp	Orangutan	Rhesus	Marmoset	Mouse	Rat	Cow	Pig	Guinea Pig	Dog	Elephant	Opossum	Chicken
<i>rs3803036</i>	X	X	X	X	X	X	X	X	X	X	X	X	X
<i>rs1520562</i>	X	X	X	X					X		X		
<i>rs1358228</i>	X	X	X	X	X	X	X	X	X	X	X		
<i>rs17306116</i>	X	X	X	X						X	X		
<i>rs790436</i>	X	X	X	X					X	X	X		
<i>rs1558726</i>	X	X	X	X	X	X			X		X		
<i>rs741525</i>	X	X		X			X	X	X	X	X		
<i>rs7134216</i>	X	X	X	X			X		X				
<i>rs4764971</i>	X	X	X			X	X			X	X		

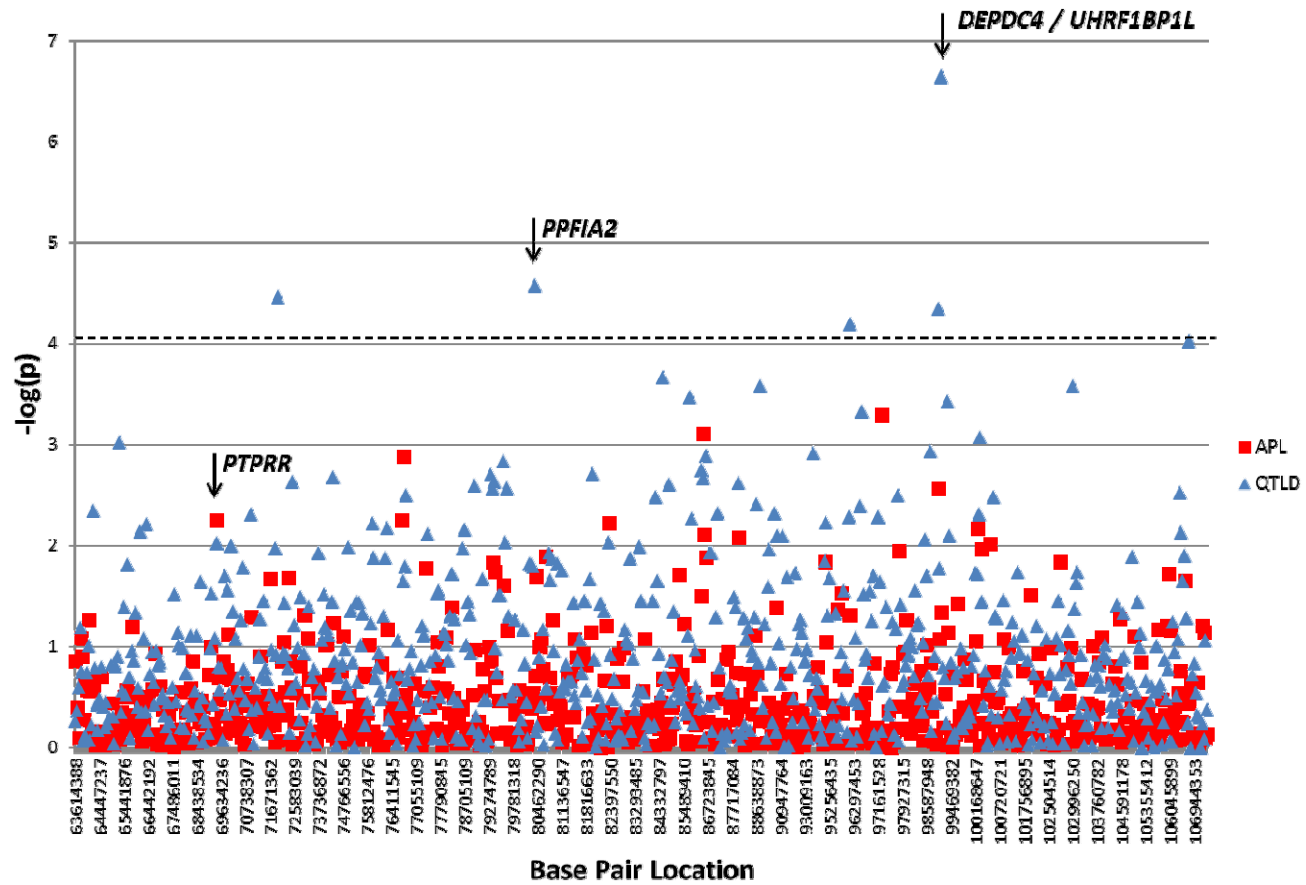


Figure 12: Association in the Presence of Linkage (APL) and Quantitative Trait Linkage Disequilibrium (QTLD) Association Results by $-\log(p)$.

P-values for each SNP are stacked in the same vertical position and indicated by separate symbols. The blue triangles Δ indicate average of two eyes (avg) SPH QTL results. The red squares \square indicate the high myopia by SPH APL results. The dashed line --- indicates the Bonferroni significance threshold by number of SNPs. Base pairs are given in human genome build 36.2, chromosome 12. (© Felicia Hawthorne, 2012)

3.2.3 International High Myopia Cohort

Three candidate SNPs were selected from both the qualitative and from the quantitative test results, one of which overlapped, giving five SNPs in total (Table 15). SNPs were selected based on their association probabilities and overlap between qualitative and quantitative test results. The SNPs selected from qualitative test results were located in or near *PTPRR*, *UHRF1BP1L* and *UTP20*. The SNPs selected from quantitative test results were located in or near *DEPDC4*, *UHRF1BP1L* (same SNP from qualitative test results), and *PPFIA2*.

As in the discovery cohort, none of the SNPs tested in the independent Caucasian, family based, high-grade myopia cohort was significant in tests using the qualitative SPH trait definition. One of the two SNPs in PTP genes approached significance: *rs17306116* intronic in *PPFIA2* ($p = 7.37 \times 10^{-2}$). In tests using the quantitative SPH trait definition, two SNPs had p-values below 0.05, but only one survived multiple testing correction criteria: *rs7134216* in *UHRF1BP1L* ($p = 2.63 \times 10^{-3}$). SNPs in/near the two PTP genes approached significance: *rs3803036* (*PTPRR*; 1.50×10^{-2}) and *rs17306116*

(*PPFIA2*; 6.59×10^{-2}). Both qualitative and quantitative SE results were comparable to SPH results (Table 15).

Table 15: Validation of the Most Significantly Associated SNPs in an Independent High Myopia Cohort.

Qualitative (Qual.) and quantitative (Quant.) association results for five candidate (based on significance and proximity to a known gene) SNPs genotyped in an independent high myopia cohort for dioptric sphere (SPH) and spherical equivalence (SE). Base pairs are based on human genome build 36.2, chromosome 12.

Base Pair Location	SNP	Gene Location	Qual. SPH p-value	Quant. SPH p-value	Qual. SE p-value	Quant. SE p-value
69425930	<i>rs3803036</i>	Nonsyn. <i>PTPRR</i>	0.881	1.50X10 ⁻²	0.943	1.18X10 ⁻²
80351222	<i>rs17306116</i>	Intronic <i>PPFIA2</i>	7.37X10 ⁻²	6.59X10 ⁻²	6.28X10 ⁻²	1.81X10 ⁻²
99043879	<i>rs7134216</i>	Intronic <i>UHRF1BP1L</i>	0.114	2.63X10 ⁻³	0.173	1.64X10 ⁻³
99155927	<i>rs4764971</i>	Exonic <i>DEPDC4</i>	0.555	0.172	0.551	0.210
100195248	<i>rs824311</i>	3 kb upstream <i>UTP20</i>	0.509	0.806	0.460	0.850

3.2.4 The Twin Eye Study

We also sought evidence of replication of our most strongly associated SNPs in an independent cohort of twins not ascertained on the basis of refractive error, for whom genome-wide genotyping and imputation had previously been carried out (Hysi, Young et al. 2010). As shown in Table 16, none of our SNPs demonstrated evidence of replication in this cohort; however, one of our most significantly associated quantitative SNPs that was not selected for validation in the high-grade myopia validation cohort, *rs1520562*, had a SPH p-value of 2.4×10^{-2} for quantitative, 7.5×10^{-2} for qualitative testing and was directionally consistent with our discovery data.

3.2.5 Concordance of SPH and SE Endophenotypes and Complete Multi-Ethnic Cohort in Discovery Data

Though this paper focuses on qualitative high myopia determined by SPH measurements and the quantitative trait SPH due to their relation to the ocular tissues discussed, it should be noted that other tests were performed in the discovery cohort, but not reported. In addition, by SE qualitative high myopia as well as quantitative testing was performed. Qualitative tests for SE revealed many of the same most significantly associated candidate SNPs and genes as those in SPH tests (Table 17). Quantitative tests for SPH and SE were also concordant for both the avg of both eyes as well as the better of the two eyes, though there was some shuffling of the order of the most significantly associated SNPs (Table 18; data not shown). As no SNPs in the

qualitative data were statistically significant, the additional tests do not drop any SNPs from statistical significance. In the quantitative testing, the three SNPs in the candidate genes presented in this paper all withstood statistical significance cut-offs after correction for multiple testing (4212 tests, Table 13).

Additionally, as previously noted, the discovery cohort contained an additional 114 individuals of Hispanic, Latino, Asian or African American descent which were excluded from analyses to avoid ethnic stratification issues. Ethnic stratification was of particular concern in QTLD testing, which utilized founder genotypes that can be skewed by population stratification (Havill, Dyer et al. 2005). However, the entire, multi-ethnic cohort was also analyzed independently for APL testing, which was less susceptible to population stratification, as well as QTLD testing. The most significant SNPs for both APL and QTLD were very similar between the Caucasian-only and the complete cohort (Tables 17 and 18).

Table 16: Validation of the Most Significantly Associated SNPs in a Previously Genotyped Independent Cohort.

Qualitative (Qual.) and quantitative (Quant.) association results for most significant SNPs from our discovery data which were previously genotyped and analyzed in an independent twin dataset. Base pairs are based on human genome build 36.2, chromosome 12.

Base Pair Location	SNP	Gene Location	Qual. SPH p-value	Quant. SPH p-value
69425930	<i>rs3803036</i>	Nonsyn. in <i>PTPRR</i>	0.73	0.15
71970854	<i>rs1520562</i>	> 600 kb from nearest gene	0.075	0.024
76672201	<i>rs1358228</i>	76 kb upstream <i>NAV3</i>	0.17	0.32
78976016	<i>rs7315130</i>	> 100 kb from nearest gene	0.86	0.97
80351222	<i>rs17306116</i>	Intronic <i>PPFIA2</i>	0.82	0.99

Table 17: APL Concordance with SPH, SE and Mixed Ethnicities.

Marker / Gene Location	SE	Marker / Gene Location	SPH	Marker / Gene Location	Caucasian SPH	Marker / Gene Location	Caucasian SE
<i>rs741525</i> 55 kb from <i>SLC9A7P1</i>	1.55X10 ⁻³	<i>rs741525</i> 55 kb from <i>SLC9A7P1</i>	6.28X10 ⁻⁴	<i>rs741525</i> 55 kb from <i>SLC9A7P1</i>	5.09X10 ⁻⁴	<i>rs790436</i>	9.98X10 ⁻⁴
<i>rs3803036</i> nonsynonymous <i>PTPRR</i>	2.17X10 ⁻³	<i>rs7134216</i> intronic <i>UHRF1BP1L</i>	8.00X10 ⁻⁴	<i>rs790436</i>	7.80X10 ⁻⁴	<i>rs1358228</i> 76 kb upstream <i>NAV3</i>	1.60X10 ⁻³
<i>rs2698746</i>	2.43X10 ⁻³	<i>rs3803036</i> nonsynonymous <i>PTPRR</i>	1.22X10 ⁻³	<i>rs1358228</i> 76 kb upstream <i>NAV3</i>	1.29X10 ⁻³	<i>rs741525</i> 55 kb from <i>SLC9A7P1</i>	2.12X10 ⁻³
<i>rs7134216</i> intronic <i>UHRF1BP1L</i>	3.10X10 ⁻³	<i>rs1370780</i> 5' UTR <i>LOC253724</i>	1.90X10 ⁻³	<i>rs7134216</i> intronic <i>UHRF1BP1L</i>	2.74X10 ⁻³	<i>rs2698746</i>	4.54X10 ⁻³
<i>rs790436</i>	3.35X10 ⁻³	<i>rs1358228</i> 76 kb upstream <i>NAV3</i>	2.34X10 ⁻³	<i>rs1493418</i>	4.40X10 ⁻³	<i>rs7134216</i> intronic <i>UHRF1BP1L</i>	4.71X10 ⁻³
<i>rs1358228</i> 76 kb upstream <i>NAV3</i>	3.59X10 ⁻³	<i>rs12300992</i> 27 kb upstream <i>MYBPC1</i>	4.94X10 ⁻³	<i>rs3803036</i> nonsynonymous <i>PTPRR</i>	5.65X10 ⁻³	<i>rs7297574</i> intronic <i>MGAT4C</i>	5.34X10 ⁻³
<i>rs1389496</i> 30 kb from <i>LOC552889</i>	4.11X10 ⁻³	<i>rs4842643</i> 36 kb upstream <i>LOC728084</i>	5.71X10 ⁻³	<i>rs953832</i>	5.69X10 ⁻³	<i>rs3803036</i> nonsynonymous <i>PTPRR</i>	5.68X10 ⁻³
<i>rs17779858</i> intronic <i>TMTC2</i>	8.54X10 ⁻³	<i>rs824311</i> 3 kb upstream <i>UTP20</i>	5.91X10 ⁻³	<i>rs4573768</i>	5.92X10 ⁻³	<i>rs1163038</i> intronic <i>PTPRQ</i>	7.15X10 ⁻³

Table 18: QTL Concordance with SPH, SE and Mixed Ethnicities.

Marker / Gene Location	SE	Marker / Gene Location	SPH	Marker	Caucasian SPH	Marker / Gene Location	Caucasian SE
rs7134216 intronic <i>UHRF1BP1L</i>	2.84X10 ⁻⁶	rs4764971 3' UTR <i>DEPDC4</i> , intronic <i>ACTR6</i>	5.46X10 ⁻⁷	rs4764971 3' UTR <i>DEPDC4</i> , intronic <i>ACTR6</i>	2.25X10 ⁻⁷	rs7134216 intronic <i>UHRF1BP1L</i>	4.64X10 ⁻⁶
rs4764971 3' UTR <i>DEPDC4</i> , intronic <i>ACTR6</i>	3.94X10 ⁻⁵	rs7134216 intronic <i>UHRF1BP1L</i>	3.10X10 ⁻⁶	rs17306116 intronic <i>PPFIA2</i>	2.65X10 ⁻⁵	rs4764971 3' UTR <i>DEPDC4</i> , intronic <i>ACTR6</i>	2.01X10 ⁻⁵
rs12297646	4.24X10 ⁻⁵	rs17306116 intronic <i>PPFIA2</i>	9.01X10 ⁻⁶	rs1520562	3.51X10 ⁻⁵	rs12814689	6.93X10 ⁻⁵
rs12814689	8.24X10 ⁻⁵	rs1520562	4.95X10 ⁻⁵	rs7134216 intronic <i>UHRF1BP1L</i>	4.49X10 ⁻⁵	rs3817552 nonsynonymous <i>MYBPC1</i>	6.95X10 ⁻⁵
rs3817552 nonsyn. in <i>MYBPC1</i>	9.58X10 ⁻⁵	rs11104117 intronic <i>MGAT4C</i>	1.57X10 ⁻⁴	rs1558726	6.36X10 ⁻⁵	rs1971036 66 kb from <i>MIR4303</i>	1.47X10 ⁻⁴
rs7304135	1.36X10 ⁻⁴	rs1558726	1.94X10 ⁻⁴	rs1045741 3' UTR <i>PRDM4</i>	9.38X10 ⁻⁵	rs1163038 intronic <i>PTPRQ</i>	1.87X10 ⁻⁴
rs1971036 66 kb from <i>MIR4303</i>	1.43X10 ⁻⁴	rs7315130	2.19X10 ⁻⁴	rs12814689	2.12X10 ⁻⁴	rs17805748 intronic <i>HCFC2</i>	1.99X10 ⁻⁴
rs1163038 intronic <i>PTPRQ</i>	2.07X10 ⁻⁴	rs10506977	2.21X10 ⁻⁴	rs17805748 intronic <i>HCFC2</i>	2.59X10 ⁻⁴	rs7304135	2.95X10 ⁻⁴

3.3 Conclusions

Genetic loci for myopia, the most common ocular disorder with predispositions to ocular morbidities when pathologic, have been identified for over twenty genomic regions. However, the causal variants within many of these linkage peaks have yet to be elucidated. The linkage peak on chromosome 12, *MYP3*, is one of the largest and has been independently replicated numerous times (Young, Ronan et al. 1998; Farbrother, Kirov et al. 2004; Nurnberg, Jacobi et al. 2008; Li, Guggenheim et al. 2009). To refine the *MYP3* locus, we conducted SNP qualitative and quantitative association testing using our high myopia family cohort. Association candidate SNPs were genotyped in an independent high myopia cohort as well as screened in a previously genotyped twin cohort. We present the first mapping association study within the *MYP3* locus with independent cohort validations.

The qualitative high myopia and quantitative SPH analyses of *MYP3* both yielded potentially interesting SNPs. While none of the SNPs in the qualitative analyses were statistically significant after correction for multiple testing, SNPs approaching significance were further evaluated as candidates. The high number of significant SNPs in quantitative analyses can likely be attributed to their location in a well-established linkage region, as well as the increased power of using quantitative data rather than qualitative classifications. Strict affection status cut-offs and consequently low numbers

of affected individuals in the qualitative data may have contributed to reduced power resulting in higher p-values.

Interestingly, qualitative and quantitative analyses had overlap in their most significantly associated SNPs (Table 13) and biological connections between some candidate genes. The fourth most significantly associated SNP in both tests was the same intronic SNP located in *UHRF1BP1L*. Four of the five most significant SNPs in the qualitative analyses had p-values less than 0.05 in quantitative analyses, including the SNP located in the PTP gene *PTPRR*, which is functionally related to another candidate gene from the quantitative data, *PPFIA*.

3.3.1 Validation in Replicate Cohorts

Independent validation, using a Caucasian high-grade myopia cohort, of our most significant association SNPs for both qualitative and quantitative testing validated one quantitative SNP, *rs7134217* within *UHRF1BP1L*. The significance of this SNP overlapped between both qualitative and quantitative discovery cohort results, but was only replicated for quantitative association in this second Caucasian high-grade myopia validation cohort. One of the two PTP genes genotyped approached significance in qualitative testing, *rs71306116* in *PPFIA2*. However, this SNP was not a top candidate in our qualitative association and none of our qualitative results in the discovery cohort reached statistical significance criteria. Both of the two SNPs in PTP candidate genes

had suggestive association in quantitative association assessment in this high-grade myopia validation cohort - *rs3803036* (*PTPRR*) and *rs1730611* (*PPFIA2*). Only the SNP within *PPFIA2* was statistically significant in the discovery quantitative testing, however, *PTPRR* did approach statistical significance in our data as well. In total, three of the five SNPs chosen for follow-up genotyping were nominally significant or statistically significant in a second high-grade myopia cohort, supporting their association with myopia.

In a second independent twin cohort that did not contain data for all of our most significantly associated SNPs, one of the most significant SNPs from the discovery cohort showed potentially interesting results. The SNP, *rs1520562*, is not near any known genes; however, it is in a region that is conserved largely by higher mammals including primates. The conservation pattern suggests that the area should be thoroughly screened for regulatory elements that may affect vision in this subset of mammals. Since this second replicate cohort was not collected with preferential selection for highly myopic individuals (twin cohort average of -0.40 D compared to discovery cohort average of -4.78 D) and used a higher cut-off in qualitative testing (-6 D compared to our -5 D cut-off), it is possible that this twin cohort lacked the power to identify some of the variants from our study. Additionally, since these data were previously collected, we were not able to screen all candidate SNPs. Considering these

limitations, it is highly encouraging that this SNP nominally replicated in the independent twin cohort. The overlap suggests that results obtained in the discovery cohort may be representative of others not tested.

3.3.2 Novel *MYP3* Candidate Genes

One of the largest limitations in our discovery cohort was the SNP coverage given the large size of the *MYP3* locus. It is possible that variants within the spacing of our coverage have been missed; however, cost limitations prohibited higher density coverage of the region. Our association data were also limited by the number of samples in the discovery genotyping cohort. Despite these limitations, quantitative association testing yielded several strong candidates withstanding conservative significance cut-offs. Our high-grade myopia validation cohort most strongly supported *UHRF1BP1L*; however, *PTPRR* and *PPFIA2* may also be candidate genes worthy of further consideration given they both approached significance in this replicate cohort as quantitative traits. Further validation and refinement of these three novel *MYP3* candidate genes is necessary to make claims regarding their involvement in myopic progression.

4. Genomic Convergence of Expression and Association

Independently designed, collected and reported ocular expression data were used to prioritize candidate genes from association testing. Genes that were within 100 kb of the most significantly associated SNPs in *MYP3* were screened and prioritized by differential ocular expression. Given that myopia can be considered a failure of normal growth, genes involved in normal growth were considered likely candidates, and those with differential expression in central retina, RPE, choroid and/or sclera between fetal and adult eyes were prioritized.

4.1 Methods

4.1.1 Ocular Tissues Relevant to Myopic Development

In normal eye growth, the eye is able to determine and regulate its AL to sharply focus images on the retinal plane. Visual cues interpreted by the retina set off a signaling cascade from the retina, to the RPE, to the choroid and ultimately to the scleral wall, all of which regulate growth. The thicknesses of the posterior tissues, including the retina, RPE, choroid and sclera, of the eye are altered during normal growth and development in an effort to achieve emmetropia or normal vision. Changes in the size and/or shape of the optic nerve and cornea are also seen in myopic individuals. Since changes in all of the tissues examined in this study have been seen in myopic eyes, changes in any or all of these tissues may contribute to myopic development (Rada, Shelton et al. 2006).

We hypothesized that genes which when altered contribute to the development of myopia, may be part of normal growth and development mechanisms in ocular tissues showing myopic associated clinical phenotypes. We assessed differentially expressed genes between rapidly growing fetal tissues relative to their mature adult counterparts. We examined the function of those differentially expressed genes to extrapolate information regarding the mechanisms of ocular disease relating to excess axial growth and other associated physical characteristics.

4.1.2 Overlap with *MYP3* Association

All candidate genes from Table 13 were expressed in all tissues and age groups tested; as such, none could be eliminated for lack of expression in the relevant tissues. All fold changes below are presented as fetal relative to adult expression. Genes with probes were considered differentially expressed if the expression difference was significant by FDR correction. Genes of interest for validation were determined by their relation to candidate genes from the association analyses, their degree of fold change, probe concordance, and expression level (Table 19).

4.1.3 RT-qPCR Validation

Candidate genes within 100 kb of the most significantly associated SNPs in the *MYP3* association results were compared with genes identified by microarray analysis as significantly differentially expressed. Genes that were the same or directly,

functionally related to candidate genes in at least one tissue type were validated using RT-qPCR with Taqman® (Foster City, California, USA) Gene Expression Assays (Table 20). Genes of interest in the expression analysis were determined by their relation to candidate genes from the association analyses, their degree of differential expression, concordance of probes within the same genes, and their level of expression (Table 19). RT-qPCR for each gene was performed for all tissue types, rather than just the tissue(s) of known overlap. Each gene was validated with four biological replicates of each adult central and 24-week central tissue, in addition to one non-template control. Each biological replicate contained equal amounts of total RNA pooled from the tissue of two individuals. In total, RNA from the tissue of eight individuals was used for each gene per tissue type. Each biological replicate was carried out in four technical replicates of RT-qPCR. Expression of adult retina and RPE were averaged and compared to 24-week retina/RPE since they could not be surgically separated. Each plate of quantitative real time assays contained the two control genes *GAPDH* (MIM 138400) and *18S* for each biological replicate of each tissue type. Reverse transcription reactions were performed with the Applied Biosystems (ABI) High Capacity cDNA Reverse Transcription Kit per manufacturer's protocol (Carlsbad, California, USA). RT-qPCR was carried out on an ABI 7900 (Carlsbad, California, USA) per the Taqman® (Foster City, California, USA) Gene Expression Assays protocol. Fold changes and standard deviation errors in each

tissue type were calculated by the $2^{-\Delta\Delta CT}$ method with normalization by the two housekeeping genes (Livak and Schmittgen 2001). Technical replicates were removed if the standard deviation was greater than 0.5 and no biological replicates were removed.

Table 19: Differentially Expressed Genes Related to Candidate Genes from *MYP3* Association.

Fold change (FC) and p-value for each differentially expressed probe (given on separate lines) of genes related to *MYP3* association candidates. Underlined genes were selected for follow up validation by RT-qPCR. Multiple values for each gene indicate multiple probes within the same gene. 'NS' indicates the fold change was not statistically significant.

Genes	Retina/RPE		Choroid		Sclera	
	FC	p-value	FC	p-value	FC	p-value
<i>ACTR6</i>	NS	NS	1.47	2.70×10^{-3}	1.08	6.20×10^{-3}
<u><i>PPFIA2</i></u>	NS	NS	2.35	1.3×10^{-3}	1.5	1.6×10^{-3}
<u><i>PTPRF</i></u>	1.24	2.65×10^{-5}	6.42	7×10^{-4}	1.11	1×10^{-4}
	1.19	2.65×10^{-5}	NS	NS	1.11	3.3×10^{-3}
<u><i>PTPRR</i></u>	1.44	2.65×10^{-5}	3.04	4.7×10^{-3}	NS	NS
<i>UHRF1</i>	NS	NS	NS	NS	1.31	6.2×10^{-3}

Table 20: Taqman® Gene Expression Assay Identification Numbers.

Gene	Assay ID
<i>PPFIA2</i>	Hs00170308_m1
<i>PTPRF</i>	Hs00160858_m1
<i>PTPRR</i>	Hs00373136_m1
<i>18S</i>	Hs03003631_g1
<i>GAPDH</i>	Hs02758991_g1

4.2 Results

When filtered by candidate genes from the qualitative and/or quantitative association results, only two genes to select from for validation by RT-qPCR were found to be significantly differentially expressed in the microarray data. Fold changes for all genes selected for validation are displayed in Figure 13 with biological variation as error bars. All significant or nominally significant SNPs were considered when creating lists of candidates (genes within 100 kb of SNP). All candidate genes from the association under consideration were included on the microarray but were not statistically significant for differential expression. The overall fold change trend upon validation was consistent with the fold changes from the microarray data with slight degree variation, except in some cases where the expression was very low and/or fold changes were small (Figure 13; data not shown).

4.2.1 RT-qPCR Validation

The three genes selected for RT-qPCR validation were protein tyrosine phosphatase (PTP) related genes: *PTPRR* and *PPFIA2* and *PTPRF* (MIM 179590), which is not a candidate from the association, however, it is the namesake interacting gene of *PPFIA2*. In the retina/RPE and choroid all three genes were found to be up-regulated in fetal relative to adult tissue specific expression. In the sclera, *PTPRF* was up-regulated while *PTPRR* and *PPFIA2* were slightly down-regulated in fetal relative to adult expression. *PTPRR*, a candidate from the qualitative high myopia association data, did not show expression in the adult RPE. As a result the retina/RPE fold change could not be calculated. Instead a fold change comparing only the adult retina to the fetal retina/RPE is presented. The fold change for retina/RPE (without adult RPE) was 3.49-fold higher expression in fetal tissue; however, absence in adult RPE limits conclusions based on this data. The fold change for the choroid was 3.22 and the sclera showed a fold change in the opposite direction of -1.49, where the adult was more highly expressed. *PPFIA2*, a candidate gene from the quantitative SPH association testing, showed a 2.48 fold change in the fetal choroid relative to the adult, while the -1.22 fold change in the sclera was opposite the direction of the array data (possibly explained by the low overall level of expression). The retina/RPE was not significant in array data, but showed a 1.83 fold change in RT-qPCR. Interestingly, *PTPRF*, which interacts with

PPFIA2, showed larger fold changes: 4.20 in retina/RPE, 7.53 in choroid, and 1.43 in sclera. The retina/RPE fold changes for *PTPRF* were much larger; however, the choroid and sclera were consistent with the microarray data.

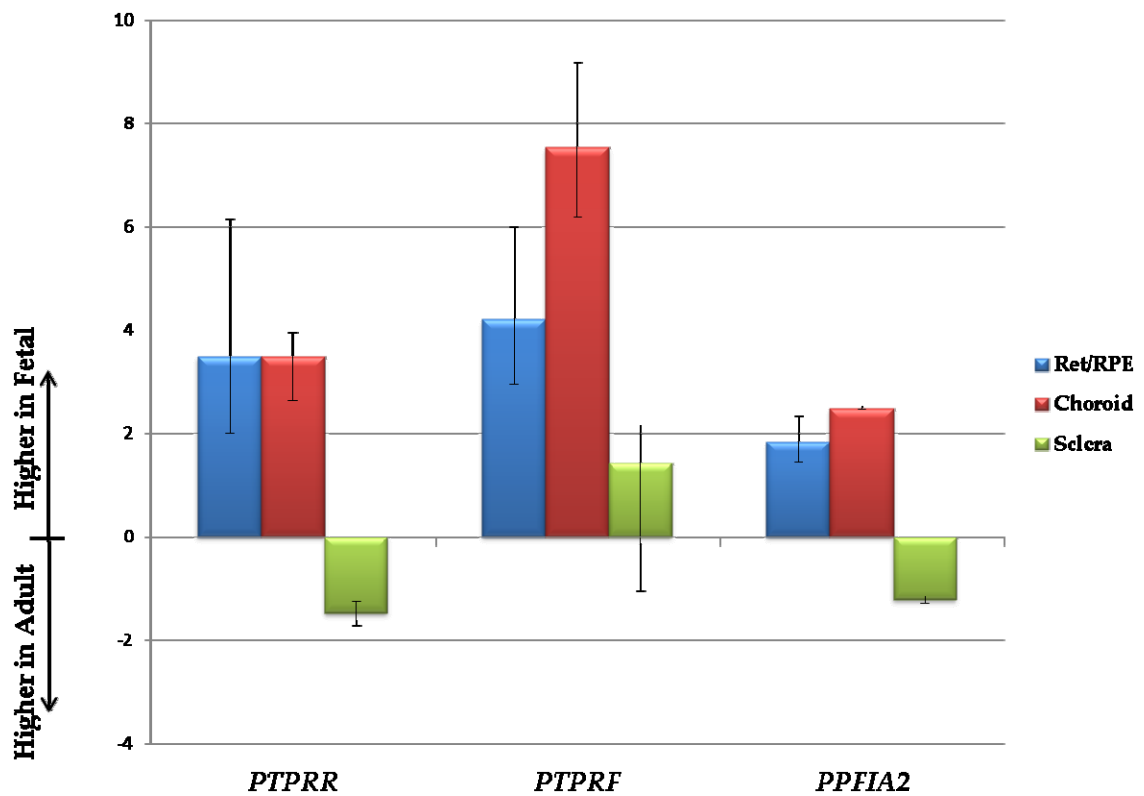


Figure 13: Fetal Versus Adult Fold Changes of Real Time Quantitative PCR (RT-qPCR) Validated Genes.

The columns from left to right for each gene represent the retina/RPE (blue), choroid (red), and sclera (green). Fold changes (left axis) were calculated by the $\Delta\Delta C_t$ Method. Biological variation is shown by error bars for each tissue/gene.

4.3 Conclusions

The association data revealed a high number of possible candidate genes. To filter our candidates we utilized genomic convergence with concurrent whole genome expression analyses. As procurement is nearly impossible, little is known about the mechanism of myopic development from affected human tissues. We decided to use rapidly growing fetal eyes as a human model, since we hypothesized that genes implicated in the exaggerated eye growth of myopic development might show differential expression in fetal relative to adult relevant posterior, central tissues. Two genes from our association analyses in addition to several related genes were independently found to show differential expression in rapidly growing fetal ocular tissues relative to adult ocular tissues.

4.3.1 Genomic Convergence of Association Candidates and Ocular Expression.

One of our candidate genes in the qualitative association data, *PTPRR*, was found to be more highly expressed in the rapidly growing fetal retina/RPE (* not detected in adult RPE) and choroid while slightly more highly expressed in the grown adult sclera. From our quantitative association data, *PPFIA2* and its namesake

interacting gene, *PTPRF*, both were found to be differentially expressed in fetal relative to adult ocular tissues. Like *PTPRR*, *PPFIA2* showed higher expression in the rapidly growing fetal retina/RPE and choroid while higher expression in the adult sclera.

PTPRF showed similar, though more pronounced, patterns with retina/RPE and choroid expression but showed higher expression in the rapidly growing fetal sclera (Figure 13).

Overall, in the microarray data and in all three PTP genes we followed up, the tissue with the highest fold changes was the choroid. The lack of high fold changes in the retina/RPE may have been caused by the averaging methods used since the fetal tissues could not be separated.

4.3.2 Limitations of Ocular Expression Prioritization

The expression data were limited by the sample number and the tissues, which we could not separate in fetal samples. Our estimation of tissues in a complex compared to separate tissues is likely imprecise. The low fold change differences we found in the retina/RPE may be an artifact of our testing. Better tissue isolation techniques will need to be developed for future expression analyses. However, despite these limitations, two of our candidate genes from the association data were supported by the expression data. *PTPRR*, *PPFIA2* and its namesake interacting gene, *PTPRF*, were found to be differentially expressed in central ocular tissues. This overlap supports our model of eye growth for myopic development and use of these expression data both in other known

myopia loci and also in detailed pathway analyses to look for targets within the known loci. However, our high-grade myopia validation cohort most strongly supported *UHRF1BP1L*, which was not differentially expressed in our data. Differential expression may have been missed by the microarray data, or it may not be differentially expressed. While the expression data has been shown to be a useful tool in prioritizing candidates, we have shown that it cannot be used to exclude candidates.

4.3.3 MYP3 Candidate Genes

The expression data alone cannot be used to identify candidates; however, we have shown additional support of two candidates which were interesting from the association data. Since the number of candidates from the discovery association cohort was too large to screen all of them, an effective prioritization step was necessary. Here we have shown that utilizing genomic expression in prioritizing candidates revealed two strong candidates, *PTPRR* and *PPFIA2*, with functional relation to one another, and provided insights into their possible mechanistic roles in myopic progression.

5. Conclusions

5.1 Implications of Genomic Convergence

5.1.1 Ocular Growth as a Model for Myopic Development

It is widely accepted that a visual feedback mechanism regulates eye growth (Wallman and Winawer 2004), yet no known pathways directly connect the retina to the choroid or sclera where despite prominent physical changes large expression fold changes in animal models have not been identified (Stone and Khurana 2010). Many of the animal models of myopia have been assessed for differential expression of genes. However, few models have been analysed for differential tissue expression using whole genome arrays. Many studies of expression in animal models have instead focused on more cost effective candidate gene approaches utilizing RT-qPCR. These studies have yielded a number of genes which have been replicated in other models or genetic studies, but they do not constitute an overall signalling mechanism for ocular growth (Stone and Khurana 2010). Our model is likely an over estimation of potential contributors, but unlike other models is directly taken from human tissue types. Despite these limitations we believe this data can be used to further understand ocular growth and development and associated diseases.

While these hypotheses require further testing, we have provided a novel framework in which to interpret myopia candidate genes. Early analyses of the

functional classifications of myopic-associated genes may help elucidate their potential roles in disease progression, particularly in the case of unexpected tissues with differential expression of these genes. Next, a deeper understanding of the mechanisms connecting these tissues may be better studied using canonical pathways. The most significant canonical pathways in all adult versus fetal tissues involved signaling, activation, and cell cycle regulation and included fewer molecules for consideration (Table 6). Genes whose mutations may confer an increased risk for axial elongation or myopia associated clinical features may be components of these pathways regardless of their differential expression. We have shown that the data supports existing ideas that myopic development may result from disruptions to growth and/or signaling pathways in any of all of the tissues presented either through the same or convergent means. Comparisons to animal models of myopia have shown a high degree of similarity given the large differences between the models. We have only scratched the surface of the possibilities with this vast resource with one common ocular disease. Clues to many other diseases may also be hidden in this data.

5.1.2 Candidates Genes for Myopic Development from Animal Models

In the retina, sonic hedgehog and vasoactive intestinal peptide have been identified as up-regulated in animal models of myopia (Stone and Khurana 2010), both of which were expressed higher in our adult relative to fetal retina/RPE (data not

shown). Other implicated signalling molecules identified which are differentially expressed in other tissues include bone morphogenic and retinoic acid receptors (Stone and Khurana 2010). Full pathway analyses, made possible by whole genome expression data, of genes in these and other identified signalling pathways may elucidate possible mechanistic roles in myopic development.

5.1.3 Whole Genome Array Studied of Animal Models of Myopic Development

Whole genome array studies performed in animal models of myopia have only included one tissue or tissue complex, none of which directly line up with our human tissues or complexes (Table 21). Two studies, both in the chick, have performed array analyses of the retina in different models of myopia, which did not have overlap with one another in reported genes. Two of the major genes reported by McGlenn et al. (McGlenn, Baldwin et al. 2007) were also differentially expressed in our retina/RPE: *EDNRB* (MIM131244) and *VIP* (MIM 192320). *EDNRB* was also differentially expressed in our choroid, albeit in the opposite direction. Given our model is of normal growth, rather than myopic growth, genes cannot necessarily be expected to have differential growth in the same direction. These genes may be expressed differently when growth is disrupted so long as they are a part of the growth process. Another gene they identified, *BMP2* (MIM 112261), was differentially expressed in two of our other tissues, the optic nerve and cornea. *SPTBN1* (MIM 182790), a differentially expressed gene found in

myopic induced chick retina reported by Schippert et al. (Schippert, Schaeffel et al. 2008) was also differentially expressed in our retina/RPE. Five other genes reported in the study were present in one or more of our other tissues (Table 21). The other array expression study, by Shelton et al. (Shelton, Troilo et al. 2008), of a myopia model tested the choroid/RPE in a marmoset model. Two of their reported major differentially expressed genes were differentially expressed in two tissues each in our data: *FGF2* (MIM 134920) in the choroid and cornea, *TGFBI* (MIM 601692) in the optic nerve and cornea. Similar to our analyses, Zhou et al. (Zhou, Rappaport et al. 2006) performed array analyses of mouse sclera during and after development. As in that study, we found *ELN* (MIM 130160) and numerous collagens to be differentially expressed in each of our fibrous tissues, the sclera, optic nerve and cornea. Future studies of whole genome expression of a myopia induced animal model using the same tissues would provide a better assessment of our growth data as a model for myopic development - particularly for those tissue types in which we found overlap but have not been tested in an animal model of myopia. Despite the limitations in the differences between tissue and model types, the overlap given the limited data available for comparison suggests our model may have potential.

Table 21: Our Human Expression Array Study Compared to Expression Array Studies of Animal Growth or Myopia.

Up/down-regulated refer to treated (to induce myopia) or adult tissues relative to control or fetal tissues. Major up/down-regulated genes from other studies which overlap in our data are listed for our study. *FDR not used for adult versus fetal optic nerve in our study. FC is fold change.

	Our Study	(McGlenn, Baldwin et al. 2007)	(Schippert, Schaeffel et al. 2008)	(Shelton, Troilo et al. 2008)	(Zhou, Rappaport et al. 2006)
Species	Human	Chick	Chick	Marmoset	Mouse
Myopia Model	Growth/Development	Form-deprivation	Positive lens wear	Binocular lens	Growth/Development
Tissue(s)	Retina/RPE Choroid Sclera Optic Nerve Cornea	Retina	Retina	Choroid/RPE	Sclera
Array	Illumina HumanHT-12 v4	Affymatrix Chicken GeneChips	Affymatrix Chicken GeneChips	Atlas Plastic Human 12k	Affymatrix Mouse 430 2.0
Significance cut-off	5% FDR *	13% FDR	6% FDR	Student t-test $p \leq 0.05$	5% FDR, top 1000
FC cut-off	> 1.5	none, 1.4 for validation	> 1.5	none	> 3
# up-regulated genes	Retina/RPE: 652 Choroid: 2780 Sclera: 526 Optic Nerve: 193 Cornea: 2176	269	67	183	210
# down-regulated genes	Retina/RPE: 533 Choroid: 3666 Sclera: 823	19	56	21	508

Major up-regulated genes	Optic Nerve: 1986				
	Cornea: 1696				
	Retina: <i>EDNRB</i> , <i>VIP</i>	<i>EDNRB</i> , <i>IL-18</i>	<i>SHQ1</i> , <i>ATE1</i> , <i>ELF1</i> , <i>GRB2</i> , <i>OSBP2</i> , <i>SPTBN1</i>	<i>TGFBI</i> , <i>FGF2</i>	
	Choroid:				
	Sclera:				<i>KIF5A</i> , <i>EXPI</i> , <i>VTN</i> , <i>NEUROD1</i>
Major down-regulated genes	Optic Nerve: <i>SPTBN1</i>				
	Cornea: <i>ELF1</i> , <i>TGFBI</i> , <i>FGF2</i>				
	Retina/RPE: <i>SPTBN1</i> , Collagens	<i>BMP2</i> , <i>CTGF</i> , <i>VIP</i> , <i>LOC404534</i> , <i>MKP-2</i>	<i>pp-URP</i> , <i>CD226</i> , <i>ABCC10</i>	<i>PTPRB</i>	
	Choroid: <i>EDNRB</i> , <i>ELF1</i> , <i>CD226</i> , <i>FGF2</i> , Collagens				
	Sclera: <i>ATE1</i> , <i>ELN</i> , <i>Collagens</i>				<i>ELN</i> , <i>TGFBI</i> , Collagens
	Optic Nerve: <i>BMP2</i> , <i>ABCC10</i> , <i>TGFBI</i> , <i>ELN</i> , Collagens				
Cornea: <i>BMP2</i> , <i>OSBP2</i> , <i>ABCC10</i> , <i>ELN</i> , Collagens					

5.1.4 Differentially Expressed Genes within Known Myopia Linkage Loci

In addition to genes previously implicated in myopic development or progression, genes located within MIM recognized genomic loci for myopia were screened for differential expression in adult versus fetal retina/RPE, choroid, and sclera. A number of genes in all but four loci were identified as significantly, differentially expressed in at least one of the fetal versus adult tissues. Appendix C contains a listing of all of these genes and their associated fold changes and significance.

5.2 Novel Insights into Possible Biological Mechanisms for Refractive Error

5.2.1 Protein Tyrosine Phosphatases (PTPs)

Interestingly the two candidate genes from the association data (one from the qualitative and one from the quantitative), located within *MYP3* that were found to be differentially expressed in ocular tissues, were both PTP related genes. PTP's are enzymes that remove a phosphate group from the amino acid tyrosine. These proteins play a role in the regulation of signal transduction by relaying signals from outside the cell that regulate cell growth, division, maturation and function (Andersen, Jansen et al. 2004; Tonks 2006). Although PTP genes seem ubiquitous, several studies have implicated them in tissue specific diseases and functions as well as various cancers (Andersen, Jansen et al. 2004; Wang, Shen et al. 2004; Tonks 2006; Chen, Yoshida et al.

2011; Ozaltin, Ibsirlioglu et al. 2011). Ozaltin et al. have shown that mutations in *PTPRO* (MIM 600579) are causal for early onset nephrotic syndrome (Ozaltin, Ibsirlioglu et al. 2011). Chen et al showed *PTPσ* regulates synapse number of zebrafish olfactory neurons (Chen, Yoshida et al. 2011). There has also been one PTP related gene previously associated with rapid ocular growth and lies within the *MYP3* locus; microarray work validated by real time assays of choroid/RPE expression in marmoset eyes undergoing lens treatment to induce rapid ocular growth showed differential expression of PTP receptor type B (*PTPRB*; MIM 176882) (Shelton, Troilo et al. 2008).

5.2.1.1 PTP Enrichment in *MYP3* Quantitative Analyses

Interestingly, in the complete quantitative association results, a pattern was detected in functionally related PTP genes (*PPFIA2*, *PPP1R12A* [MIM 602021], *PTPRB*, *PTPRR*, *PTPRQ* [MIM 603317], *DUSP6* [MIM 602748] and *DYRK2* [MIM 603496]), two of which are our candidate genes. While most of these SNPs were not individually statistically significant, in the quantitative association this subset of SNPs was significantly more likely to have p-values below 0.5 than the rest ($p = 1.2 \times 10^{-5}$) (Figure 14). In addition to *PTPRR* and *PPFIA2*, some or all of these genes may also play a role in the development of myopia and their functional relatedness may provide insight into a possibly pathway. It is also potentially interesting that many other known myopia loci contain PTP related genes (Table 22).

Table 22: PTP Related Genes in Known Myopia Linkage Loci.

Myopia Loci were taken from NEIBank: Candidate Disease Loci – Myopia and Hornbeak et al 2009.

Locus	Location	Genes
<i>MYP1</i>	Xq28	<i>DUSP9, MTM1, MTMR1</i>
<i>MYP2</i>	18p11.31	<i>PTPN2, PTPRM</i>
<i>MYP3</i>	12q21 – q23	<i>DUSP6, DYRK2, PP1R12A, PPFIA2, PTPRB, PTPRR, PTPRQ</i>
<i>MYP4</i>	7q36	<i>PTPRN2</i>
<i>MYP5</i>	17q21 – q22	<i>MTMR4</i>
<i>MYP6</i>	22q12	<i>DUSP18, MTMR</i>
<i>MYP10</i>	8p23	<i>MTMR9</i>
<i>MYP12</i>	2q37.1	<i>DUSP28</i>
<i>MYP14</i>	1p36	<i>EYA3</i>
<i>MYP16</i>	5p15.33-15.2	<i>MTMR12</i>
<i>MYP18</i>	14q22.1-24.2	<i>STYX</i>

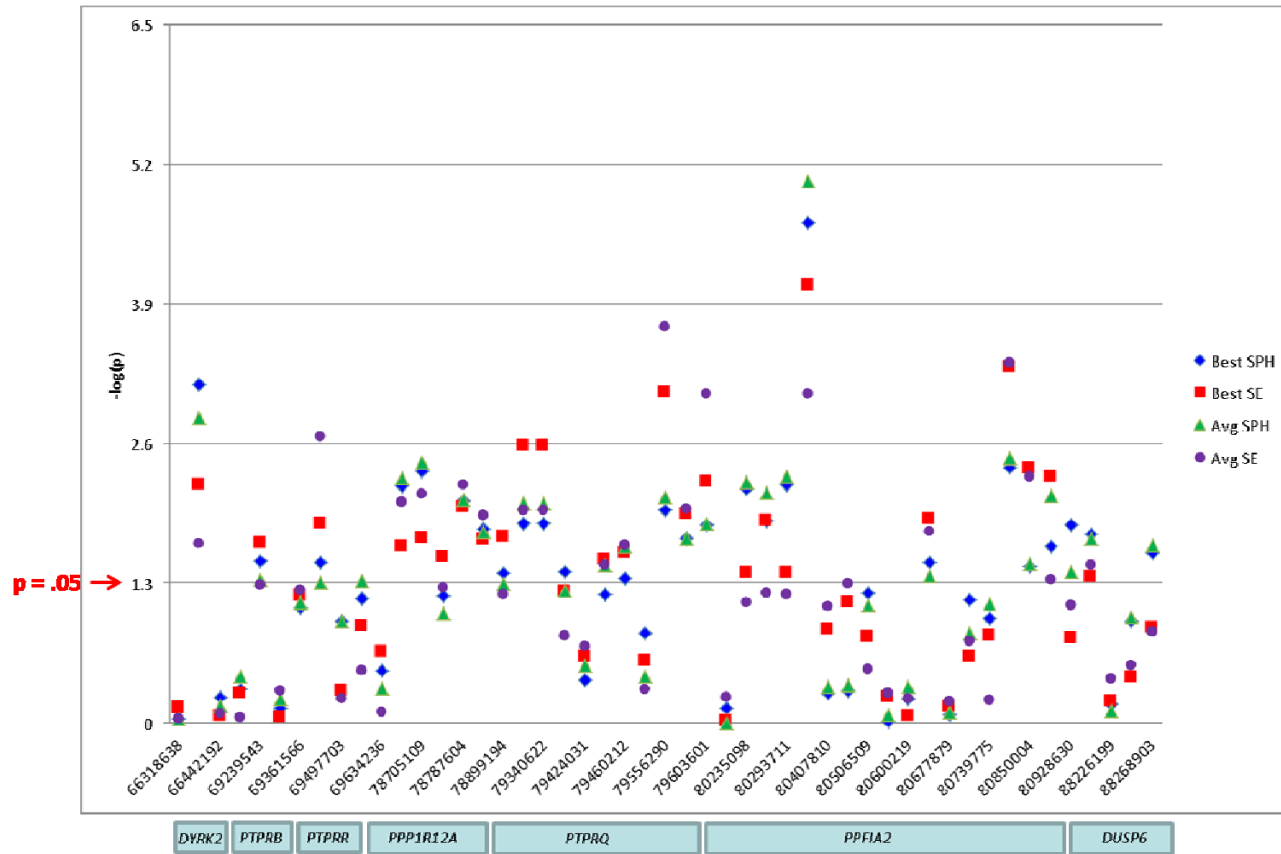


Figure 14: Quantitative Association by $-\log(p)$ for All SNPs in PTP Related Genes.

SNPs are placed adjacent to one another for the purposes of this graph, but they are not representative of the chromosomal distance between genes. SPH is sphere; SE is spherical equivalence; avg is average of both eyes; best is the least myopic eye.

5.2.2 *PTPRR* and *PPFIA2* as *MYP3* Candidates for Myopic Development

It is intriguing to consider that *PTPRR*, *PPFIA2* or other PTP genes might be involved in the development of high myopia or the variation of our endophenotype, SPH, by regulating ocular cell growth and division. Myopic eyes tend to be longer (as measured by our endophenotype, SPH) with thinner posterior tissues (Atchison, Jones et al. 2004). The exact mechanism for myopic development is still largely unknown, however, generally considered to result from signaling molecules triggered by light in the retina passed through to choroid and sclera, termed the retino-scleral cascade. The result of this cascade leads the structural changes we see of matrix degradation, scleral tissue loss/thinning and axial elongation (McBrien and Gentle 2003; Atchison, Jones et al. 2004).

5.2.2.1 *PTPRR*

PTPs are involved in numerous aspects of cellular control (Andersen, Jansen et al. 2004; Tonks 2006). PTP receptors are recruited by PTPs which create binding sites that activate signaling pathways or regulate catalytic activity (Pawson and Scott 2005). PTP receptors make up 21 of the PTP family members. *PTPRR* shares a gene symbol (considered synonymous) with *PTPRQ*, which, when overexpressed, inhibits cell proliferation and induces apoptosis (Oganesian, Poot et al. 2003). *PTPRQ* has been identified as one of a subgroup of PTP receptors, which have different primary

biological activities (Oganesian, Poot et al. 2003). This subgroup acts as active phosphoinositide phosphatases that regulate cell proliferation (Oganesian, Poot et al. 2003) making genes, such as *PTPRR*, an early and frequent target of silencing in some forms of cancer (Menigatti, Cattaneo et al. 2009). *PTPRR* has also been shown to be a key negative regulator of *MAPK* signaling in androgen-regulated expression (Shi, Zhang et al. 2011). *PTPRR* in mice have distinct localization of each isoforms, all of which contain the kinase interacting motif necessary to bind and inactivate *MAPK* by dephosphorylation (Hendriks, Dilaver et al. 2009). In mice, two of these isoforms of *PTPRR* localize on the membranes of endocytotic vesicles like those used for glutamate or other cell signaling molecules (Van Den Maagdenberg, Bachner et al. 1999; Dilaver, Schepens et al. 2003). *PTPRR* may be involved in the development of high myopia by a change in its ability to bind to or dephosphorylate *MAPK* leading to increased *MAPK* growth signals. These signals could affect glutamate-gated, or other neuronal signals, ion channels in the photoreceptors or other retinal synaptic cells' vesicular synaptic terminals. As in some neurons of the brain, glutamate is a common neurotransmitter in the retina in photoreceptors, bipolar and ganglion cells (Rodieck 1998). Increased neurotransmitter production and/or release across synapses could disrupt the normal response to neuronal signals converted from photon capture. These abnormal signals may increase axial elongation of the eye beyond normal growth, particularly afflicting

those posterior tissues surrounding the macular region responsible for high acuity vision. Increased expression of *PTPRR* in rapidly growing fetal retina/RPE (*not present in adult RPE) and choroid may be the result of normal developmental or growth regulators suggesting it plays a role in reigning in ocular growth. Disruption of this proteins function may account for the rapid growth seen in highly myopic individuals during early childhood that slows into adulthood (Figure 15). As normal growth regulators slow, the need for this protein would also decrease.

5.2.2.2 *PPFIA2*

PPFIA2 is a member of the leukocyte common antigen-related (LAR) PTP interacting protein family liprin. Liprins are proposed to act as scaffolding proteins for recruitment and anchoring of LAR PTPs (Wei, Zheng et al. 2011). Vertebrates have four homologs of liprin- α (1-4) each enriched in different synaptic and non-synaptic cell populations (Spangler, Jaarsma et al. 2011). Liprin- α 's are thought to be essential elements of the active zone at the pre-synaptic plasma membrane by guiding synaptic vessels to their fusion sites and regulating neurotransmitter releases (Spangler, Jaarsma et al. 2011). Liprin- α 2 in the brain is preferentially localized in excitatory synapses, like the hippocampal mossy fiber nerve endings that release glutamate via synaptic vesicles (Spangler, Jaarsma et al. 2011). *PPFIA2* is a liprin α 2 known to be down regulated by androgens in prostate cancer cell lines (Fujinami, Uemura et al. 2002). *PPFIA2* may be

involved in the variation of the SPH phenotype, which is decreased in myopic patients, by altering the release of glutamate. Mutations in *PPFIA2* could affect its ability to guide glutamate filled synaptic vesicles to their fusion sites, thereby disrupting the signaling cascade throughout the retina and possibly onto other ocular tissues (Figure 15). Alterations in the normal signaling cascade may disrupt the normal process of emmetropization.

Converse to *PTPRR*, the function of *PPFIA2* seems more likely to be a positive regulator of cell growth which fits with its moderate increase in expression in rapidly growing retina/RPE, and choroid. *PPFIA2* may result in smaller growth increases found more commonly in moderate myopic individuals, picked up by our quantitative analyses, rather than the extreme changes seen in highly myopic individuals, which were qualitatively assessed.

5.2.3 *UHRF1BP1L*, *ACTR6*, *DEPDC4* and *NAV3* as *MYP3* Candidates for Myopic Development

5.2.3.1 *UHRF1BP1L*

While physically close genes *UHRF1BP1L*, *ACTR6* and *DEPDC4* were not directly supported by our ocular expression data, they still may be interesting genes for future work. Particularly *UHRF1BP1L*, one of the most significantly associated SNPs in both qualitative and quantitative data which was replicated by an independent high myopia cohort for quantitative SPH may be of interest. *UHRF1BP1L* binds to *UHRF1*,

which regulates topoisomerase II alpha (*TOP2A*; MIM 126430) (Hopfner, Mousli et al. 2000) and retinoblastoma (*RB1*; MIM 180200) (Jeanblanc, Mousli et al. 2005) gene expression, indicating a possible link to regulation of cell growth and proliferation within the retina. *UHRF1* binds to the methylated promoter of *RB1* suppressing its translation (Jeanblanc, Mousli et al. 2005). Over expression of *UHRF1* has been shown to down regulate *RB1* expression, which itself acts as a tumor suppressor of excess growth (Jeanblanc, Mousli et al. 2005). *UHRF1BP1L* could be involved in myopic development by regulating the expression of other genes, such as *RB1* or *TOP2A*, via its interactions with *UHRF1* ultimately contributing to increased axial growth (Figure 15). This may explain why differential expression may not exist in the relevant ocular tissues during growth. Interestingly, *TOP2A*, had significantly lower expression in the adult retina/RPE, choroid, and sclera (-1.88, -56.64, and -5.43 respectively). Pathway analysis of differentially expressed genes may help uncover a more precise possible mechanism for this genes' role in myopic progression.

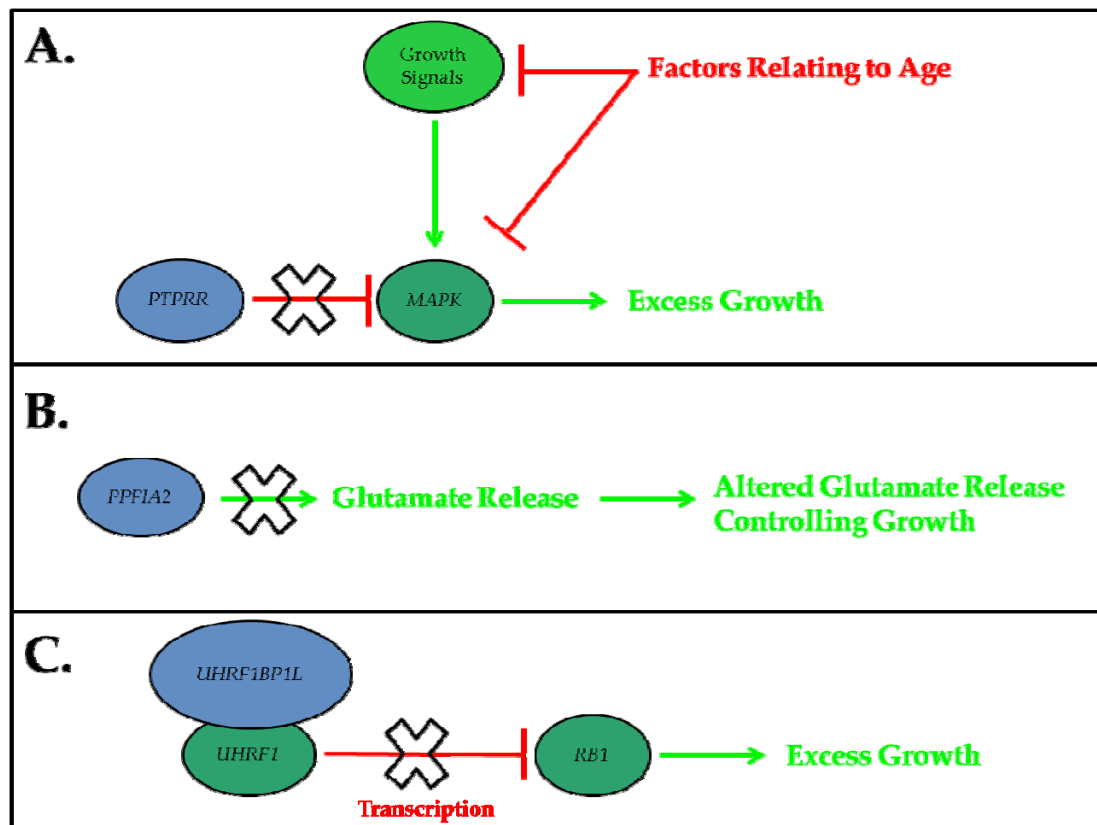


Figure 15: Possible Mechanistic Roles for Novel Candidates *PTPRR*, *PPFA2* and *UHRF1BP1L*.

A) Disruption of *PTPRR* may allow excess *MAPK* regulated growth, which would decline over time as growth signals slow. B) Disruptions to *PPFA2* may alter retinal neurotransmitter release affecting local growth regulatory mechanisms. C) Changes to *UHRF1BP1L* may affect *UHRF1*'s ability to block transcription on growth stimulants such as *RB1*. (© Felicia Hawthorne, 2012)

5.2.3.2 *ACTR6*, *DEPDC4* and *NAV3*

Other candidates which were not supported by either validation cohorts or expression data may also be considered. *ACTR6* is an actin-related protein, which could

be involved in the scleral extracellular matrix remodeling seen in myopic individuals. *DEPDC4* is a DEP (Dishevelled, Egl-10 and Pleckstrin: the three genes originally found with it) domain containing protein. *DEPDC4* is involved in G-protein signaling which in the retina regulates stimulation by light and could also be part of a signaling pathway resulting in myopic development. It is also potentially interesting that two known myopia loci contain genes functionally related to *DEPDC4*. *DEPDC7* is in *MYP7* (MIM 609256) and *DEPDC5* is in *MYP6* (MIM 608908). Lastly, *NAV3*, with two of the ten most significant SNPs from qualitative data upstream of it should be considered in future studies. This gene is believed to be involved in neuron navigation and has been proposed to play roles in diseases from cancer to Alzheimer's (Shioya, Obayashi et al. 2010; Carlsson, Ranki et al. 2012). However, how (if at all) *NAV3* may be involved in myopic growth remains unclear.

5.3 Future Directions

5.3.1 Ocular Expression

5.3.1.1 Candidates in Genomic Myopia Loci

The ocular growth expression data for the retina/RPE, choroid, and sclera yielded many genes from known myopia loci which are differentially expressed (Appendix C). Some regions such as *MYP1* have long lists of differentially expressed genes, while others such as *MYP4* have fewer than 15. As with the *MYP3* locus, the

genotype information in these regions should be compared to the differentially expressed genes and their pathways to identify and prioritize novel candidates.

5.3.1.2 Animal Model Comparison by Tissue

This expression data has been preliminarily compared to expression array data from existing models of myopic development; however, no perfect tissue matches have been performed. To gain a better assessment of normal human ocular growth as a model for myopic development, whole genome tissue expression studies must be completed in one or more animal models of myopia, using the same tissues as in our study. Then the data could be more accurately compared for similarities and differences within each tissue type.

5.3.2 Refinement of the *MYP3* locus

5.3.2.1 Validation by Additional Cohorts and/or Ethnicities

Validation of the candidate SNPs for myopic development within the *MYP3* locus was completed in one independent cohort of the same ethnicity and screened in a previously genotyped cohort. Screening these genes for quantitative association in additional cohorts is necessary to understand the frequency of their possible impact in a general population. In particular, they should be screened in Asian cohorts, where myopic prevalence is continually rising.

5.3.2.2 Tagging SNPs

In addition to further validation with a larger sample pool, these genes should be further refined. Tagging SNPs within this and other populations may help identify regions of either shared or novel mutations affecting myopic progression. It is unlikely that sequencing for variants that segregate within families would yield causal mutations, as the strongest evidence for association for all of the candidates was that of quantitative traits measuring disease severity. Refinement of the genes may uncover hotspots for mutation or regions of functional importance which could affect the quantitative trait SPH.

5.3.2.3 Functional Validation

Once fine mapping of the candidate genes is complete, any candidate mutations would need to be functionally tested for alterations to the gene product and subsequent changes in ocular growth. These mutations could be cloned into cell lines to measure protein product and assess protein efficiency. However, the best method of functionally validating any candidate mutations within these genes would be to create an animal model (such as zebrafish morpholinos) to screen for phenotypic changes consistent with myopic development.

5.3.2.4 Differential Expression in Animal Models of Myopia

Another future direction to validate these novel candidate genes would be to specifically test for differential expression of them in one or more animal models of myopia. Differential expression of these candidates may have been missed in other array studies due to varying significance criteria or tissue selection. RT-qPCR of the candidate genes in all relevant tissues between control and myopic eyes might help to validate or exclude existing candidates.

5.4 Conclusions

5.4.1 Ocular Growth as a Model for Myopia

There has been shown strong preliminary evidence for normal ocular growth as a surrogate model for the rapid growth seen in myopic development. Many candidate genes implicated in the development of myopia from genetic and animal model studies were replicated using our model. Additionally, this pool of data can be used to prioritize candidates within candidate genomic regions (which is of particular use in very large regions such as *MYP3*). Lastly, the functional and pathway information contained in this data can be used to interpret candidates and infer potential biological mechanisms for disease development or progression.

5.4.2 Refinement of the *MYP3* Locus

Three novel candidates for high myopia have been identified from the *MYP3* locus – *PTPRR*, *PPFIA2*, and *UHRF1BP1L*. All three candidates have either suggestive or strong supporting evidence in at least one additional high myopia cohort. They also all have known functions which could explain their roles in disease progression. Two genes, *PTPRR* and *PPFIA2*, also showed genomic convergence with our novel proposed model for myopic development, while the third, *UHRF1BP1L*, may have convergence via its pathways. Two of these candidates, *PTPRR* and *PPFIA2*, are both functionally related PTP genes belonging to a large group identified within the *MYP3* locus as being enriched for significance to myopic quantitative association, which may indicate a possible mechanism involved in the development and/or progression of myopia.

Appendix A

Candidate Genomic Loci Identified for Myopia by Linkage.

Those regions with locus names and MIM numbers have been approved by the Human Genome Organization Gene Nomenclature Committee. Some regions have been identified for overlapping myopia classifications. Replicate (R) studies listed only for differing myopia severities. † Indicates suggestive evidence for locus (at least one LOD score > 2, < 3). * Estimated D based on axial length (AL) ($\Delta 1 \text{ mm} \approx 3 \text{ D}$ refractive error; average AL ~ 24 mm (Nakanishi, Yamada et al. 2009)).

Locus	MIM	Cytogenic Location	Reference Study	Myopia Severity
Quantitative Myopia				
<i>MYP14</i>	610320	1p36	(Wojciechowski, Moy et al. 2006)	Mean -3.46 D
		1q41	(Fan, Barathi et al. 2012)	AL 20.48 – 38.03 mm
		2p23.2 †	(Wojciechowski, Moy et al. 2006)	Mean -3.46 D
		3q29 †	(Abbott, Li et al. 2012)	9 to -29 D
		4q28.3 †	(Wojciechowski, Moy et al. 2006)	Mean -3.46 D
		5q14.2	(Zhu, Hewitt et al. 2008)	11.7 to -14.7 D *
		5q35.1 – q35.2	(Abbott, Li et al. 2012)	9 to -29 D
		†		
		6q13 – q16.1 †	(Abbott, Li et al. 2012)	9 to -29 D
		6q14.1 - q15 †	(Zhu, Hewitt et al. 2008)	11.7 to -14.7 D *
<i>MYP17</i>	608367	7p15	(Ciner, Wojciechowski et al. 2008)	Mean -2.87 D
		7q11.23 – q21.2 †	(Abbott, Li et al. 2012)	9 to -29 D
		9p23 †	(Wojciechowski, Moy et al. 2006)	Mean -3.46 D
		10q25.3 †	(Zhu, Hewitt et al. 2008)	11.7 to -14.7 D *
		14q32.13 †	(Zhu, Hewitt et al. 2008)	11.7 to -14.7 D *
		15q14	(Solouki, Verhoeven et al. 2010)	-19 to 10 D
All Myopia				
<i>MYP8</i>	609257	3q26	(Hammond, Andrew et al. 2004)	< 0 D

<i>MYP9</i>	609258	4q12	(Hammond, Andrew et al. 2004)	< 0 D
<i>MYP10</i>	609259	8p23	(Hammond, Andrew et al. 2004)	< 0 D
<i>MYP7</i>	609256	11p13	(Hammond, Andrew et al. 2004)	< 0 D

Mild to Moderate Myopia

<i>MYP12(R)</i>	609995	2q37.1	(Chen, Stankovich et al. 2007)	-0.50 to -10.25 D
<i>MYP10 (R)</i>	609259	6q23.3 †	(Ciner, Ibay et al. 2009)	< -1 D
		8p23 †	(Stambolian, Ciner et al. 2005)	< -1 D
		11p15.1 †	(Ciner, Ibay et al. 2009)	< -1 D
		12p12.3 - p11.23 †	(Ciner, Ibay et al. 2009)	< -1 D
		14q32.2 †	(Stambolian, Ibay et al. 2004)	< -1 D
<i>MYP6</i>	608908	15q25	(Hysi, Young et al. 2010)	< -1 D
		20p11.21 - q13.12 †	(Ciner, Ibay et al. 2009)	< -1 D
		22q12	(Stambolian, Ibay et al. 2004)	< -1 D
		Xq21.1 - q21.33 †	(Stambolian, Ciner et al. 2005)	< -1 D

High Myopia

<i>MYP14 (R)</i>	610320	1p36 †	(Li, Guggenheim et al. 2009)	< -5 D
<i>MYP21</i>	614167	1p22.2	(Shi, Li et al. 2011)	-6.27 to -20 D
		2p24.1 †	(Li, Guggenheim et al. 2009)	< -5 D
<i>MYP12</i>	609995	2p14 †	(Li, Guggenheim et al. 2009)	< -5 D
		2q37.1	(Paluru, Nallasamy et al. 2005)	-7.25 D to -27 D
<i>MYP11</i>	609994	3p13 †	(Li, Guggenheim et al. 2009)	< -5 D
<i>MYP16</i>	612554	4q22 - q27	(Zhang, Guo et al. 2005)	-5 D to -20 D
<i>MYP19</i>	613969	5p15.33-15.2	(Lam, Tam et al. 2008)	< -6 D
		5p15.1-p13.3	(Ma, Shen et al. 2010)	< -6 D
		5q23.3 †	(Li, Guggenheim et al. 2009)	< -5 D
		5q31.1 †	(Li, Guggenheim et al. 2009)	< -5 D
		5q33.1 †	(Li, Guggenheim et al. 2009)	< -5 D
		6p24.1 †	(Li, Guggenheim et al. 2009)	< -5 D
		(R)		6q14.1 †
<i>MYP17 (R)</i>	608367	7p15	(Paget, Julia et al. 2008)	< -5 D

<i>MYP4</i>	608367	7p14.1 †	(Li, Guggenheim et al. 2009)	< -5 D
		7q36 †	(Naiglin, Gazagne et al. 2002)	Mean -13.05 D
<i>MYP15</i>	612717	9q34.11 †	(Li, Guggenheim et al. 2009)	< -5 D
		10p14	(Li, Guggenheim et al. 2009)	< -5 D
		10p11.21	(Li, Guggenheim et al. 2009)	< -5 D
		10q21.1	(Nallasamy, Paluru et al. 2007)	< -5 D
<i>MYP3</i>	603221	11q24.1	(Nakanishi, Yamada et al. 2009)	AL > 28 mm
		12p11.21 †	(Li, Guggenheim et al. 2009)	< -5 D
		12q12-q15 †	(Li, Guggenheim et al. 2009)	< -5 D
		12q21 - q23	(Young, Ronan et al. 1998)	-6.25 D to -15 D
		13q12.12	(Shi, Qu et al. 2011)	< -6 D
<i>MYP18</i>	255500	13q33.3 †	(Li, Guggenheim et al. 2009)	< -5 D
		14q11.2 †	(Yang, Xiao et al. 2009)	< -6 D
		14q22.1-q24.2 †	(Yang, Xiao et al. 2009)	< -6 D
<i>MYP5</i>	608474	15q12 - q13	(Yu, Li et al. 2007)	High (unknown criteria)
		15q21.1 †	(Li, Guggenheim et al. 2009)	< -5 D
		15q26.2 †	(Li, Guggenheim et al. 2009)	< -5 D
		16p11.2 †	(Li, Guggenheim et al. 2009)	< -5 D
		17p12	(Li, Guggenheim et al. 2009)	< -5 D
		17q21 - q22	(Paluru, Ronan et al. 2003)	-5.5 D to -50 D
		18p11.31	(Young, Ronan et al. 1998)	-6 D to -21 D
<i>MYP2</i>	160700	18q12.1	(Li, Guggenheim et al. 2009)	< -5 D
<i>MYP6 (R)</i>	608908	19p13.3 - p13.12 †	(Li, Guggenheim et al. 2009)	< -5 D
		19q13.32 †	(Li, Guggenheim et al. 2009)	< -5 D
		20q13.13 †	(Li, Guggenheim et al. 2009)	< -5 D
		22q12.3 †	(Li, Guggenheim et al. 2009)	< -5 D
<i>MYP13</i>	300613	Xq23 - q27.2 †	(Zhang, Guo et al. 2006); (Zhang, Li et al. 2007)	-6 D to -20 D; < -7 D
<i>MYP1</i>	310460	Xq28	(Schwartz, Haim et al. 1990)	-6.75 to -11.25 D

Appendix B

Adult Versus Fetal Retina/RPE

Gene	FC	P-value	Gene	FC	P-value
<i>CRHR1</i>	-8.5	0.0003	<i>INMT</i>	21.09	2.65E-05
<i>FLJ40244</i>	-8.11	0.0012	<i>C5ORF48</i>	9.79	0.0004
<i>LOC100133528</i>	-5.25	0.0025	<i>GCGR</i>	5.33	5.29E-05
<i>CYP24A1</i>	-4.65	0.0026	<i>ASCL4</i>	5.17	0.0046
<i>ETFB</i>	-4.31	2.65E-05	<i>HAND1</i>	4.37	0.0018
<i>C13ORF23</i>	-4.1	0.0059	<i>LOC399706</i>	4.08	0.0003
<i>NUP155</i>	-3.49	0.0036	<i>HNMT</i>	3.9	0.0044
<i>ZNF92</i>	-3.4	0.0002	<i>KIR2DL3</i>	3.8	5.29E-05
<i>MAGED4</i>	-3.38	0.0001	<i>NRP2</i>	3.72	0.0001
<i>C20ORF118</i>	-3.36	0.0055	<i>DLX6</i>	3.52	0.0005
<i>KRT6A</i>	-3.28	0.0011	<i>FOXR1</i>	3.42	0.0015
<i>SNIP</i>	-3.2	0.0068	<i>OR52A1</i>	3.41	0.0001
<i>ASB6</i>	-3.17	0.0064	<i>LOC100127983</i>	3.36	0.0068
<i>KIF4A</i>	-3.16	0.0008	<i>HERV-FRD</i>	3.35	0.0005
<i>FAM19A1</i>	-3.09	0.0042	<i>40610</i>	3.33	0.0025
<i>MMD2</i>	-3.08	0.0001	<i>IL1RN</i>	3.3	0.0036
<i>LRRIQ3</i>	-3.05	0.0008	<i>DEFB119</i>	3.14	2.65E-05
<i>SGOL2</i>	-3.01	0.0018	<i>EDNRB</i>	3.12	0.0002
<i>KLK12</i>	-2.97	0.0068	<i>MAGEA11</i>	3.1	0.0005
<i>TDGF1</i>	-2.96	0.0001	<i>MT1M</i>	3.02	2.65E-05
<i>NNAT</i>	-2.94	2.65E-05	<i>LOC389834</i>	3	2.65E-05
<i>LOC651746</i>	-2.92	0.0002	<i>FAM55A</i>	2.99	0.0003
<i>OTOS</i>	-2.92	0.0008	<i>DCST2</i>	2.97	5.29E-05
<i>COL6A6</i>	-2.89	0.0046	<i>LOC646085</i>	2.94	0.0003
<i>ZWILCH</i>	-2.88	0.0008	<i>RHO</i>	2.93	2.65E-05
<i>SSX2</i>	-2.86	0.0068	<i>CAMP</i>	2.93	0.0037
<i>NSBP1</i>	-2.84	2.65E-05	<i>BEST3</i>	2.91	0.0003
<i>RIPPLY2</i>	-2.81	2.65E-05	<i>MICB</i>	2.86	2.65E-05
<i>COL2A1</i>	-2.74	0.0002	<i>LGSN</i>	2.86	0.005
<i>TTY17B</i>	-2.74	0.005	<i>HUS1</i>	2.82	0.005
<i>TTY9A</i>	-2.73	0.0036	<i>LRRC25</i>	2.8	0.0068
<i>BPY2C</i>	-2.68	0.0072	<i>FAM55D</i>	2.77	0.0025
<i>KIAA0514</i>	-2.65	2.65E-05	<i>EPYC</i>	2.76	0.0012
<i>LOC653889</i>	-2.64	0.0002	<i>KCNJ14</i>	2.74	0.0008
<i>MATK</i>	-2.62	0.0006	<i>VCAM1</i>	2.73	0.005
<i>TREML2P</i>	-2.6	0.0025	<i>GJA8</i>	2.69	0.0008
<i>BTBD17</i>	-2.59	2.65E-05	<i>KRTAP19-4</i>	2.65	0.0018
<i>SLC18A2</i>	-2.54	0.0008	<i>OR13F1</i>	2.64	0.0068
<i>PAMR1</i>	-2.54	0.0036	<i>LOC653075</i>	2.63	0.0005
<i>ABHD11</i>	-2.53	0.0019	<i>CYP2A7</i>	2.63	0.0068

Adult Versus Fetal Choroid

Gene	FC	P-value	Gene	FC	P-value
<i>HBG1</i>	-617.57	0.0007	<i>SERPINA3</i>	550.49	0.0007
<i>COL9A1</i>	-165.29	0.0007	<i>SAA1</i>	344.94	0.0007
<i>HBG2</i>	-159.85	0.0007	<i>MT1M</i>	221.47	0.0007
<i>HCG2P7</i>	-117.26	0.0013	<i>PLA2G2A</i>	220.99	0.0007
<i>HBA1</i>	-98.16	0.0007	<i>SNTN</i>	179.32	0.0027
<i>GRIK1</i>	-92.66	0.0007	<i>C19ORF12</i>	174.68	0.0007
<i>APLNR</i>	-75.93	0.0007	<i>LOC100128693</i>	139.44	0.0013
<i>HBM</i>	-74.74	0.0007	<i>LOC100132620</i>	137.85	0.0007
<i>DUXAP3</i>	-66.52	0.0027	<i>TTC21B</i>	123.34	0.0013
<i>DMC1</i>	-65	0.0027	<i>ZNF273</i>	112.7	0.0027
<i>NLRP8</i>	-62.8	0.0027	<i>LOC100132518</i>	108.2	0.0007
<i>GRIK1</i>	-62.17	0.0007	<i>IL1RL1</i>	96.02	0.0007
<i>LOC100128084</i>	-55.69	0.0013	<i>GTF2IRD2B</i>	86.41	0.0007
<i>TOP2A</i>	-55.64	0.0007	<i>LOC100132540</i>	85.5	0.0024
<i>ARMCX6</i>	-54.79	0.0024	<i>NNMT</i>	84.35	0.0007
<i>LOC645452</i>	-50.32	0.0027	<i>PPIL3</i>	80.97	0.0007
<i>IGF1</i>	-45.62	0.0007	<i>RUNDC2B</i>	80.95	0.0007
<i>FCAR</i>	-45.56	0.0027	<i>LOC729652</i>	80.46	0.0007
<i>KCNK4</i>	-45.45	0.0007	<i>STAG3L1</i>	74.06	0.0007
<i>CRTAP</i>	-43.96	0.0007	<i>PRIM2</i>	69.86	0.0013
<i>CXCL12</i>	-43.05	0.0007	<i>SNHG10</i>	68.88	0.0007
<i>UBE2C</i>	-42.86	0.0007	<i>BCAS4</i>	67.49	0.0007
<i>CDKN2AIPNL</i>	-41.93	0.0047	<i>LOC100134172</i>	66.89	0.0007
<i>COL4A5</i>	-39.77	0.0007	<i>LOC100129445</i>	65.3	0.0007
<i>KIAA1751</i>	-36.97	0.0027	<i>PTER</i>	65.12	0.0027
<i>SFRP4</i>	-36.3	0.0007	<i>GNPTAB</i>	64.42	0.0047
<i>TRIM24</i>	-36.18	0.0007	<i>TRIM16L</i>	60.82	0.0047
<i>CCT7</i>	-35.79	0.0024	<i>CHI3L2</i>	59.38	0.0007
<i>NCAPG</i>	-35.44	0.0007	<i>LOC202134</i>	59.22	0.0007
<i>MCART1</i>	-34.88	0.0027	<i>LOC100128562</i>	58.77	0.0007
<i>COL1A2</i>	-34.43	0.0024	<i>TAF8</i>	58.48	0.0007
<i>LRRC37B2</i>	-34.37	0.0027	<i>PPID</i>	58.47	0.0007
<i>LOC100128505</i>	-34.36	0.0027	<i>LOC651192</i>	53.93	0.0007
<i>ARHGAP28</i>	-33.11	0.0007	<i>LOC728054</i>	52.7	0.0013
<i>AP1S1</i>	-32	0.0024	<i>LOC647592</i>	52.36	0.0007
<i>GPC3</i>	-31.98	0.0007	<i>STAP2</i>	49.61	0.0027
<i>LOC399900</i>	-31.51	0.0027	<i>ZNF100</i>	49.02	0.0007
<i>HBZ</i>	-30.9	0.0007	<i>TEX11</i>	48.84	0.0013
<i>LAMA1</i>	-30.8	0.0007	<i>SLA2</i>	47.56	0.0007
<i>IP6K2</i>	-30.51	0.0007	<i>ST20</i>	46.86	0.0007

Adult Versus Fetal Sclera

Gene	FC	P-value	Gene	FC	P-value
<i>ACOX1</i>	-125.11	0.0065	<i>MYOC</i>	6.4	3.69E-05
<i>EYA2</i>	-96.93	0.0016	<i>ABCF2</i>	5.47	0.0004
<i>KRTAP5-6</i>	-91.07	0.0003	<i>FMO3</i>	4.1	0.0021
<i>GRIA1</i>	-32.41	0.0012	<i>SLPI</i>	3.92	3.69E-05
<i>CDON</i>	-9.68	0.0011	<i>PLA2G2A</i>	3.64	3.69E-05
<i>CDC45L</i>	-9.61	3.69E-05	<i>GLDN</i>	3.26	3.69E-05
<i>MRI1</i>	-9.43	0.0009	<i>AKR1B10</i>	3.14	3.69E-05
<i>SNIP</i>	-8.94	0.0001	<i>SLC26A4</i>	3.14	3.69E-05
<i>MAL2</i>	-8.59	3.69E-05	<i>SCNN1A</i>	3.08	3.69E-05
<i>FOXL2</i>	-8.04	0.0007	<i>CCL15</i>	2.94	0.0012
<i>KCNIP2</i>	-7.92	0.0016	<i>KCNE1</i>	2.9	0.0001
<i>COL11A1</i>	-7.81	0.0044	<i>COMP</i>	2.78	3.69E-05
<i>UBASH3A</i>	-7.43	0.0001	<i>CD69</i>	2.72	0.0021
<i>S100A12</i>	-7.15	3.69E-05	<i>C10ORF81</i>	2.59	7.37E-05
<i>NEU3</i>	-7.05	3.69E-05	<i>TCEAL6</i>	2.58	3.69E-05
<i>KIAA1549</i>	-6.56	3.69E-05	<i>SCGB3A2</i>	2.57	3.69E-05
<i>DEFA4</i>	-6.3	0.0027	<i>CHI3L2</i>	2.56	3.69E-05
<i>TCF2</i>	-6.26	0.0046	<i>COL4A3</i>	2.56	0.0011
<i>PTGER3</i>	-6.14	0.0011	<i>LIN28</i>	2.54	0.0007
<i>DDX25</i>	-6.01	0.0021	<i>SAA1</i>	2.54	0.0007
<i>RASSF5</i>	-5.98	0.0046	<i>MMP3</i>	2.53	3.69E-05
<i>BUB1</i>	-5.94	0.0005	<i>ABCC2</i>	2.51	3.69E-05
<i>RPE</i>	-5.92	0.0046	<i>KRTAP9-3</i>	2.49	0.0003
<i>MATN4</i>	-5.91	0.0027	<i>MMP12</i>	2.43	0.0011
<i>KLK3</i>	-5.75	0.0004	<i>MT1M</i>	2.42	3.69E-05
<i>CACNA1G</i>	-5.73	0.0021	<i>CYP4F12</i>	2.39	3.69E-05
<i>METTL1</i>	-5.71	0.0004	<i>OR7D2</i>	2.39	0.0003
<i>HBM</i>	-5.71	0.0027	<i>SERPINA3</i>	2.39	0.0005
<i>ARPP-21</i>	-5.67	0.0054	<i>ASB11</i>	2.35	0.0027
<i>AGR2</i>	-5.61	0.0012	<i>GPR88</i>	2.34	3.69E-05
<i>ALDH4A1</i>	-5.44	0.0035	<i>PDPN</i>	2.34	0.0024
<i>TOP2A</i>	-5.43	3.69E-05	<i>LOC100130988</i>	2.29	0.0046
<i>HRH3</i>	-5.37	0.0072	<i>ANGPTL7</i>	2.27	3.69E-05
<i>TBC1D29</i>	-5.35	0.0016	<i>NNMT</i>	2.27	3.69E-05
<i>OR1E2</i>	-5.31	0.0033	<i>GBP2</i>	2.25	3.69E-05
<i>MIR1258</i>	-5.3	7.37E-05	<i>INMT</i>	2.25	3.69E-05
<i>GPR44</i>	-5.22	0.0072	<i>MYOC</i>	2.22	3.69E-05
<i>COL6A6</i>	-5.18	3.69E-05	<i>KRT28</i>	2.22	0.0062
<i>TRIM29</i>	-5.17	0.0062	<i>ZBTB16</i>	2.21	3.69E-05
<i>RHBDF2</i>	-5.12	0.0007	<i>KGFLP1</i>	2.21	0.0007

Adult Versus Fetal Optic Nerve

Gene	FC	P-value	Gene	FC	P-value
<i>COL1A1</i>	-205.22	0.0043	<i>BCAS1</i>	1695.34	0.0067
<i>COL3A1</i>	-171.4	0.0043	<i>BCAS1</i>	1105.48	0.0075
<i>COL1A2</i>	-100.87	0.0043	<i>MAG</i>	111.21	0.0043
<i>C5ORF13</i>	-97.75	0.0043	<i>S1PR5</i>	79.37	0.0055
<i>CPNE4</i>	-73.78	0.0075	<i>ZNF488</i>	50.7	0.0075
<i>MMP15</i>	-63.99	0.0067	<i>GPX3</i>	47.64	0.0043
<i>PRND</i>	-63.09	0.0043	<i>RAB11FIP4</i>	43.7	0.008
<i>SEMA5B</i>	-60.69	0.008	<i>FA2H</i>	38.01	0.0075
<i>COL1A2</i>	-60.34	0.0043	<i>MAL</i>	25.43	0.0043
<i>CDH7</i>	-60.03	0.0067	<i>CENTA1</i>	24.84	0.0043
<i>C20ORF103</i>	-59.18	0.008	<i>SEPT4</i>	22.55	0.0043
<i>PCDH12</i>	-46.03	0.0075	<i>COBL</i>	19.78	0.0043
<i>COL5A1</i>	-45.92	0.0043	<i>MAP6D1</i>	18.84	0.0043
<i>TBC1D10C</i>	-44.02	0.0067	<i>SEPT4</i>	18.7	0.0043
<i>KAL1</i>	-43.22	0.0043	<i>COL4A3</i>	17.72	0.0067
<i>APOA1</i>	-36.38	0.0075	<i>APOD</i>	16.26	0.0043
<i>HS.204481</i>	-35.77	0.0055	<i>QDPR</i>	14.35	0.0043
<i>TNC</i>	-34.88	0.0043	<i>PRODH</i>	12.89	0.0043
<i>FNDC1</i>	-33.21	0.0043	<i>MIR1974</i>	12.05	0.0173
<i>RSPO4</i>	-31.26	0.0055	<i>APLP1</i>	12.02	0.0043
<i>FOXL2</i>	-29.21	0.0054	<i>CAPN3</i>	11.78	0.0087
<i>COL5A2</i>	-26.92	0.0043	<i>PPP1R14A</i>	11.55	0.0043
<i>TNFRSF25</i>	-24.92	0.0043	<i>PCTK3</i>	11.43	0.0043
<i>CDC20B</i>	-24.3	0.0043	<i>MIR1978</i>	11.06	0.0043
<i>SLIT1</i>	-23.74	0.008	<i>SLC7A2</i>	9.89	0.0043
<i>THSD1</i>	-23.04	0.008	<i>TP53INP2</i>	9.58	0.0043
<i>SLC16A14</i>	-22.9	0.008	<i>C7ORF41</i>	9.54	0.0043
<i>OCA2</i>	-22.81	0.0075	<i>MT1X</i>	8.93	0.0043
<i>ARSE</i>	-21.69	0.0066	<i>BCYRN1</i>	8.92	0.0043
<i>SPON1</i>	-20.66	0.0043	<i>COL4A4</i>	8.89	0.0067
<i>MYH7</i>	-20.65	0.008	<i>DBNDD2</i>	8.63	0.0043
<i>UNC13C</i>	-20.63	0.0043	<i>FAM107A</i>	8.21	0.0043
<i>FBN2</i>	-20.57	0.0043	<i>CDKN1A</i>	8.09	0.0173
<i>NKD2</i>	-20.31	0.0043	<i>SYNM</i>	7.74	0.0087
<i>MMP25</i>	-20	0.0043	<i>ENPP2</i>	7.67	0.0173
<i>MXRA5</i>	-19.37	0.0043	<i>C10ORF116</i>	7.64	0.0043
<i>C20ORF46</i>	-18.85	0.0075	<i>CHN2</i>	7.47	0.0043
<i>VCAN</i>	-18.8	0.0043	<i>S100A8</i>	7.38	0.0353
<i>DACT1</i>	-18.02	0.0043	<i>ENPP2</i>	7.22	0.0173
<i>NMU</i>	-18.02	0.0067	<i>RGS1</i>	7.05	0.0043

Adult Versus Fetal Cornea

Gene	FC	P-value	Gene	FC	P-value
<i>LOC100134134</i>	-1252.45	0.0043	<i>MAMDC2</i>	205.77	0.0043
<i>OGN</i>	-612.53	0.0043	<i>AKR1C2</i>	192.43	0.0043
<i>MEG3</i>	-451.89	0.0043	<i>KRT24</i>	181.18	0.0043
<i>COL5A1</i>	-321.1	0.0043	<i>ADH7</i>	174.83	0.0043
<i>FAM180A</i>	-277.35	0.0043	<i>ZBTB16</i>	156.59	0.0039
<i>OGN</i>	-274.14	0.0043	<i>ANGPTL7</i>	142.31	0.0043
<i>THBS2</i>	-265.3	0.0043	<i>CA3</i>	114	0.0039
<i>DPT</i>	-256.95	0.0043	<i>IL20RA</i>	111.17	0.0043
<i>SOCS1</i>	-250.99	0.0043	<i>AKR1C4</i>	109.18	0.0043
<i>THRA</i>	-228.18	0.0043	<i>SLURP1</i>	99.65	0.0039
<i>PXDN</i>	-217.78	0.0043	<i>SLC47A1</i>	89.77	0.0039
<i>IGDCC4</i>	-211.63	0.0043	<i>IFI27</i>	82.06	0.0043
<i>COL1A1</i>	-209.79	0.0043	<i>INMT</i>	81.8	0.0039
<i>COL3A1</i>	-161.78	0.0043	<i>GJB4</i>	81.42	0.0043
<i>RASL11B</i>	-157.22	0.0043	<i>MME</i>	74.43	0.0043
<i>MMP23B</i>	-154.42	0.0043	<i>MYOC</i>	74.2	0.0043
<i>KCNIP4</i>	-148.3	0.0043	<i>EFCBP1</i>	73.56	0.0039
<i>PCDH17</i>	-147.06	0.0043	<i>TMEM45B</i>	68.26	0.0039
<i>MFAP2</i>	-143.13	0.0043	<i>STEAP4</i>	66.43	0.0039
<i>NTM</i>	-131.38	0.0043	<i>PLK5P</i>	66.16	0.0039
<i>COCH</i>	-131.04	0.0043	<i>HSD11B1</i>	63.84	0.0039
<i>UNQ1940</i>	-126.31	0.0043	<i>ECM1</i>	63.1	0.0043
<i>SRPX</i>	-126.27	0.0043	<i>NQO1</i>	58.54	0.0043
<i>CAPN6</i>	-103.79	0.0043	<i>CRTAC1</i>	54.78	0.0043
<i>HBG1</i>	-99.54	0.0043	<i>KRT27</i>	47.54	0.0043
<i>FBN2</i>	-93.03	0.0043	<i>CALML3</i>	46.96	0.0043
<i>HBA2</i>	-89.18	0.0043	<i>PTPN22</i>	46.1	0.0039
<i>THY1</i>	-86.78	0.0043	<i>COL8A1</i>	43.63	0.0039
<i>SOX11</i>	-81.66	0.0043	<i>PSCA</i>	40.4	0.0043
<i>SMO</i>	-80.53	0.0043	<i>ZBTB16</i>	40.19	0.0043
<i>C1QTNF1</i>	-79.43	0.0043	<i>ECM1</i>	38.83	0.0043
<i>MMP23A</i>	-78.59	0.0043	<i>SOD3</i>	37.61	0.0043
<i>COL11A1</i>	-75.57	0.0043	<i>MICALCL</i>	37.6	0.0043
<i>PMEPA1</i>	-74.45	0.0043	<i>AGXT2L1</i>	36.92	0.0039
<i>CCND2</i>	-73.66	0.0043	<i>CYP26A1</i>	35.79	0.0043
<i>HBG2</i>	-70.49	0.0043	<i>FAM164C</i>	35.05	0.0039
<i>SCXA</i>	-69.87	0.0043	<i>ALDH3A1</i>	34.93	0.0043
<i>SNCAIP</i>	-63.58	0.0043	<i>SYT8</i>	34.61	0.0043
<i>PYCR1</i>	-62.75	0.0043	<i>RGS7BP</i>	34.48	0.0039
<i>C1QTNF5</i>	-61.52	0.0043	<i>CLCA4</i>	34	0.0043

Central Versus Peripheral Retina

Gene	FC	P-value	Gene	FC	P-value
<i>DKK1</i>	-10.22	0.0625	<i>PRPH</i>	14.65	0.0625
<i>LOC493869</i>	-4.43	0.0625	<i>PMP2</i>	7.4	0.0625
<i>ID3</i>	-4.31	0.0625	<i>NEFL</i>	6.97	0.0625
<i>FXYD6</i>	-3.61	0.0625	<i>POU4F1</i>	5.79	0.0625
<i>GAGE2B</i>	-3.47	0.0625	<i>NEFM</i>	5.67	0.0625
<i>KCNJ13</i>	-3.31	0.0625	<i>RASGRP3</i>	5.37	0.0625
<i>ERP27</i>	-2.96	0.0625	<i>DDX12</i>	4.71	0.0625
<i>ATP1A2</i>	-2.92	0.0625	<i>AHNAK2</i>	4.68	0.0625
<i>ZIC2</i>	-2.83	0.0625	<i>NEFH</i>	4.5	0.0625
<i>XLKD1</i>	-2.78	0.0625	<i>ISLR2</i>	4.43	0.0625
<i>CYR61</i>	-2.74	0.0625	<i>SNCG</i>	4.38	0.0625
<i>HOPX</i>	-2.64	0.0625	<i>ANXA2</i>	4.17	0.0625
<i>PPP1R3C</i>	-2.59	0.0625	<i>FABP3</i>	3.99	0.0625
<i>SFRS3</i>	-2.51	0.0625	<i>STMN2</i>	3.85	0.0625
<i>ATOH8</i>	-2.49	0.0625	<i>CDC42BPA</i>	3.82	0.0625
<i>TSPAN1</i>	-2.46	0.0625	<i>POU4F2</i>	3.69	0.0625
<i>COL2A1</i>	-2.41	0.0625	<i>LDLR</i>	3.64	0.0625
<i>ID4</i>	-2.41	0.0625	<i>ADCY3</i>	3.61	0.0625
<i>SNORA12</i>	-2.41	0.0625	<i>CPLX1</i>	3.57	0.0625
<i>C14ORF173</i>	-2.4	0.0625	<i>IRX2</i>	3.5	0.0625
<i>BTG2</i>	-2.39	0.0625	<i>L1CAM</i>	3.46	0.0625
<i>FOS</i>	-2.39	0.0625	<i>DLC1</i>	3.39	0.0625
<i>LOC441550</i>	-2.35	0.0625	<i>PTH1R</i>	3.35	0.0625
<i>RHOD</i>	-2.35	0.0625	<i>TNFRSF21</i>	3.32	0.0625
<i>MT1H</i>	-2.34	0.0625	<i>RBPM2</i>	3.19	0.0625
<i>LOC137107</i>	-2.33	0.0625	<i>TSC22D3</i>	3.05	0.0625
<i>SPHK1</i>	-2.33	0.0625	<i>EOMES</i>	3.03	0.0625
<i>EPHA2</i>	-2.31	0.0625	<i>UCHL1</i>	3.01	0.0625
<i>LOC642567</i>	-2.29	0.0625	<i>EBF1</i>	2.99	0.0625
<i>LOC644037</i>	-2.26	0.0625	<i>QPRT</i>	2.96	0.0625
<i>CDH23</i>	-2.24	0.0625	<i>VSNL1</i>	2.92	0.0625
<i>PPIB</i>	-2.23	0.0625	<i>STMN2</i>	2.87	0.0625
<i>LOC550112</i>	-2.22	0.0625	<i>MAP1A</i>	2.83	0.0625
<i>LOC643308</i>	-2.17	0.0625	<i>TSPAN8</i>	2.82	0.0625
<i>MT1G</i>	-2.17	0.0625	<i>SLC6A17</i>	2.82	0.0625
<i>VASH1</i>	-2.15	0.0625	<i>TMSB10</i>	2.81	0.0625
<i>ID1</i>	-2.14	0.0625	<i>HBA1</i>	2.79	0.0625
<i>C4ORF23</i>	-2.12	0.0625	<i>C1QTNF1</i>	2.75	0.0625
<i>LITAF</i>	-2.12	0.0625	<i>FOXF2</i>	2.75	0.0625
<i>SLC45A2</i>	-2.11	0.0625	<i>TMEM97</i>	2.73	0.0625

Central Versus Peripheral Choroid

Gene	FC	P-value	Gene	FC	P-value
<i>HDC</i>	-5.28	0.0625	<i>ACTB</i>	12.68	0.0938
<i>KIAA1199</i>	-4.44	0.0313	<i>ZNF674</i>	11.44	0.0938
<i>SPARCL1</i>	-4.36	0.0313	<i>ROCK2</i>	6.11	0.0938
<i>B4GALT5</i>	-4.32	0.0938	<i>LOC100132727</i>	5.92	0.0938
<i>DAPL1</i>	-4.25	0.0625	<i>LOC100130053</i>	5.52	0.0938
<i>C6ORF48</i>	-4.21	0.0313	<i>LOC100129758</i>	5.5	0.0625
<i>TFF3</i>	-4.12	0.0625	<i>ANKRD30B</i>	4.86	0.0938
<i>C15ORF24</i>	-4	0.0313	<i>RPL11</i>	4.74	0.0625
<i>ABCA4</i>	-3.9	0.0313	<i>LOC100133465</i>	4.63	0.0938
<i>SMOC2</i>	-3.86	0.0313	<i>MYH11</i>	4.57	0.0938
<i>LITAF</i>	-3.85	0.0313	<i>CALD1</i>	4.43	0.0313
<i>PTCD2</i>	-3.69	0.0625	<i>IGLL1</i>	4.4	0.0313
<i>CDON</i>	-3.65	0.0625	<i>LOC100132593</i>	4.38	0.0938
<i>C12ORF48</i>	-3.63	0.0313	<i>A2M</i>	4.33	0.0313
<i>AGPAT5</i>	-3.51	0.0313	<i>PPP1R1B</i>	4.21	0.0938
<i>CPNE3</i>	-3.51	0.0625	<i>CLUAP1</i>	4.16	0.0313
<i>PLEKHH2</i>	-3.49	0.0313	<i>BIN3</i>	4.13	0.0313
<i>MRPL51</i>	-3.46	0.0313	<i>HS.19339</i>	4.13	0.0625
<i>HMGN2</i>	-3.45	0.0938	<i>VCAM1</i>	4.09	0.0625
<i>PI16</i>	-3.38	0.0313	<i>AQP7P2</i>	3.98	0.0938
<i>GINS2</i>	-3.26	0.0313	<i>TSC22D3</i>	3.9	0.0938
<i>OLFM2</i>	-3.21	0.0625	<i>ATOH8</i>	3.83	0.0625
<i>MMP2</i>	-3.2	0.0313	<i>BOLA2</i>	3.78	0.0313
<i>MAN1C1</i>	-3.2	0.0313	<i>ORC6L</i>	3.78	0.0938
<i>GAPDH</i>	-3.17	0.0313	<i>ARRDC2</i>	3.68	0.0313
<i>FHL1</i>	-3.17	0.0625	<i>RPS14</i>	3.64	0.0625
<i>C18ORF18</i>	-3.17	0.0938	<i>LOC100133760</i>	3.56	0.0938
<i>MGST1</i>	-3.15	0.0625	<i>DCPS</i>	3.47	0.0625
<i>PLTP</i>	-3.1	0.0625	<i>LOC645979</i>	3.38	0.0938
<i>C14ORF45</i>	-3.06	0.0625	<i>CYP4X1</i>	3.29	0.0625
<i>SERPINB1</i>	-3.06	0.0625	<i>C17ORF56</i>	3.27	0.0313
<i>LOC388524</i>	-3.04	0.0938	<i>GPER</i>	3.25	0.0313
<i>LUM</i>	-2.98	0.0625	<i>WDHD1</i>	3.21	0.0313
<i>CCDC107</i>	-2.97	0.0313	<i>TYR</i>	3.2	0.0938
<i>C13ORF33</i>	-2.95	0.0313	<i>ARID4B</i>	3.17	0.0313
<i>BOLA1</i>	-2.95	0.0938	<i>DLC1</i>	3.17	0.0625
<i>SRR</i>	-2.94	0.0313	<i>ENG</i>	3.17	0.0938
<i>SPON1</i>	-2.94	0.0313	<i>TMEM19</i>	3.09	0.0313
<i>KLHL9</i>	-2.9	0.0938	<i>PRPF40A</i>	3.09	0.0625
<i>RPL7A</i>	-2.89	0.0625	<i>SORCS1</i>	3.03	0.0313

Central Versus Peripheral Sclera

Gene	FC	P-value	Gene	FC	P-value
<i>FANCI</i>	-6.33	0.0625	<i>DAPP1</i>	14.98	0.0625
<i>ZMAT4</i>	-5.38	0.0625	<i>LOC100132593</i>	13.1	0.0625
<i>C20ORF103</i>	-4.87	0.0625	<i>USP49</i>	9.4	0.0625
<i>MAPK10</i>	-4.32	0.0625	<i>ATP5F1</i>	8.04	0.0625
<i>MYO16</i>	-4.29	0.0625	<i>LOC727808</i>	7.95	0.0625
<i>TRIM24</i>	-3.96	0.0625	<i>LOC100133772</i>	7.43	0.0625
<i>TNIK</i>	-3.93	0.0625	<i>LOC643509</i>	5.7	0.0625
<i>FAM86B1</i>	-3.91	0.0625	<i>LOC645895</i>	5.69	0.0625
<i>FLJ40194</i>	-3.88	0.0625	<i>KIAA1751</i>	5.66	0.0625
<i>SIRT4</i>	-3.88	0.0625	<i>FAM73A</i>	5.16	0.0625
<i>ST8SIA4</i>	-3.69	0.0625	<i>FAM175A</i>	5.13	0.0625
<i>CDK5R1</i>	-3.61	0.0625	<i>LOC100132585</i>	5.03	0.0625
<i>CDC42</i>	-3.6	0.0625	<i>IL17RD</i>	4.92	0.0625
<i>ELF2</i>	-3.6	0.0625	<i>LOC440704</i>	4.83	0.0625
<i>HS.120893</i>	-3.58	0.0625	<i>LOC646996</i>	4.65	0.0625
<i>LOC644670</i>	-3.53	0.0625	<i>LOC399900</i>	4.57	0.0625
<i>LOC81691</i>	-3.52	0.0625	<i>CYCSL1</i>	4.53	0.0625
<i>GAL3ST3</i>	-3.51	0.0625	<i>LOC100131989</i>	4.47	0.0625
<i>PROX1</i>	-3.51	0.0625	<i>C9ORF80</i>	4.44	0.0625
<i>EIF2C3</i>	-3.49	0.0625	<i>ATG12</i>	4.14	0.0625
<i>TJP2</i>	-3.45	0.0625	<i>LOC100128098</i>	4.05	0.625
<i>LOC100134361</i>	-3.41	0.0625	<i>CD68</i>	4.03	0.0625
<i>KCNJ4</i>	-3.34	0.0625	<i>TMEM17</i>	3.97	0.0625
<i>SMC4</i>	-3.32	0.0625	<i>C14ORF153</i>	3.93	0.0625
<i>C17ORF65</i>	-3.29	0.0625	<i>LOC644642</i>	3.87	0.0625
<i>HS.570189</i>	-3.29	0.0625	<i>ZNF394</i>	3.74	0.0625
<i>COX11</i>	-3.28	0.0625	<i>LOC401098</i>	3.72	0.0625
<i>S100A1</i>	-3.27	0.0625	<i>DTWD2</i>	3.7	0.0625
<i>ZSCAN5A</i>	-3.24	0.0625	<i>ZNF786</i>	3.68	0.0625
<i>KCNK4</i>	-3.21	0.0625	<i>MPZL2</i>	3.58	0.0625
<i>HS.154948</i>	-3.19	0.0625	<i>C21ORF58</i>	3.55	0.0625
<i>LOC653075</i>	-3.19	0.0625	<i>RGS5</i>	3.49	0.0625
<i>SRD5A1</i>	-3.14	0.0625	<i>C15ORF63</i>	3.45	0.0625
<i>RGS20</i>	-3.13	0.0625	<i>BTBD6</i>	3.36	0.0625
<i>OTX2</i>	-3.12	0.0625	<i>CLIC4</i>	3.34	0.0625
<i>LOC220930</i>	-3.07	0.0625	<i>DENR</i>	3.31	0.0625
<i>PPFIA2</i>	-3.06	0.0625	<i>PPP1R10</i>	3.22	0.0625
<i>DTX1</i>	-3.04	0.0625	<i>C10ORF10</i>	3.19	0.0625
<i>TEKT1</i>	-3.01	0.0625	<i>LOC727865</i>	3.18	0.0625
<i>PHACTR3</i>	-3	0.0625	<i>ZNF223</i>	3.16	0.0625

Appendix C

Symbol	MIM	Ret/RPE FC	p-value	Choroid FC	p-value	Sclera FC	p-value
MYP1							
<i>AFF2</i>	300806	-1.31	2.65X10 ⁻⁵				
<i>ATP6AP1</i>	300197			1.68	0.0007		
<i>BCAP31</i>	300398	1.06	0.0005	2.09	0.0007	1.1	0.0001
<i>BRCC3</i>	300617					-1.41	0.0004
<i>CD99L2</i>		1.09	0.0005				
<i>CSAG1</i>		-1.56	0.0012	-3.14	0.0047		
<i>CXorf40B</i>				-2.18	0.0027		
<i>DNASE1L1</i>	300081			-3.21	0.0027		
<i>GAB3</i>	300482			-4.39	0.0007		
<i>GDI1</i>	300104	1.07	0.0005			1.1	0.0024
<i>HCFC1</i>	300019			-1.71	0.0007		
<i>HMGB3</i>	300193	-1.56	2.65X10 ⁻⁵	-4.16	0.0007	-1.35	0.0046
<i>IDS</i>	300823	1.12	0.0001	1.44	0.0007		
<i>L1CAM</i>	142623			3.49	0.0013	-1.78	0.0046
<i>LAGE3</i>	300060	-1.06	0.005	-4.56	0.0007	-1.1	7.37X10 ⁻⁵
<i>MAGEA1</i>	300016			5.97	0.0047		
<i>MAGEA3</i>	300174	1.28	0.0018				
<i>MAMLD1</i>	300120	-1.16	0.0036				
<i>MPP1</i>	305360	1.09	0.005				
<i>PNCK</i>	300680	-1.28	2.65X10 ⁻⁵				
<i>PNMA3</i>	300675					-1.35	3.69X10 ⁻⁵
<i>PNMA6A</i>						-1.58	3.69X10 ⁻⁵
<i>PRRG3</i>	300685	-1.36	0.0005	-3.17	0.0027	-1.43	0.0003
<i>RENBP</i>	312420	1.29	0.0008			1.27	0.0007
<i>SSR4</i>	300090	-1.1	0.0012				
<i>TAZ</i>	300069	1.34	0.0012				
<i>TMEM185A</i>	300031	-1.12	0.0001	-1.92	0.0027	1.44	0.0016
<i>TMEM187</i>	300059			-2.81	0.0007		
<i>TMLHE</i>	300777	1.1	0.0068				
<i>VBP1</i>	300133			-4.51	0.0047		
MYP2							
<i>FLJ35776</i>		1.24	0.0005				
MYP3							
<i>ACTR6</i>				1.47	0.0027	1.08	0.0062
<i>ALX1</i>	601527	1.13	0.0003	-3.09	0.0007		
<i>ANKS1B</i>	607815			-1.53	0.0036	-1.39	0.0062
<i>APAF1</i>	602233					-1.08	0.0062
<i>ARL1</i>	603425			-5.22	0.0007	-1.13	0.0007
<i>ATP2B1</i>	108731			-2.7	0.0007		
<i>BTBD11</i>				4.16	0.0024		
<i>C12orf23</i>				-7.1	0.0007		

<i>C12orf48</i>				-11.39	0.0007	-1.61	0.0001
<i>C12orf64</i>				2.13	0.008		
<i>CCDC53</i>						1.07	7.37X10 ⁻⁵
<i>CCDC59</i>		-1.07	0.005				
<i>CHPT1</i>						1.21	0.0016
<i>CRADD</i>	603454			1.92	0.0027	1.14	0.0046
<i>DUSP6</i>	602748	-1.47	0.0036	2.37	0.0007		
				-13.01	0.0007		
<i>E2F7</i>	612046						
<i>EEA1</i>	605070			2.61	0.0007		
<i>EPYC</i>	601657	2.76	0.0012				
<i>FGD6</i>	613520			-2.75	0.0007		
<i>GAS2L3</i>				2.86	0.0007		
<i>GLT8D2</i>				-3.42	0.0007	-1.15	0.0062
<i>GNPTAB</i>	252500	1.68	0.0068	64.42	0.0047	1.93	0.0033
<i>IGF1</i>	147440			-45.62	0.0007	-1.62	0.0003
				-2.73	0.0027		
<i>KITLG</i>	145250			-5.71	0.0007		
				-3.35	0.0007		
<i>LOC100128191</i>						-1.21	0.0062
<i>LOC144481</i>			-3.23	0.008			
<i>LOC643770</i>						1.36	0.0016
<i>LTA4H</i>	151570					-1.05	0.0024
<i>METAP2</i>	601870					1.06	0.0007
<i>MRPL42</i>	611847	-1.22	0.005				
<i>MTERFD3</i>		1.38	0.0036				
<i>NEDD1</i>	600372			-3.47	0.0047		
<i>NFYB</i>	189904			-2.58	0.0013		
<i>NTN4</i>	610401					1.23	7.37X10 ⁻⁵
<i>NUDT4</i>	609229	1.29	5.29X10 ⁻⁵	2.39	0.0007		
<i>PLXNC1</i>	604259			-23.87	0.0007	-1.66	0.0003
<i>PPFIA2</i>	603143			-2.35	0.0013	-1.5	0.0016
<i>PRDM4</i>	605780	1.08	0.0005				
<i>PTPRQ</i>	603317	-1.51	0.0002	-5.63	0.0007		
<i>PTPRR</i>	602853	1.44	2.65X10 ⁻⁵	3.04	0.0047		
<i>PWP1</i>		-1.12	0.0005				
<i>RASSF9</i>	610383	1.28	0.0003				
<i>RFX4</i>	603958			-3.13	0.0047		
<i>RIC8B</i>	609147	1.12	0.0003				
<i>SLC17A8</i>	605583			-4.71	0.0007	-2.27	0.0046
<i>SLC25A3</i>	600370	-1.65	0.0018	-5.51	0.0007	-1.77	0.0033
<i>SLC6A15</i>	607971	-1.35	2.65X10 ⁻⁵				
<i>SOCS2</i>	605117	-1.33	0.005			1.16	0.0001
<i>SPIC</i>	612568					1.27	0.0024
<i>TDG</i>	601423	-1.1	0.0008	1.93	0.0007		
<i>TMTC2</i>		-1.34	2.65X10 ⁻⁵				
<i>TMTC3</i>						-1.21	0.0062

<i>TSPAN31</i>	181035					1.09	0.0011
<i>UTP20</i>	612822			36.99	0.0007	1.48	0.0016
MYP4							
<i>EN2</i>	131310	1.38	0.0036	7.09	0.0007	1.46	0.0011
<i>FAM62B</i>		1.13	0.0008	2.34	0.0007	1.14	7.37X10 ⁻⁵
<i>LMBR1</i>	174500			-2.53	0.0007		
<i>LOC100132707</i>		1.59	2.65E-05				
<i>LOC202781</i>			⁻⁵ .63	0.008			
<i>NCAPG2</i>	608532	-1.15	0.0008	-3.32	0.0013	-1.32	0.0011
<i>NOM1</i>	611269	-1.42	0.0018				
<i>RBM33</i>				2.9	0.0013		
<i>RNF32</i>		1.21	0.005			1.27	0.0046
<i>SHH</i>	120200	1.77	0.0008				
<i>VIPR2</i>	601970					-1.23	0.0062
MYP5							
<i>AKAP1</i>	602449			-2.57	0.0027		
<i>APPBP2</i>	605324			-2.77	0.0047	-1.06	7.37X10 ⁻⁵
<i>C17orf71</i>	613175	-1.1	0.0002	-1.8	0.0027	-1.11	0.004
<i>CA4</i>	114760			3.27	0.0013		
<i>CUEDC1</i>						-1.11	0.0012
<i>DHX40</i>	607570	-1.1	0.0002	-2.34	0.0013		
				-3.36	0.0027		
<i>GDPD1</i>		-1.14	0.0025				
<i>HLF</i>	142385			-3.24	0.008	1.17	0.0024
<i>LOC645638</i>						1.31	3.69X10 ⁻⁵
<i>MKS1</i>	209900					-1.23	0.0011
<i>OR4D1</i>		-1.36	0.0068				
<i>PRR11</i>				-4.43	0.0013	-2.67	3.69X10 ⁻⁵
<i>PTRH2</i>	608625			3.75	0.0007		
<i>RAD51C</i>	602774			-3.8	0.0027		
<i>RPS6KB1</i>	608938	1.11	0.0001	2.31	0.0007	1.11	0.0008
<i>SCPEP1</i>		1.19	2.65X10 ⁻⁵				
<i>SFRS1</i>	600812			1.39	0.0081		
<i>TRIM25</i>	600453	1.14	0.0005				
<i>TRIM37</i>	253250			-4.65	0.0047		
<i>TUBD1</i>	607344					1.22	3.69X10 ⁻⁵
MYP6							
<i>APOL1</i>	181500					1.42	0.0001
<i>APOL2</i>	181500	1.3	0.0008	3.47	0.008	1.51	3.69X10 ⁻⁵
<i>APOL3</i>	607253	1.28	0.0005			1.5	3.69X10 ⁻⁵
<i>APOL6</i>	607256	1.57	0.0025				
<i>C1QTNF6</i>				-5.21	0.0007	-1.56	0.0004
<i>C22orf28</i>				-3.84	0.008	-1.19	7.37X10 ⁻⁵
<i>C22orf30</i>		-1.08	2.65X10 ⁻⁵			-1.07	0.0003
<i>DRG1</i>	603952	-1.09	0.0003			-1.07	0.0011
<i>EIF4ENIF1</i>	607445			-1.92	0.008		

<i>EMID1</i>	608926	-1.64	0.0003	-3.57	0.0007	-1.73	0.0004
<i>EWSR1</i>	133450	-1.06	0.0012	1.93	0.0007		
<i>FBXO7</i>	260300			-2.21	0.008		
				-3.04	0.0013		
<i>FOXRED2</i>				-4.38	0.0007	-1.18	0.0033
				-5.31	0.0027		
<i>HMGXB4</i>	604702			-2.46	0.0027	-1.18	0.0046
<i>HPS4</i>	203300	1.72	0.0008	-4.19	0.0047	1.78	0.0033
<i>HSCB</i>	608142	-1.17	0.0018	-17.44	0.0027		
				-3.24	0.0007		
<i>INPP5J</i>	606481			2.18	0.0027		
<i>KREMEN1</i>	609898	-1.29	0.0012	-2.46	0.008	-1.4	0.0033
<i>LARGE</i>	236670	-1.17	0.0036			-1.28	0.0016
		-1.08	0.0012				
<i>LIF</i>	159540	1.18	0.0018				
<i>MCM5</i>	602696	-1.21	0.0025	-2.37	0.0007	-1.23	0.0031
<i>MN1</i>	156100	-1.21	2.65X10 ⁻⁵	-4.33	0.0007		
		-1.17	5.29X10 ⁻⁵	-3.99	0.0007		
<i>MORC2</i>		-1.3	0.0001			-1.13	0.0024
<i>MPST</i>	602496	-1.29	2.65X10 ⁻⁵				
<i>MTMR3</i>	603558			-5.27	0.0007		
<i>MYH9</i>	153640	1.11	5.29X10 ⁻⁵				
		1.14	0.0001				
<i>NEFH</i>	105400	1.59	0.0012				
<i>PATZ1</i>	605165			-2.74	0.0013		
<i>RASL10A</i>	602220					-1.9	3.69X10 ⁻⁵
<i>RBM9</i>	612149			-3.59	0.0007	-1.19	3.69X10 ⁻⁵
						-1.42	0.0062
<i>RHBDD3</i>						-1.21	0.0011
<i>RNF215</i>				-1.84	0.008		
<i>SEZ6L</i>	607021	-2.12	0.0001				
<i>SF3A1</i>	605595	-1.11	0.0036			-1.18	0.0033
<i>SFI1</i>	612765	1.29	0.0001				
<i>SMTN</i>	602127	1.2	0.0005				
<i>TCN2</i>	275350	-1.25	0.0012				
<i>TFIP11</i>	612747	1.23	0.0036	7.02	0.0047	1.22	0.0046
<i>THOC5</i>	612733			1.95	0.0007		
<i>TTC28</i>		-1.3	0.0008				
<i>YWHAH</i>	113508					-1.07	7.37X10 ⁻⁵
MYP7							
<i>ABTB2</i>		-1.22	0.0036				
<i>C11orf41</i>	612297	-1.27	5.29X10 ⁻⁵	-3.99	0.0013	-1.48	0.0001
<i>CAPRIN1</i>	601178	1.05	0.0044	-7.42	0.0007	1.1	0.0062
<i>CAT</i>	115500	-1.24	2.65X10 ⁻⁵	-3.56	0.0047		
				-5.64	0.0047		
<i>CD44</i>	107269			2.19	0.0047		
<i>COMMD9</i>	612299	-1.11	0.0003				

<i>CSTF3</i>	600367	-1.12	0.0018	-2.74	0.0007	-1.17	0.0007
<i>DEPDC7</i>	612294					-1.89	0.0062
<i>DKFZ</i>				4.99	0.0013	1.39	0.0001
<i>p686K1684</i>							
<i>EIF3M</i>	609641	-1.21	0.0012	-7.19	0.0047		
<i>ELP4</i>	606985					-1.36	0.0007
<i>FBXO3</i>	609089			-3.33	0.0047		
<i>FJX1</i>	612206	-1.47	0.0018				
<i>NAT10</i>	609221			1.73	0.0013		
<i>PAMR1</i>		-2.54	0.0036	-6.47	0.0007	-2.15	0.0016
<i>QSER1</i>						-1.3	0.0062
<i>RCN1</i>	602735	1.07	0.0012	1.59	0.0047	-1.15	0.0001
<i>SLC1A2</i>	600300			-3.43	0.0007		
<i>TRIM44</i>	612298					1.11	3.69X10 ⁻⁵
MYP8							
<i>AADACL1</i>	613234	1.25	0.0001	2.28	0.0007	1.25	0.0001
		1.36	0.0018				
<i>ACTL6A</i>	604958	-1.18	0.0005	-3.54	0.0047		
<i>ATP11B</i>	605869	1.18	2.65X10 ⁻⁵			1.15	0.0011
<i>B3GALNT1</i>	111400	-1.12	5.29X10 ⁻⁵	-2.09	0.0027	-1.07	0.0033
				-6.57	0.0007	-1.41	0.0046
<i>BCHE</i>	177400	-1.24	0.0012	-7.81	0.0007	-1.65	0.0005
		-1.48	0.0001	-16.23	0.0007	-1.81	0.0003
<i>CLDN11</i>	601326			4.05	0.0007		
<i>ECT2</i>	600586	1.25	0.0003			-1.28	0.0001
<i>EIF5A2</i>	605782	1.47	2.65X10 ⁻⁵	3.26	0.0007	1.26	0.0003
<i>FLJ46066</i>						1.57	0.0024
<i>FXR1</i>	600819			-2.51	0.0007		
<i>GNB4</i>	610863			-17.25	0.0027		
<i>GOLIM4</i>	606805			-3.27	0.0027		
<i>GPR160</i>		-1.25	0.0036				
<i>KCNMB2</i>	605214					-1.25	0.0062
<i>LRRC31</i>				5.01	0.0007		
<i>NLGN1</i>	600568			-2.24	0.0027	-1.08	0.0033
<i>PDCD10</i>	603285			-4.24	0.0047	-1.38	0.0062
<i>RPL22L1</i>				2.1	0.008		
<i>SEC62</i>		1.12	5.29X10 ⁻⁵			1.13	3.69X10 ⁻⁵
<i>SERPINI1</i>	602445			-13.28	0.0007		
				-3.42	0.008		
<i>SLITRK3</i>	609679			-2.46	0.0027	-1.2	7.37X10 ⁻⁵
<i>TNFSF10</i>	603598	1.88	0.0003			1.56	0.0001
<i>TNIK</i>	610005			-6.63	0.0007	-2.23	0.0007
<i>USP13</i>	603591			-2.47	0.0047	-1.16	0.0001
<i>ZMAT3</i>				-2.44	0.0007		
				-6.44	0.0047		
MYP9							
<i>C4orf14</i>		-1.16	0.0002			-1.25	0.0062

<i>CEP135</i>	611423	1.14	0.0005					
<i>CLOCK</i>	601851	1.26	0.0008			1.18	0.0062	
<i>DCUN1D4</i>	612977	1.11	2.65X10 ⁻⁵	2.49	0.0007	1.24	3.69X10 ⁻⁵	
					1.09	0.0003		
<i>FIP1L1</i>	607686			2.44	0.008	-1.08	0.0062	
<i>KDR</i>	191306			-2.88	0.008			
<i>KIAA1211</i>		-1.38	2.65E-05		-1.47	0.0007		
<i>KIT</i>	164920	-1.12	0.0002					
		-1.1	0.0018					
<i>NMU</i>	605103			-2.91	0.0013	-2.29	3.69X10 ⁻⁵	
<i>SCFD2</i>						-1.4	0.0024	
<i>SGCB</i>	600900	-1.17	0.0012					
<i>SRD5A3</i>	611715	1.21	0.0068					
<i>USP46</i>	612849			-3.97	0.0007			
<i>MYP11</i>								
<i>ADH1B</i>	103720			12.39	0.0013	2.15	3.69X10 ⁻⁵	
<i>ADH5</i>	103710	-1.18	0.0068					
<i>AGXT2L1</i>		1.19	0.0036			1.49	0.0001	
<i>ANK2</i>	106410					1.11	0.0062	
<i>BANK1</i>	152700			1.76	0.0047			
<i>C4orf32</i>						1.22	7.37X10 ⁻⁵	
<i>CAMK2D</i>	607708			-2.93	0.0027			
<i>CCDC109B</i>						1.15	3.69X10 ⁻⁵	
<i>CENPE</i>	117143	1.11	0.0036	-2.63	0.0007	-1.27	0.0062	
<i>CFI</i>	217030	1.33	5.29X10 ⁻⁵					
<i>CXXC4</i>	611645	-1.24	2.65X10 ⁻⁵	-3.69	0.0013	-1.59	0.0004	
<i>CYP2U1</i>	610670			2.29	0.0047	1.24	3.69X10 ⁻⁵	
<i>DDIT4L</i>	607730	1.44	0.0001	11.27	0.0007			
<i>DNAJB14</i>		1.17	0.0012	1.94	0.0007	1.08	0.0046	
<i>EMCN</i>	608350	1.36	0.005	-7.41	0.0013			
<i>FLJ43963</i>						1.61	0.0046	
<i>GSTCD</i>				-1.41	0.008	-1.37	3.69X10 ⁻⁵	
<i>H2AFZ</i>	142763	-1.1	0.0025	-3.57	0.0024	-1.16	0.0007	
<i>HADH</i>	231530			-2.28	0.0007	-1.06	0.0007	
<i>LOC729218</i>				2.02	0.0027			
<i>LRIT3</i>		1.48	0.0003					
<i>MAD2L1</i>	601467	-1.27	0.0012	-3.95	0.0007	-2.23	0.0003	
<i>METAP1</i>	610151	-1.1	0.0012	-1.92	0.008	-1.13	0.0062	
<i>NDST3</i>	603950					-1.85	3.69X10 ⁻⁵	
<i>NDST4</i>				1.95	0.0047			
<i>NPNT</i>	610306			2.9	0.0007			
<i>PAPSS1</i>	603262	-1.22	2.65X10 ⁻⁵	-3.42	0.0007	-1.18	0.0001	
<i>PDE5A</i>	603310	1.24	0.0001			1.14	0.0033	
		1.23	0.0036					
<i>PITX2</i>	137600			-2.82	0.0007			
				-10.15	0.0007			
<i>RG9MTD2</i>				-3.64	0.0047	-1.32	0.0003	

<i>TRAM1L1</i>		-1.66	0.0008	-6.71	0.0007	-1.87	0.0033
<i>TSPAN5</i>				-2.15	0.008	-1.42	3.69X10 ⁻⁵
<i>MYP12</i>							
<i>ATG16L1</i>	610767			1.65	0.0027		
<i>DGKD</i>	601826	-1.52	0.0012			-1.13	0.0033
<i>SAG</i>	181031	1.33	0.0018			1.76	0.0062
<i>MYP13</i>							
<i>ACSL4</i>	300157					1.19	0.0007
<i>AIFM1</i>	300169	1.09	0.0001				
		1.04	0.0068				
		-1.27	0.0012				
<i>AMOT</i>	300410	-1.15	0.0008	-4.94	0.0024		
<i>C1GALT1C1</i>	300611	1.15	0.0019	3.02	0.0007		
<i>CAPN6</i>	300146	1.28	0.0068			-1.24	0.0016
<i>CXorf64</i>		-1.45	0.0036				
<i>DCX</i>	300067	-1.43	2.65X10 ⁻⁵			-1.63	3.69X10 ⁻⁵
<i>GPR119</i>	300513					-2.37	0.0046
<i>GRIA3</i>	300699					-1.19	0.0062
						-1.19	0.0062
<i>IL13RA1</i>	300119	1.41	2.65X10 ⁻⁵			1.23	3.69X10 ⁻⁵
<i>KLHL13</i>	300655			-5.14	0.0007	-1.8	0.0001
<i>LAMP2</i>	300257	1.21	2.65X10 ⁻⁵	2.04	0.0007	1.11	0.0005
				1.77	0.0007	1.19	3.69X10 ⁻⁵
<i>LHFPL1</i>	300566	1.27	0.0018				
<i>NKAP</i>	300766			-7.38	0.0007		
<i>NKRF</i>	300440			1.46	0.008		
<i>PGRMC1</i>	300435	-1.14	2.65X10 ⁻⁵	-3.59	0.0007	-1.09	0.0062
<i>PLS3</i>	300131	1.19	5.29X10 ⁻⁵			1.14	3.69X10 ⁻⁵
<i>RAP2C</i>						1.13	0.0033
<i>SH2D1A</i>	300490			2.41	0.0013		
				2.41	0.0013		
<i>SLC25A14</i>	300242			2.71	0.0007		
				-2.07	0.0047		
<i>SLC25A43</i>	300641					1.32	0.0003
<i>SMARCA1</i>	300012			-3.04	0.0007		
<i>THOC2</i>		1.13	5.29X10 ⁻⁵	2.61	0.0047		
				1.79	0.0007		
<i>UBE2A</i>	312180					-1.19	0.0062
<i>UPF3B</i>	300298			2.14	0.0007	1.09	0.0016
<i>UTP14A</i>	300508	-1.18	0.0012				
		-1.26	2.65X10 ⁻⁵				
<i>WDR44</i>						1.29	3.69X10 ⁻⁵
<i>XIAP</i>	300079			-3.14	0.0007		
<i>XIAP</i>	300079			-3.14	0.0007		
<i>ZCCHC12</i>	300701	-1.55	2.65X10 ⁻⁵				
<i>ZNF280C</i>				2.39	0.0007	1.13	0.0062
<i>MYP14</i>							

<i>AKR7A2</i>	603418			-2.22	0.0007		
<i>ALPL</i>	146300					-1.35	3.69X10 ⁻⁵
<i>ARID1A</i>	603024	-1.15	0.0003	-4.07	0.0007	-1.1	0.0007
<i>C1orf151</i>		1.31	0.0036	28.03	0.0007	1.61	0.0011
<i>CAMK2N1</i>				-2.57	0.0007		
<i>CAPZB</i>	601572	1.13	2.65X10 ⁻⁵			1.06	0.0046
<i>CCDC21</i>		-1.22	0.0018	-4.76	0.0007	-1.28	7.37X10 ⁻⁵
<i>CLIC4</i>	606536					1.22	0.0062
<i>CNKSR1</i>		1.16	0.0003				
<i>DDOST</i>	602202					-1.05	0.0033
<i>DHDDS</i>	608172					-1.17	0.0033
<i>DNAJC8</i>	173393			2.02	0.0007	1.04	0.0007
<i>E2F2</i>	600426			-4.3	0.0007	-1.44	0.0001
<i>ECE1</i>	145500			-3.71	0.0027		
<i>EIF4G3</i>	603929					-1.07	0.0046
<i>EPHA8</i>	176945	-1.74	2.65X10 ⁻⁵				
<i>EPHB2</i>	600997	-1.51	2.65X10 ⁻⁵	-2.17	0.0047	-1.55	3.69X10 ⁻⁵
		-2.43	2.65X10 ⁻⁵			-3.49	3.69X10 ⁻⁵
<i>EXTL1</i>	601738	1.26	0.0036				
<i>EYA3</i>	601655	1.43	0.0025				
<i>FAM46B</i>		1.73	0.0025	4.26	0.0047	2.06	0.0027
<i>FGR</i>	164940	1.8	0.0012			1.29	0.0033
						1.36	0.0004
<i>FUCA1</i>	230000	-1.13	0.0025	-3.8	0.0013	-1.16	0.0033
<i>GALE</i>	230350			5.94	0.0013	-1.12	0.0046
<i>HMGN2</i>	163910	-1.34	2.65X10 ⁻⁵	-2.65	0.0007	-1.34	0.0001
		-1.18	5.29X10 ⁻⁵	-3.36	0.0007	-1.15	0.0005
				-20.42	0.0007		
<i>HNRNPR</i>	607201	-1.16	0.0003				
		-1.12	0.0008				
<i>HSPG2</i>	142461			-5.68	0.0007		
<i>ID3</i>	600277			-2.39	0.0007		
<i>IL28RA</i>	607404	1.56	2.65X10 ⁻⁵	10.55	0.0007	1.6	3.69X10 ⁻⁵
<i>KIF17</i>	605037			-3.75	0.0007	-1.76	0.0007
<i>LDLRAP1</i>	603813	1.5	5.29X10 ⁻⁵				
<i>MAN1C1</i>		-1.16	0.0036	-4.3	0.0027		
				-6.31	0.0007		
<i>MAP3K6</i>	604468	1.38	0.0003	5.72	0.0024	1.32	3.69X10 ⁻⁵
<i>MECR</i>	608205	-1.25	0.0018			-5.04	0.0011
						-1.63	0.0024
<i>MRTO4</i>						-1.28	0.0001
<i>MUL1</i>	612037			-1.37	0.0027		
<i>NBPF3</i>	612992	1.07	0.0012	-1.81	0.0027		
<i>PAFAH2</i>	602344	-1.12	0.0025				
<i>PDIK1L</i>	610785	-1.17	0.0036	-3.77	0.0007	-1.23	0.0024
<i>PHACTR4</i>	608726	-1.13	5.29X10 ⁻⁵			-1.08	0.0024
<i>PLA2G2A</i>	114500			220.99	0.0007	3.64	3.69X10 ⁻⁵

<i>PLA2G5</i>	601192	1.34	0.0008			2.01	3.69X10 ⁻⁵
<i>PTPRU</i>	602454	1.18	0.0018			1.15	0.0016
<i>RUNX3</i>	600210			-3.22	0.0007		
<i>SEPN1</i>						-1.1	0.0007
<i>SFN</i>	601290	1.72	0.0036				
<i>SLC9A1</i>	107310	1.13	5.29X10 ⁻⁵				
<i>SRRM1</i>	605975			2.25	0.0007		
<i>STMN1</i>	151442	-1.31	2.65X10 ⁻⁵	-9.18	0.0007	-1.64	3.69X10 ⁻⁵
		-2	0.0005	-19.87	0.0007	-2.45	0.0004
<i>SYF2</i>	607090	-1.11	0.0018	-1.87	0.008	1.11	0.0003
<i>TCEA3</i>	604128			-4.3	0.0027		
<i>TCEB3</i>	600786			1.93	0.0007		
<i>TRNAU1AP</i>				-1.86	0.008	-1.23	0.0057
<i>P</i>				-1.69	0.0007		
<i>USP48</i>		1.12	0.0068	1.65	0.0027		
<i>WDTC1</i>				-6.1	0.0007		
<i>XKR8</i>						-1.21	0.0033
<i>YTHDF2</i>	152430	-1.1	0.0003				
<i>ZDHHC18</i>		-1.23	0.0012			-1.22	0.0007
<i>ZNF436</i>	611703			-5.07	0.0007		
<i>ZNF593</i>				2.47	0.0013		
<i>MYP15</i>							
<i>ZWINT</i>	609177	-1.41	0.005	-4.33	0.0047	-1.5	0.0024
				-11.1	0.0007	-2.38	7.37X10 ⁻⁵
						-3.73	0.0016
<i>MYP17</i>							
<i>CDCA7L</i>	609685	-1.27	0.0012	-4.03	0.0007	-1.64	0.0003
<i>HIBADH</i>	608475	1.12	0.0018				
<i>HNRNPA2B1</i>	600124			2.16	0.0047		
<i>HOXA2</i>	604685			6.29	0.0007		
<i>HOXA3</i>	142954	1.41	0.0003	1.97	0.0027		
<i>HOXA5</i>	142952			4.62	0.0013	1.68	3.69X10 ⁻⁵
<i>HOXA6</i>	142951	1.21	5.29X10 ⁻⁵	3.14	0.0007		
<i>HOXA7</i>	142950	1.41	0.0018				
<i>HOXA9</i>	142956	1.39	0.0012				
<i>IGF2BP3</i>	608259	-1.53	5.29X10 ⁻⁵	-9.9	0.0007	-1.7	3.69X10 ⁻⁵
<i>JAZF1</i>	606246			-2.08	0.0013		
<i>KLHL7</i>	611119			1.63	0.0027	1.19	0.0005
<i>NFE2L3</i>	604135	-1.18	0.0068				
<i>NPVF</i>		-1.46	0.005				
<i>NPY</i>	162640	-1.72	2.65X10 ⁻⁵				
<i>NUPL2</i>		-1.13	0.0012				
		-1.16	0.0008				
<i>OSBPL3</i>	606732					1.28	0.0033
<i>OTX2</i>	600037	-1.44	0.0002				
		-1.18	2.65X10 ⁻⁵				
		-1.35	2.65X10 ⁻⁵				

SKAP2	605215					1.5	3.69X10 ⁻⁵
						1.35	7.37X10 ⁻⁵
TAX1BP1	605326			-1.34	0.0047		
				-3.7	0.0013		
TOMM7	607980			1.7	0.0047	1.07	0.0007
				2.22	0.0024	1.07	3.69X10 ⁻⁵
TRA2A	602718	-1.12	0.0025				
MYP18							
ACTN1	102575	1.22	5.29X10 ⁻⁵	2.61	0.0007	1.19	3.69X10 ⁻⁵
ACTR10				-3.27	0.0047		
ADAM21	603713					-2.32	0.0004
ARG2	107830	1.16	0.0036	2.26	0.0047		
ARID4A	180201			-5.24	0.0007	1.15	0.0024
				-4.31	0.0027		
ATG14	613515	-1.4	0.0018				
ATL1	606439			-2.94	0.0013		
BMP4	112262	-1.55	0.0036	-5.01	0.008	1.11	0.0011
C14orf101				-2.9	0.0007		
C14orf135		-1.09	0.0036	-2.45	0.0007	-1.11	0.0046
		-1.13	0.0002	-1.75	0.0027		
C14orf149				-1.65	0.008		
C14orf162				3.55	0.0047		
C14orf37		-1.29	2.65X10 ⁻⁵	-5.23	0.0007	-1.27	0.0024
		-1.39	0.0005	-3.18	0.0007	-1.31	0.0011
C14orf38		1.35	0.0003				
CDKN3	123832					-1.94	0.0005
COX16		1.52	2.65X10 ⁻⁵	41.27	0.0007	1.62	0.0016
DAAM1	606626			-1.66	0.0047		
DLGAP5				-10.45	0.0007	-2.58	3.69X10 ⁻⁵
DPF3	601672	1.19	0.0068				
DPP3	606818			-4.69	0.0047		
ERO1L		1.27	2.65X10 ⁻⁵	3.4	0.0007	1.34	3.69X10 ⁻⁵
EXD2				-2.63	0.008		
FRMD6	614555			-7.37	0.0047		
				-8.18	0.0007		
FUT8	602589			-3.87	0.0007		
GMFB	601713			1.45	0.0027		
GNG2	606981	-1.8	0.0005	-12.83	0.0007		
GNPNAT1		1.11	0.005	2.33	0.0007		
GPHB5	609652			2.33	0.008		
HIF1A	603348			2.93	0.0007		
HSPA2	140560			-3.51	0.0007		
KIAA0247		1.13	0.0018				
KTN1	600381			-1.9	0.0047		
LGALS3	153619	2.51	2.65X10 ⁻⁵			1.44	3.69X10 ⁻⁵
LOC283553			-2.27	0.008			
MAP4K5	604923			2.46	0.0007		

MAX	154950	1.3	0.0008	-3.55	0.0007		
				2.21	0.0007		
MTHFD1	172460	-1.17	0.0068				
NID2	605399			-7.03	0.0024	-1.4	0.0011
NIN	608684			-3.7	0.0047		
NUMB	603728			1.38	0.0027	1.08	3.69X10 ⁻⁵
PAPLN		1.36	0.0002				
PCNX				1.75	0.0007		
PELI2							
PIGH	600154	1.11	0.0003			1.27	7.37X10 ⁻⁵
PLEK2	608007	1.33	0.0025				
PLEKHG3		1.26	5.29X10 ⁻⁵				
PLEKHH1		1.13	0.0008				
PPM1A	606108			-5.81	0.0007		
PSEN1	104311	-1.44	0.0068	-2.27	0.0027		
PTGDR	604687	1.65	0.0001	6.39	0.0007	1.3	0.0011
				1.96	0.008		
PYGL	613741			2.18	0.0007	1.09	0.0011
RDH11	607849	1.14	2.65X10 ⁻⁵	1.96	0.0007		
RDH12	608830	1.66	0.0003				
RTN1	600865	-1.58	0.0018	2.36	0.008		
SCARNA20		-1.24	0.005				
SIPA1L1				-2.91	0.0007		
SIX1	601205					-1.49	0.0024
SIX4	606342	1.41	0.0018				
SIX6	606326	-1.23	2.65X10 ⁻⁵			-1.95	0.0004
SLC35F4						-3.19	0.0001
SLC38A6		1.18	0.0005			1.16	0.0003
SMOC1	608488	-1.55	0.0068	-2.63	0.0047		
SNAPC1	600591			-3.69	0.0027		
SYNE2	608442			-3.56	0.0007		
				-1.63	0.0047		
TMX1	610527	-1.09	0.0008	23.05	0.0047		
TRIM9	606555	-1.25	0.0001				
		-1.16	0.0002				
TRMT5	611023	-1.19	2.65X10 ⁻⁵	-5.38	0.0007	-1.17	3.69X10 ⁻⁵
WDHD1	608126	-1.35	0.0025			-1.25	0.0011
WDR89		1.12	0.0018			-1.85	0.0024
		-1.32	0.0025				
ZBTB1						1.32	0.0016
ZFYVE1	605471					1.1	0.0046
MYP19							
CMBL	613379			-3.85	0.0007		
DAP	600954			-1.93	0.0013		
LOC255167				-7.01	0.0027		
MED10	612382	-1.11	0.0018			-1.12	0.0003
MTRR	236270			-1.56	0.0047		

<i>SEMA5A</i>	609297	-1.29	0.0025	-19.6	0.0007	-1.9	3.69×10^{-5}
<i>SRD5A1</i>	184753	-1.22	0.0002	-5.21	0.0007	-1.4	3.69×10^{-5}

References

- Abbott, D., Y. J. Li, et al. (2012). "An international collaborative family-based whole genome quantitative trait linkage scan for myopic refractive error." Mol Vis **18**: 720-729.
- Abecasis, G. R. and W. O. Cookson (2000). "GOLD--graphical overview of linkage disequilibrium." Bioinformatics **16**(2): 182-183.
- Adams, J. A. (2006). "Endothelium and cardiopulmonary resuscitation." Crit Care Med **34**(12 Suppl): S458-465.
- Akagi-Kurashige, Y., K. Kumagai, et al. (2012). "Vascular endothelial growth factor gene polymorphisms and choroidal neovascularization in highly myopic eyes." Investigative Ophthalmology & Visual Science **53**(4): 2349-2353.
- Almasy, L. and J. Blangero (1998). "Multipoint quantitative-trait linkage analysis in general pedigrees." Am. J. Hum. Genet. **62**(5): 1198-1211.
- Andersen, J. N., P. G. Jansen, et al. (2004). "A genomic perspective on protein tyrosine phosphatases: gene structure, pseudogenes, and genetic disease linkage." FASEB J **18**(1): 8-30.
- Annamaneni, S., C. H. Bindu, et al. (2011). "Association of vitamin D receptor gene start codon (Fok1) polymorphism with high myopia." Oman J Ophthalmol **4**(2): 57-62.
- Ashby, R. S., P. L. Megaw, et al. (2009). "Changes in the expression of Pax6 RNA transcripts in the retina during periods of altered ocular growth in chickens." Exp Eye Res **89**(3): 392-397.
- Atchison, D. A., C. E. Jones, et al. (2004). "Eye shape in emmetropia and myopia." Invest. Ophthalmol. Vis. Sci. **45**(10): 3380-3386.
- Barbara M. Wirostko, M. R. E., MD; and Alon Harris, MS, PhD (2009). "The Vascular Theory in Glaucoma: A focus on the endothelial cells." Glaucoma Today(April): 25-27.

Benjamini, Y. H., Yosef (1995). "Controlling the false discovery rate: a practical and powerful approach to multiple testing." Journal of the Royal Statistical Society Series B (Methodological) **57**(1): 289–300.

Bhat, S. P., S. A. Rayner, et al. (2004). "Pax-6 expression in posthatch chick retina during and recovery from form-deprivation myopia." Dev Neurosci **26**(5-6): 328-335.

Bowes Rickman, C., J. N. Ebright, et al. (2006). "Defining the human macula transcriptome and candidate retinal disease genes using EyeSAGE." Investigative Ophthalmology & Visual Science **47**(6): 2305-2316.

Brown, D. M., K. Vandenburg, et al. (1995). "Novel frameshift mutations in the procollagen 2 gene (COL2A1) associated with Stickler syndrome (hereditary arthropathopathy)." Hum Mol Genet **4**(1): 141-142.

Burton, T. C. (1989). "The influence of refractive error and lattice degeneration on the incidence of retinal detachment." Trans. Am. Ophthalmol. Soc. **87**: 143-155.

Carlson, C. S., M. A. Eberle, et al. (2004). "Selecting a maximally informative set of single-nucleotide polymorphisms for association analyses using linkage disequilibrium." Am. J. Hum. Genet. **74**(1): 106-120.

Carlsson, E., A. Ranki, et al. (2012). "Potential role of a navigator gene NAV3 in colorectal cancer." Br J Cancer **106**(3): 517-524.

Chakravarti, S., J. Paul, et al. (2003). "Ocular and scleral alterations in gene-targeted lumican-fibromodulin double-null mice." Investigative Ophthalmology & Visual Science **44**(6): 2422-2432.

Chen, C. Y., J. Stankovich, et al. (2007). "Linkage replication of the MYP12 locus in common myopia." Investigative Ophthalmology & Visual Science **48**(10): 4433-4439.

Chen, K. C., E. Hsi, et al. (2012). "MicroRNA-328 may influence myopia development by mediating the PAX6 gene." Investigative Ophthalmology & Visual Science **53**(6): 2732-2739.

Chen, X., A. Xue, et al. (2011). "Assessment of exonic single nucleotide polymorphisms in the adenosine A(2A) receptor gene to high myopia susceptibility in Chinese subjects." Mol Vis **17**: 486-491.

Chen, X., T. Yoshida, et al. (2011). "Protein tyrosine phosphatase sigma regulates the synapse number of zebrafish olfactory sensory neurons." J. Neurochem.

Chen, Y. P., P. M. Hocking, et al. (2011). "Selective breeding for susceptibility to myopia reveals a gene-environment interaction." Investigative Ophthalmology & Visual Science **52**(7): 4003-4011.

Chen, Z. T., I. J. Wang, et al. (2009). "The association of haplotype at the lumican gene with high myopia susceptibility in Taiwanese patients." Ophthalmology **116**(10): 1920-1927.

Ciner, E., G. Ibay, et al. (2009). "Genome-wide scan of African-American and white families for linkage to myopia." Am J Ophthalmol **147**(3): 512-517 e512.

Ciner, E., R. Wojciechowski, et al. (2008). "Genomewide scan of ocular refraction in African-American families shows significant linkage to chromosome 7p15." Genet Epidemiol **32**(5): 454-463.

Cordell, H. J. and D. G. Clayton (2005). "Genetic association studies." Lancet **366**(9491): 1121-1131.

Curtin, B. J., T. Iwamoto, et al. (1979). "Normal and staphylomatous sclera of high myopia. An electron microscopic study." Arch Ophthalmol **97**(5): 912-915.

Dilaver, G., J. Schepens, et al. (2003). "Colocalisation of the protein tyrosine phosphatases PTP-SL and PTPBR7 with beta4-adaptin in neuronal cells." Histochem Cell Biol **119**(1): 1-13.

Fan, Q., V. A. Barathi, et al. (2012). "Genetic variants on chromosome 1q41 influence ocular axial length and high myopia." PLoS Genet **8**(6): e1002753.

Farbrother, J. E., G. Kirov, et al. (2004). "Linkage analysis of the genetic loci for high myopia on 18p, 12q, and 17q in 51 U.K. families." Invest. Ophthalmol. Vis. Sci. **45**(9): 2879-2885.

Faulkner, A. E., M. K. Kim, et al. (2007). "Head-mounted goggles for murine form deprivation myopia." J. Neurosci. Methods **161**(1): 96-100.

Flammer, J., S. Orgul, et al. (2002). "The impact of ocular blood flow in glaucoma." Prog Retin Eye Res **21**(4): 359-393.

Fledelius, H. C. and A. C. Christensen (1996). "Reappraisal of the human ocular growth curve in fetal life, infancy, and early childhood." Br. J. Ophthalmol. **80**(10): 918-921.

Francomano, C. A., R. M. Liberfarb, et al. (1987). "The Stickler syndrome: evidence for close linkage to the structural gene for type II collagen." Genomics **1**(4): 293-296.

Fujinami, K., H. Uemura, et al. (2002). "Liprin-alpha2 gene, protein tyrosine phosphatase LAR interacting protein related gene, is downregulated by androgens in the human prostate cancer cell line LNCaP." Int J Mol Med **10**(2): 173-176.

Gao, H., M. R. Frost, et al. (2011). "Patterns of mRNA and protein expression during minus-lens compensation and recovery in tree shrew sclera." Mol Vis **17**: 903-919.

Gordon, R. A. and P. B. Donzis (1985). "Refractive development of the human eye." Arch. Ophthalmol. **103**(6): 785-789.

Hammond, C. J., T. Andrew, et al. (2004). "A susceptibility locus for myopia in the normal population is linked to the PAX6 gene region on chromosome 11: a genomewide scan of dizygotic twins." Am J Hum Genet **75**(2): 294-304.

Han, W., K. H. Leung, et al. (2009). "Association of PAX6 polymorphisms with high myopia in Han Chinese nuclear families." Investigative Ophthalmology & Visual Science **50**(1): 47-56.

Han, W., M. K. Yap, et al. (2006). "Family-based association analysis of hepatocyte growth factor (HGF) gene polymorphisms in high myopia." Invest Ophthalmol Vis Sci **47**(6): 2291-2299.

Hansen, A. C. (1963). "The collagen diseases: eye manifestations." J Natl Med Assoc **55**: 8-12.

Havill, L. M., T. D. Dyer, et al. (2005). "The quantitative trait linkage disequilibrium test: a more powerful alternative to the quantitative transmission disequilibrium test for use in the absence of population stratification." BMC Genet. **6 Suppl 1**: S91.

Hendrickson, A. (1992). "A morphological comparison of foveal development in man and monkey." Eye (Lond) **6 (Pt 2)**: 136-144.

Hendriks, W. J., G. Dilaver, et al. (2009). "PTPRR protein tyrosine phosphatase isoforms and locomotion of vesicles and mice." Cerebellum 8(2): 80-88.

Hesse, C., D. R. Schroeder, et al. (2010). "beta2-Adrenoceptor gene variation and systemic vasodilatation during ganglionic blockade." J Physiol 588(Pt 14): 2669-2678.

Hewitt, A. W., L. S. Kearns, et al. (2007). "PAX6 mutations may be associated with high myopia." Ophthalmic Genet 28(3): 179-182.

Hildebrand, G. D. and A. R. Fielder (2011). Anatomy and Physiology of the Retina. Pediatric Retina. J. R. a. S. Olitsky, Springer Berlin Heidelberg: pp 39-65.

Ho, D. W., M. K. Yap, et al. (2012). "Association of High Myopia with Crystallin Beta A4 (CRYBA4) Gene Polymorphisms in the Linkage-Identified MYP6 Locus." PLoS One 7(6): e40238.

Hodge, S. E. (1993). "Linkage analysis versus association analysis: distinguishing between two models that explain disease-marker associations." Am J Hum Genet 53(2): 367-384.

Hopfner, R., M. Mousli, et al. (2000). "ICBP90, a novel human CCAAT binding protein, involved in the regulation of topoisomerase IIalpha expression." Cancer Res 60(1): 121-128.

Hornbeak, D. M. and T. L. Young (2009). "Myopia genetics: a review of current research and emerging trends." Curr. Opin. Ophthalmol. 20(5): 356-362.

Hotelling, H. (1931). "The Generalization of Student's Ratio." The Annals of Mathematical Statistics 2(3): 360-378.

Hwang, Y. H. and Y. Y. Kim (2012). "Myopic optic disc changes in adolescents." Ophthalmology 119(4): 885-886.

Hysi, P. G., C. L. Simpson, et al. (2012). "Common polymorphisms in the SERPINI2 gene are associated with refractive error in the 1958 British Birth Cohort." Investigative Ophthalmology & Visual Science 53(1): 440-447.

Hysi, P. G., T. L. Young, et al. (2010). "A genome-wide association study for myopia and refractive error identifies a susceptibility locus at 15q25." Nat Genet 42(10): 902-905.

- Inamori, Y., M. Ota, et al. (2007). "The COL1A1 gene and high myopia susceptibility in Japanese." Hum Genet **122**(2): 151-157.
- Irizarry, R. A., B. Hobbs, et al. (2003). "Exploration, normalization, and summaries of high density oligonucleotide array probe level data." Biostatistics **4**(2): 249-264.
- Javitt, J. C. and Y. P. Chiang (1994). "The socioeconomic aspects of laser refractive surgery." Arch. Ophthalmol. **112**(12): 1526-1530.
- Jeanblanc, M., M. Mousli, et al. (2005). "The retinoblastoma gene and its product are targeted by ICBP90: a key mechanism in the G1/S transition during the cell cycle." Oncogene **24**(49): 7337-7345.
- Jepsen, K. J., F. Wu, et al. (2002). "A syndrome of joint laxity and impaired tendon integrity in lumican- and fibromodulin-deficient mice." J Biol Chem **277**(38): 35532-35540.
- Jiang, B., M. K. Yap, et al. (2011). "PAX6 haplotypes are associated with high myopia in Han chinese." PLoS One **6**(5): e19587.
- Jobling, A. I., A. Gentle, et al. (2009). "Regulation of scleral cell contraction by transforming growth factor-beta and stress: competing roles in myopic eye growth." The Journal of biological chemistry **284**(4): 2072-2079.
- Jobling, A. I., M. Nguyen, et al. (2004). "Isoform-specific changes in scleral transforming growth factor-beta expression and the regulation of collagen synthesis during myopia progression." The Journal of biological chemistry **279**(18): 18121-18126.
- Jobling, A. I., R. Wan, et al. (2009). "Retinal and choroidal TGF-beta in the tree shrew model of myopia: isoform expression, activation and effects on function." Exp Eye Res **88**(3): 458-466.
- Jonas, J. B., G. C. Gusek, et al. (1988). "Optic disk morphometry in high myopia." Graefes Arch Clin Exp Ophthalmol **226**(6): 587-590.
- Jordan, T., I. Hanson, et al. (1992). "The human PAX6 gene is mutated in two patients with aniridia." Nat Genet **1**(5): 328-332.

Katz, J., J. M. Tielsch, et al. (1997). "Prevalence and risk factors for refractive errors in an adult inner city population." Invest. Ophthalmol. Vis. Sci. **38**(2): 334-340.

Kempen, J. H., P. Mitchell, et al. (2004). "The prevalence of refractive errors among adults in the United States, Western Europe, and Australia." Arch. Ophthalmol. **122**(4): 495-505.

Khor, C. C., Q. Fan, et al. (2010). "Support for TGFB1 as a susceptibility gene for high myopia in individuals of Chinese descent." Arch Ophthalmol **128**(8): 1081-1084.

Klein, A. P., B. Suktitipat, et al. (2009). "Heritability analysis of spherical equivalent, axial length, corneal curvature, and anterior chamber depth in the Beaver Dam Eye Study." Arch Ophthalmol **127**(5): 649-655.

Kolb, H., Nelson, R., Fernandez, E., and Jones, B (2011). Webvision - The organization of the Retina and the Visual System. Webvision - The organization of the Retina and the Visual System. H. Kolb, R. Nelson, E. Fernandez and B. Jones. <http://webvision.med.utah.edu/>.

Lam, C. Y., P. O. Tam, et al. (2008). "A genome-wide scan maps a novel high myopia locus to 5p15." Investigative Ophthalmology & Visual Science **49**(9): 3768-3778.

Lam, D. S., W. S. Lee, et al. (2003). "TGFbeta-induced factor: a candidate gene for high myopia." Investigative Ophthalmology & Visual Science **44**(3): 1012-1015.

Leveziel, N., Y. Yu, et al. (2012). "Genetic Factors for Choroidal Neovascularization Associated with High Myopia." Invest Ophthalmol Vis Sci.

Leveziel, N., Y. Yu, et al. (2012). "Genetic factors for choroidal neovascularization associated with high myopia." Investigative Ophthalmology & Visual Science **53**(8): 5004-5009.

Li, S., B. Ji, et al. (2001). "[Study on the association of pathologic myopia with HLA-DQB1 gene]." Zhonghua Yan Ke Za Zhi **37**(4): 263-266.

Li, X., B. X. Ji, et al. (2000). "[Studies of the association of pathological myopia in Chinese patients with HLA alleles]." Yi Chuan Xue Bao **27**(3): 189-194.

Li, Y. J., L. Goh, et al. (2011). "Genome-wide association studies reveal genetic variants in CTNND2 for high myopia in Singapore Chinese." Ophthalmology **118**(2): 368-375.

Li, Y. J., J. A. Guggenheim, et al. (2009). "An international collaborative family-based whole-genome linkage scan for high-grade myopia." Invest. Ophthalmol. Vis. Sci. **50**(7): 3116-3127.

Liang, C. L., E. Hsi, et al. (2011). "A functional polymorphism at 3'UTR of the PAX6 gene may confer risk for extreme myopia in the Chinese." Invest Ophthalmol Vis Sci **52**(6): 3500-3505.

Lin, H. J., Y. J. Kung, et al. (2010). "Association of the lumican gene functional 3'-UTR polymorphism with high myopia." Invest Ophthalmol Vis Sci **51**(1): 96-102.

Lin, H. J., L. Wan, et al. (2012). "Muscarinic acetylcholine receptor 3 is dominant in myopia progression." Investigative Ophthalmology & Visual Science.

Lin, H. J., L. Wan, et al. (2009). "Muscarinic acetylcholine receptor 1 gene polymorphisms associated with high myopia." Mol Vis **15**: 1774-1780.

Lin, H. J., L. Wan, et al. (2010). "The association between lumican gene polymorphisms and high myopia." Eye (Lond) **24**(6): 1093-1101.

Lin, H. J., L. Wan, et al. (2009). "Sclera-related gene polymorphisms in high myopia." Mol Vis **15**: 1655-1663.

Lin, H. J., L. Wan, et al. (2006). "The TGFbeta1 gene codon 10 polymorphism contributes to the genetic predisposition to high myopia." Mol Vis **12**: 698-703.

Linberg, K. A. and S. K. Fisher (1990). "A burst of differentiation in the outer posterior retina of the eleven-week human fetus: an ultrastructural study." Vis Neurosci **5**(1): 43-60.

Liu, H., N. Xiang, et al. (2007). "Influence of high level TGF-beta1 on scleral thickness." J Huazhong Univ Sci Technolog Med Sci **27**(5): 601-604.

Liu, H. P., Y. J. Lin, et al. (2009). "A novel genetic variant of BMP2K contributes to high myopia." J Clin Lab Anal **23**(6): 362-367.

Liu, M. G., H. Li, et al. (2008). "Comparison of gene expression during in vivo and in vitro postnatal retina development." J. Ocul. Biol. Dis. Infor. **1**(2-4): 59-72.

Liu, Y., D. Munro, et al. (2011). "Serial analysis of gene expression (SAGE) in normal human trabecular meshwork." Mol Vis **17**: 885-893.

Livak, K. J. and T. D. Schmittgen (2001). "Analysis of relative gene expression data using real-time quantitative PCR and the 2(-Delta Delta C(T)) Method." Methods **25**(4): 402-408.

Lopes, M. C., T. Andrew, et al. (2009). "Estimating heritability and shared environmental effects for refractive error in twin and family studies." Invest. Ophthalmol. Vis. Sci. **50**(1): 126-131.

Lu, B., D. Jiang, et al. (2011). "Replication study supports CTNND2 as a susceptibility gene for high myopia." Investigative Ophthalmology & Visual Science **52**(11): 8258-8261.

Lyhne, N., A. K. Sjolie, et al. (2001). "The importance of genes and environment for ocular refraction and its determiners: a population based study among 20-45 year old twins." Br. J. Ophthalmol. **85**(12): 1470-1476.

Ma, J. H., S. H. Shen, et al. (2010). "Identification of a locus for autosomal dominant high myopia on chromosome 5p13.3-p15.1 in a Chinese family." Mol Vis **16**: 2043-2054.

Majava, M., P. N. Bishop, et al. (2007). "Novel mutations in the small leucine-rich repeat protein/proteoglycan (SLRP) genes in high myopia." Hum Mutat **28**(4): 336-344.

Mak, J. Y., M. K. Yap, et al. (2012). "Association of IGF1 gene haplotypes with high myopia in Chinese adults." Arch Ophthalmol **130**(2): 209-216.

Margo, C. E. and A. Lee (1995). "Fixation of whole eyes: the role of fixative osmolarity in the production of tissue artifact." Graefe's archive for clinical and experimental ophthalmology = Albrecht von Graefes Archiv fur klinische und experimentelle Ophthalmologie **233**(6): 366-370.

Martin, E. R., M. P. Bass, et al. (2003). "Accounting for linkage in family-based tests of association with missing parental genotypes." Am. J. Hum. Genet. **73**(5): 1016-1026.

McBrien, N. A. and A. Gentle (2003). "Role of the sclera in the development and pathological complications of myopia." Prog. Retin. Eye Res. **22**(3): 307-338.

McBrien, N. A., P. Lawlor, et al. (2000). "Scleral remodeling during the development of and recovery from axial myopia in the tree shrew." Investigative Ophthalmology & Visual Science **41**(12): 3713-3719.

McGlinn, A. M., D. A. Baldwin, et al. (2007). "Form-deprivation myopia in chick induces limited changes in retinal gene expression." Invest Ophthalmol Vis Sci **48**(8): 3430-3436.

Menigatti, M., E. Cattaneo, et al. (2009). "The protein tyrosine phosphatase receptor type R gene is an early and frequent target of silencing in human colorectal tumorigenesis." Mol Cancer **8**: 124.

Metlapally, R., Y. J. Li, et al. (2009). "COL1A1 and COL2A1 genes and myopia susceptibility: evidence of association and suggestive linkage to the COL2A1 locus." Invest Ophthalmol Vis Sci **50**(9): 4080-4086.

Mordechai, S., L. Gradstein, et al. (2011). "High myopia caused by a mutation in LEPREL1, encoding prolyl 3-hydroxylase 2." Am J Hum Genet **89**(3): 438-445.

Morgan, I. and K. Rose (2005). "How genetic is school myopia?" Prog. Retin. Eye Res. **24**(1): 1-38.

Morgan, I. G. (2003). "The biological basis of myopic refractive error." Clin Exp Optom **86**(5): 276-288.

Morgan, I. G., K. Ohno-Matsui, et al. (2012). "Myopia." Lancet **379**(9827): 1739-1748.

Mu, X., S. Zhao, et al. (2001). "Gene expression in the developing mouse retina by EST sequencing and microarray analysis." Nucleic Acids Res. **29**(24): 4983-4993.

Mutti, D. O., M. E. Cooper, et al. (2011). "Vitamin D receptor (VDR) and group-specific component (GC, vitamin D-binding protein) polymorphisms in myopia." Investigative Ophthalmology & Visual Science **52**(6): 3818-3824.

Naiglin, L., C. Gazagne, et al. (2002). "A genome wide scan for familial high myopia suggests a novel locus on chromosome 7q36." Journal of medical genetics **39**(2): 118-124.

Nakanishi, H., R. Yamada, et al. (2009). "A genome-wide association analysis identified a novel susceptible locus for pathological myopia at 11q24.1." PLoS Genet **5**(9): e1000660.

Nallasamy, S., P. C. Paluru, et al. (2007). "Genetic linkage study of high-grade myopia in a Hutterite population from South Dakota." Mol Vis **13**: 229-236.

Ng, T. K., C. Y. Lam, et al. (2009). "AC and AG dinucleotide repeats in the PAX6 P1 promoter are associated with high myopia." Mol Vis **15**: 2239-2248.

Nickla, D. L. and J. Wallman (2010). "The multifunctional choroid." Prog Retin Eye Res **29**(2): 144-168.

Nishizaki, R., M. Ota, et al. (2009). "New susceptibility locus for high myopia is linked to the uromodulin-like 1 (UMODL1) gene region on chromosome 21q22.3." Eye (Lond) **23**(1): 222-229.

Nurnberg, G., F. K. Jacobi, et al. (2008). "Refinement of the MYP3 locus on human chromosome 12 in a German family with Mendelian autosomal dominant high-grade myopia by SNP array mapping." Int. J. Mol. Med. **21**(4): 429-438.

O'Connell, J. R. and D. E. Weeks (1998). "PedCheck: a program for identification of genotype incompatibilities in linkage analysis." Am. J. Hum. Genet. **63**(1): 259-266.

Oganesian, A., M. Poot, et al. (2003). "Protein tyrosine phosphatase RQ is a phosphatidylinositol phosphatase that can regulate cell survival and proliferation." Proc Natl Acad Sci U S A **100**(13): 7563-7568.

Ohno-Matsui, K., M. Akiba, et al. (2012). "Acquired Optic Nerve and Peripapillary Pits in Pathologic Myopia." Ophthalmology.

Oliveira, S. A., Y. J. Li, et al. (2005). "Identification of risk and age-at-onset genes on chromosome 1p in Parkinson disease." Am. J. Hum. Genet. **77**(2): 252-264.

Ozaltin, F., T. Ibsirlioglu, et al. (2011). "Disruption of PTPRO Causes Childhood-Onset Nephrotic Syndrome." Am. J. Hum. Genet. **89**(1): 139-147.

Paget, S., S. Julia, et al. (2008). "Linkage analysis of high myopia susceptibility locus in 26 families." Mol Vis **14**: 2566-2574.

Paluru, P., S. M. Ronan, et al. (2003). "New locus for autosomal dominant high myopia maps to the long arm of chromosome 17." Investigative Ophthalmology & Visual Science **44**(5): 1830-1836.

Paluru, P. C., S. Nallasamy, et al. (2005). "Identification of a novel locus on 2q for autosomal dominant high-grade myopia." Investigative Ophthalmology & Visual Science **46**(7): 2300-2307.

Pararajasegaram, R. (1999). "VISION 2020-the right to sight: from strategies to action." Am. J. Ophthalmol. **128**(3): 359-360.

Parssinen, O., H. M. Jauhonen, et al. (2010). "Heritability of spherical equivalent: a population-based twin study among 63- to 76-year-old female twins." Ophthalmology **117**(10): 1908-1911.

Pascolini, D. and S. P. Mariotti (2012). "Global estimates of visual impairment: 2010." Br J Ophthalmol **96**(5): 614-618.

Paul, O. L. and Z. Dmitri (2006). GDA (Genetic Data Analysis).

Pawson, T. and J. D. Scott (2005). "Protein phosphorylation in signaling--50 years and counting." Trends Biochem Sci **30**(6): 286-290.

Pesudovs, K., E. Garamendi, et al. (2006). "The Contact Lens Impact on Quality of Life (CLIQ) Questionnaire: development and validation." Invest Ophthalmol. Vis. Sci. **47**(7): 2789-2796.

Purves, D., and Augustine, G. J. et al. (2001). Anatomical Distribution of Rods and Cones. Neuroscience. G. J. A. Dale Purves, David Fitzpatrick, Lawrence C Katz, Anthony-Samuel LaMantia, James O McNamara, and S Mark Williams. Sunderland (MA), Sinauer Associates.

Quek, T. P., C. G. Chua, et al. (2004). "Prevalence of refractive errors in teenage high school students in Singapore." Ophthalmic Physiol. Opt. **24**(1): 47-55.

Rada, J. A., S. Shelton, et al. (2006). "The sclera and myopia." Exp. Eye Res. **82**(2): 185-200.

Ritchey, E. R., C. P. Zelinka, et al. (2012). "The combination of IGF1 and FGF2 and the induction of excessive ocular growth and extreme myopia." Exp Eye Res **99**: 1-16.

Rodieck, R. W. (1998). The first steps in seeing. Sunderland, Mass., Sinauer Associates.

Rose, K., R. Harper, et al. (2000). "Quality of life in myopia." Br. J. Ophthalmol. **84**(9): 1031-1034.

Rose, K. A., I. G. Morgan, et al. (2008). "Outdoor activity reduces the prevalence of myopia in children." Ophthalmology **115**(8): 1279-1285.

Samarawickrama, C., P. Mitchell, et al. (2011). "Myopia-related optic disc and retinal changes in adolescent children from Singapore." Ophthalmology **118**(10): 2050-2057.

Saw, S. M. (2003). "A synopsis of the prevalence rates and environmental risk factors for myopia." Clin. Exp. Optom. **86**(5): 289-294.

Saw, S. M., J. Katz, et al. (1996). "Epidemiology of myopia." Epidemiol. Rev. **18**(2): 175-187.

Schache, M., C. Y. Chen, et al. (2009). "Fine mapping linkage analysis identifies a novel susceptibility locus for myopia on chromosome 2q37 adjacent to but not overlapping MYP12." Mol Vis **15**: 722-730.

Schippert, R., F. Schaeffel, et al. (2008). "Microarray analysis of retinal gene expression in chicks during imposed myopic defocus." Mol. Vis. **14**: 1589-1599.

Schwartz, M., M. Haim, et al. (1990). "X-linked myopia: Bornholm eye disease. Linkage to DNA markers on the distal part of Xq." Clinical genetics **38**(4): 281-286.

Shelton, L., D. Troilo, et al. (2008). "Microarray analysis of choroid/RPE gene expression in marmoset eyes undergoing changes in ocular growth and refraction." Mol. Vis. **14**: 1465-1479.

Shen, P., X. Ding, et al. (2012). "Contribution of genetic and environmental effects on lens thickness: the Guangzhou Twin Eye study." Investigative Ophthalmology & Visual Science **53**(4): 1758-1763.

- Shi, C., K. Zhang, et al. (2011). "Gender-specific role of the protein tyrosine phosphatase receptor type R gene in major depressive disorder." J Affect Disord.
- Shi, Y., Y. Li, et al. (2011). "Exome sequencing identifies ZNF644 mutations in high myopia." PLoS Genet 7(6): e1002084.
- Shi, Y., J. Qu, et al. (2011). "Genetic variants at 13q12.12 are associated with high myopia in the Han Chinese population." Am J Hum Genet 88(6): 805-813.
- Shih, Y. F., T. C. Ho, et al. (2006). "Long-term visual prognosis of infantile-onset high myopia." Eye (Lond) 20(8): 888-892.
- Shioya, M., S. Obayashi, et al. (2010). "Aberrant microRNA expression in the brains of neurodegenerative diseases: miR-29a decreased in Alzheimer disease brains targets neurone navigator 3." Neuropathol Appl Neurobiol 36(4): 320-330.
- Silva, R. (2012). "Myopic Maculopathy: A Review." Ophthalmologica.
- Solouki, A. M., V. J. Verhoeven, et al. (2010). "A genome-wide association study identifies a susceptibility locus for refractive errors and myopia at 15q14." Nat Genet 42(10): 897-901.
- Spangler, S. A., D. Jaarsma, et al. (2011). "Differential expression of liprin-alpha family proteins in the brain suggests functional diversification." J Comp Neurol 519(15): 3040-3060.
- Stambolian, D., E. B. Ciner, et al. (2005). "Genome-wide scan for myopia in the Old Order Amish." Am J Ophthalmol 140(3): 469-476.
- Stambolian, D., G. Ibay, et al. (2004). "Genomewide linkage scan for myopia susceptibility loci among Ashkenazi Jewish families shows evidence of linkage on chromosome 22q12." Am J Hum Genet 75(3): 448-459.
- Stone, R. A. and T. S. Khurana (2010). "Gene profiling in experimental models of eye growth: clues to myopia pathogenesis." Vision Res. 50(23): 2322-2333.
- Strauss, O. (2005). "The retinal pigment epithelium in visual function." Physiol Rev 85(3): 845-881.

Sugiyama, D. T., J. C. Townsend, et al. (1993). "Support for the vasogenic theory of glaucoma: case reports and literature review." J Am Optom Assoc **64**(8): 568-582.

Sundin, O. H., S. Dharmaraj, et al. (2008). "Developmental basis of nanophthalmos: MFRP Is required for both prenatal ocular growth and postnatal emmetropization." Ophthalmic Genet **29**(1): 1-9.

Tang, W. C., S. P. Yip, et al. (2007). "Linkage and association of myocilin (MYOC) polymorphisms with high myopia in a Chinese population." Mol Vis **13**: 534-544.

Tkatchenko, T. V., Y. Shen, et al. (2009). "Mouse Experimental Myopia Has Features of Primate Myopia." Invest. Ophthalmol. Vis. Sci.

Tonks, N. K. (2006). "Protein tyrosine phosphatases: from genes, to function, to disease." Nat Rev Mol Cell Biol **7**(11): 833-846.

Tran-Viet, K. N., E. St Germain, et al. (2012). "Study of a US cohort supports the role of ZNF644 and high-grade myopia susceptibility." Mol Vis **18**: 937-944.

Tsai, M. Y., L. L. Lin, et al. (2009). "Estimation of heritability in myopic twin studies." Jpn. J. Ophthalmol. **53**(6): 615-622.

Tsai, Y. Y., C. C. Chiang, et al. (2008). "A PAX6 gene polymorphism is associated with genetic predisposition to extreme myopia." Eye (Lond) **22**(4): 576-581.

Ulmer, M., J. Li, et al. (2012). "Genome-Wide Analysis of Central Corneal Thickness in Primary Open-Angle Glaucoma Cases in the NEIGHBOR and GLAUGEN Consortia." Invest Ophthalmol Vis Sci **53**(8): 4468-4474.

Van Den Maagdenberg, A. M., D. Bachner, et al. (1999). "The mouse Ptprr gene encodes two protein tyrosine phosphatases, PTP-SL and PTPBR7, that display distinct patterns of expression during neural development." Eur J Neurosci **11**(11): 3832-3844.

Vatavuk, Z., J. Skunca Herman, et al. (2009). "Common variant in myocilin gene is associated with high myopia in isolated population of Korcula Island, Croatia." Croat Med J **50**(1): 17-22.

Veerappan, S., K. K. Pertile, et al. (2010). "Role of the hepatocyte growth factor gene in refractive error." Ophthalmology **117**(2): 239-245 e231-232.

Vieland, V. J., K. Wang, et al. (2001). "Power to detect linkage based on multiple sets of data in the presence of locus heterogeneity: comparative evaluation of model-based linkage methods for affected sib pair data." Hum Hered **51**(4): 199-208.

Vision, A. A. (2007). Statistics on Ophthalmic Industry Sales, Access Media Group LLC.

Vitale, S., M. F. Cotch, et al. (2006). "Costs of refractive correction of distance vision impairment in the United States, 1999-2002." Ophthalmology **113**(12): 2163-2170.

Vitale, S., R. D. Sperduto, et al. (2009). "Increased prevalence of myopia in the United States between 1971-1972 and 1999-2004." Arch. Ophthalmol. **127**(12): 1632-1639.

Waliszek-Iwanicka, A., M. Waliszek, et al. (2010). "Assessment of blood flow in posterior ciliary arteries and its correlation with intraocular and arterial blood pressures in patients with open angle glaucoma." Med Sci Monit **16**(10): CR501-509.

Wallman, J., M. D. Gottlieb, et al. (1987). "Local retinal regions control local eye growth and myopia." Science **237**(4810): 73-77.

Wallman, J. and J. Winawer (2004). "Homeostasis of eye growth and the question of myopia." Neuron **43**(4): 447-468.

Wang, I. J., T. H. Chiang, et al. (2006). "The association of single nucleotide polymorphisms in the 5'-regulatory region of the lumican gene with susceptibility to high myopia in Taiwan." Mol Vis **12**: 852-857.

Wang, Z., D. Shen, et al. (2004). "Mutational analysis of the tyrosine phosphatome in colorectal cancers." Science **304**(5674): 1164-1166.

Wei, Z., S. Zheng, et al. (2011). "Liprin-mediated large signaling complex organization revealed by the liprin-alpha/CASK and liprin-alpha/liprin-beta complex structures." Mol Cell **43**(4): 586-598.

Wilcoxon, F. (1945). "Individual Comparisons by Ranking Methods." Biometrics Bulletin **1**(6): 80-83.

Wildsoet, C. and J. Wallman (1995). "Choroidal and scleral mechanisms of compensation for spectacle lenses in chicks." Vision Res. **35**(9): 1175-1194.

Wistow, G., K. Peterson, et al. (2008). "NEIBank: genomics and bioinformatics resources for vision research." Mol. Vis. **14**: 1327-1337.

Wojciechowski, R., J. E. Bailey-Wilson, et al. (2010). "Association of matrix metalloproteinase gene polymorphisms with refractive error in Amish and Ashkenazi families." Investigative Ophthalmology & Visual Science **51**(10): 4989-4995.

Wojciechowski, R., C. Moy, et al. (2006). "Genomewide scan in Ashkenazi Jewish families demonstrates evidence of linkage of ocular refraction to a QTL on chromosome 1p36." Hum Genet **119**(4): 389-399.

Xie, F. and Y. G. Chen (2008). "[Influence of disulfiram on the expression of transforming growth factor-beta2 in form-deprived eyes in chicks]." Beijing Da Xue Xue Bao **40**(6): 610-615.

Xu, L., Y. Li, et al. (2007). "Characteristics of highly myopic eyes: the Beijing Eye Study." Ophthalmology **114**(1): 121-126.

Xu, X., S. Li, et al. (2009). "Sequence variations of GRM6 in patients with high myopia." Mol Vis **15**: 2094-2100.

Yang, Y., X. Li, et al. (2009). "Myopia: a collagen disease?" Med Hypotheses **73**(4): 485-487.

Yang, Z., X. Xiao, et al. (2009). "Clinical and linkage study on a consanguineous Chinese family with autosomal recessive high myopia." Mol Vis **15**: 312-318.

Yanovitch, T., Y. J. Li, et al. (2009). "Hepatocyte growth factor and myopia: genetic association analyses in a Caucasian population." Mol Vis **15**: 1028-1035.

Young, T. L., S. S. Deeb, et al. (2004). "X-linked high myopia associated with cone dysfunction." Arch Ophthalmol **122**(6): 897-908.

Young, T. L., X. D. Guo, et al. (2003). "Identification of genes expressed in a human scleral cDNA library." Mol. Vis. **9**: 508-514.

Young, T. L., S. M. Ronan, et al. (1998). "A second locus for familial high myopia maps to chromosome 12q." Am. J. Hum. Genet. **63**(5): 1419-1424.

- Young, T. L., S. M. Ronan, et al. (1998). "Evidence that a locus for familial high myopia maps to chromosome 18p." Am J Hum Genet **63**(1): 109-119.
- Young, T. L., G. S. Scavello, et al. (2004). "Microarray analysis of gene expression in human donor sclera." Mol. Vis. **10**: 163-176.
- Yu, Z., J. Zhou, et al. (2012). "Polymorphisms in the CTNND2 Gene and 11q24.1 Genomic Region Are Associated with Pathological Myopia in a Chinese Population." Ophthalmologica **228**(2): 123-129.
- Yu, Z. Q., Y. B. Li, et al. (2007). "[A genome-wide screening for pathological myopia suggests a novel locus on chromosome 15q12 - 13]." Zhonghua Yan Ke Za Zhi **43**(3): 233-238.
- Zarepari, S., A. Hero, et al. (2004). "Seeing the unseen: Microarray-based gene expression profiling in vision." Invest. Ophthalmol. Vis. Sci. **45**(8): 2457-2462.
- Zha, Y., K. H. Leung, et al. (2009). "TGFB1 as a susceptibility gene for high myopia: a replication study with new findings." Arch Ophthalmol **127**(4): 541-548.
- Zhang, F., T. Zhu, et al. (2009). "Association of lumican gene with susceptibility to pathological myopia in the northern han ethnic chinese." J Ophthalmol **2009**: 514306.
- Zhang, Q., X. Guo, et al. (2005). "A new locus for autosomal dominant high myopia maps to 4q22-q27 between D4S1578 and D4S1612." Mol Vis **11**: 554-560.
- Zhang, Q., X. Guo, et al. (2006). "Novel locus for X linked recessive high myopia maps to Xq23-q25 but outside MYP1." Journal of medical genetics **43**(5): e20.
- Zhang, Q., S. Li, et al. (2007). "Confirmation of a genetic locus for X-linked recessive high myopia outside MYP1." J Hum Genet **52**(5): 469-472.
- Zhang, Q., X. Xiao, et al. (2007). "Mutations in NYX of individuals with high myopia, but without night blindness." Mol Vis **13**: 330-336.
- Zhao, Y. Y., F. J. Zhang, et al. (2011). "The association of a single nucleotide polymorphism in the promoter region of the LAMA1 gene with susceptibility to Chinese high myopia." Mol Vis **17**: 1003-1010.

Zhong, X. W., J. Ge, et al. (2004). "Expression of pax-6 in rhesus monkey of optical defocus induced myopia and form deprivation myopia." Chin Med J (Engl) **117**(5): 722-726.

Zhou, J., E. F. Rappaport, et al. (2006). "Differential gene expression in mouse sclera during ocular development." Invest. Ophthalmol. Vis. Sci. **47**(5): 1794-1802.

Zhou, X., Q. Huang, et al. (2010). "Genetic deletion of the adenosine A2A receptor confers postnatal development of relative myopia in mice." Investigative Ophthalmology & Visual Science **51**(9): 4362-4370.

Zhou, X., F. Ji, et al. (2012). "Experimental murine myopia induces collagen type Ialpha1 (COL1A1) DNA methylation and altered COL1A1 messenger RNA expression in sclera." Mol Vis **18**: 1312-1324.

Zhu, G., A. W. Hewitt, et al. (2008). "Genetic dissection of myopia: evidence for linkage of ocular axial length to chromosome 5q." Ophthalmology **115**(6): 1053-1057 e1052.

Biography

Felicia Hawthorne was born on July 16th, 1985 in Derry, New Hampshire. She attended Clemson University in South Carolina, where she competed as a high jumper for the track team and received her Bachelor of Science in Biological Sciences in May of 2007. She was awarded the College of Agriculture, Forestry, and Life Sciences Outstanding Senior Award. Felicia then attended Duke University, joining the laboratory of Terri L. Young, MD, MBA. She received her Doctorate of Philosophy in October of 2012. In the spring of 2012, Felicia was the runner-up for the position of Graduate and Professional Young Trustee. She was also awarded a fellowship with Accelerate Brain Cancer Cure in March of 2012.